Twenty years of amino acid determination using capillary electrophoresis: A review

Hai Yen Ta, Fabrice Collin, Lucie Perquis, Véréna Poinsot, Varravaddheay Ong-Meang, Francois Couderc

Twenty years of amino acid determination using capillary electrophoresis: A review

Hai Yen TA[a], Fabrice COLLIN[a], Lucie PERQUIS[a], Véréna POINSOT[b], Varravaddheay ONG-MEANG[b], Francois COUDERC[a],

[a] Laboratoire des IMRCP, UMR 5623, Université de Toulouse, Université Toulouse III, Paul Sabatier, 31062 Toulouse Cedex 4. FRANCE

[b] I2MC, UMR1048, Université de Toulouse, Université Toulouse III Paul Sabatier, 1 avenue du Professeur Jean Poulhès, BP 84225, 31432 Toulouse Cedex 4. FRANCE

Hai Yen TA, ta@chimie.ups-tlse.fr; Fabrice COLLIN, collin@chimie.ups-tlse.fr; Lucie PERQUIS, perquis@chimie.ups-tlse.fr; Véréna POINSOT, verena.poinsot@inserm.fr; Varravaddheay ONG-MEANG, varravaddheay.ong-meang@univ-tlse3.fr

Corresponding author:

François COUDERC, couderc@chimie.ups-tlse.fr +33 (0)5 61 55 88 73. Laboratoire des IMRCP, UMR 5623, Université de Toulouse, Université Toulouse III, Paul Sabatier, 31062 Toulouse Cedex 4. FRANCE

Abstract: In this review, we have attempted to highlight the advancements in the the field of amino acid determination using capillary electrophoresis. The technique has been developed through the years, and the assessment of publications from the past twenty years reveals the different developmental processes. Although there are relatively fewer publications on capillary electrophoresis (CE) every year, the advancements in both fluorescence and UV detection techniques make it a simple and powerful tool. We showed that recent developments in the coupling of CE with mass spectrometry or conductimetry pave the way for high throughput solutions for applications in metabolomics or in clinical biology analysis. This review describes the use of these different detection methods, and reports the most advanced applications: medical studies, amino acid determination in neurosciences, metabolomics, and foodomics. Through this review, we intended to show that as a tool for amino acid detection, CE has reached an advanced stage of development.

Abbreviations: AA, amino acid; BGE, background electrolyte; C^4D, capacitively coupled contactless conductivity detection; CBQCA, 3-(4-carboxy- benzoyl)-2-

quinolinecarboxaldehyde; CS, chiral selector; CSF, cerebrospinal fluid; CTAB, cetyltrimethylammonium bromide; GABA, γ-aminobutyric acid; FA, formic acid; FITC, fluorescein isothiocyanate; Hcy, homocysteine; IAF, iodoacetomido-fluorescein; LEDIF, LED induced fluorescence; NBD-F, 4-fluoro-7-nitro-2,1,3-benzoxadiazole-labeled; Orn, ornithine; TCAC, tricarboxylic acid cycle, 18C6H4, (+)-(18-crown-6)-2,3,11,12-tetracarboxylic acid

Contents

1. Introduction

Amino acid (AAs) separation using capillary electrophoresis (CE) is a subject of particular relevance that has been discussed extensively in the past 20 years in almost 3000 articles. In particular, the topic has been reviewed by various authors. Some of the notable researchers in this field of study are Poinsot *et al*, who have published detailed review articles every 2 years [1–8]; Denoroy and Parrot, who have studied these topics for a longer period [9]; and Song *et al*, who have studied biological samples from patients with specific diseases between 2012 and 2016 [10]. This is the first review to discuss studies conducted and reported over such an extensive time period, given that 20 years is sufficient to measure technical evolutions and apprehend novelties in a field. We will describe the key works that were published during this period, and occasionally, we will refer to the basics published earlier. Fig. 1 shows the variation in the number of publications, where the phrase "capillary electrophoresis" is present in the title and "amino acid" in the abstract (source: the Web of Knowledge). We observed that there two parallel curves are formed, which indicates that CE is less frequently used in analytical studies that result in publications, and as a consequence, AA studies are also less frequently reported. When comparing these curves with those on CE/fluorescence studies on AAs, we also observed a parallel decrease. The application of CE/mass spectrometry (MS) in AA determination does not show this tendency of reduction, with MS being a considerably popular technique used in analytical experiments as well as by major organizations (*i.e*, Agilent, Sciex) manufacturing CE/MS instruments. Capacitively coupled contactless conductivity detection (C^4D) with CE is the only detection mode whose applications have increased. This is an expected observation, owing to the universality of the method; currently, it is considered a useful AA determination method.

Several studies have described the use of simple background electrolytes (BGEs) for capillary zone electrophoresis (CZE), where AAs or their derivatives migrate in proportion to their charge and in inverse proportion to the size of the solvated ion. Micellar kinetic chromatography (MEKC) involves the migration of surfactants and their associated micelles in an electrolyte. At pH values above 7, the micelles play the role of a pseudo-stationary phase

with which AAs can be associated. Therefore, a complementary criterion for separation comes into play: the partition of AAs between the pseudo-stationary phase (in which limited migration occurs) and the buffer (in which they migrate as in CZE). Cyclodextrin (CD) can also be added to the MEKC electrolyte to establish a supplementary equilibrium (AAs inside CD or outside CD), which modifies the migration dynamics of the AAs. The AA/CD complex, being considerably larger than free AAs, migrates at a different electrophoretic velocity. CD also helps separate enantiomers.

Since it is neither feasible nor desirable to peruse all 3000 research articles published over the 20-year period, we have discussed various developments in the analysis of AAs using CE coupled to UV absorbance detection, C^4D, fluorescence detection, or MS. Following this, we have discussed the various common fields of applications: metabolomics, medical science, neuroscience, and foodomics. We have presented the key findings of these articles with precision, and expect that it will assist readers in the selection of an appropriate CE method for implementation in experimental settings. We have also added a critical synthesis at the end of each section.

2. CE/UV

Most AAs do not contain a chromophore moiety, and resultantly, do not absorb UV radiation sufficiently. Only aromatic AAs (Phe, Tyr, Trp, and His) and Cys can be easily detected using UV radiation. Therefore, the labeling of an AA with a chromophore is necessary for the use of CE/UV in AA studies. A handbook on derivatization was edited 20 years ago; it describes a variety of dyes, their related bibliography, and the reaction and separation conditions in high-performance liquid chromatography (HPLC) or CE [11]. A more concise publication, which may be considered old but not outdated, was published by Toyo'oka [12]. Generally, labeling is performed off-line prior to conducting CE/UV measurements; however, specific attempts have been made to achieve on-column derivatization. Other attempts have been aimed at studying AAs without derivatization with indirect UV detection or detection of changes in the refractive indices of zones containing the AAs after CZE separation. Table 1 outlines the basic analytical conditions adopted in the studies that have been reviewed in this chapter.

2.1. CE/UV with AA derivatization

Fluorescamine is particularly suitable for AA derivatization in relevant CE separation procedures. For example, in an experiment using a robust method of taurine determination, at

pH 3, labeled taurine was observed to be negatively charged and lag behind other AAs during migration [13].

Phenylisothiocyanate (PITC) derivatization was popularly used for AA determination approximately 50 years ago (in Edman degradation reaction). In a particular study, it was used to analyze 18 L-AAs (except Trp or Asn) with a buffer containing β-cyclodextrin (β-CD). A long separation step (53 min) was required. PITC-derivatized Arg migrated close to the electroosmotic flow (EOF). The majority of AAs were separated, and only Leu and Ile comigrated. The limit of detection (LOD) ranged from 1 μM (Gly) to 4 μM (Phe) [14].

Dansyl chloride has mostly been used for the identification of AAs using CE/UV and to a lesser extent using CE/fluorescence. Jorgenson and DeArman Lukacs were the first to publish a report on CE that dealt with the separation of dansylated AAs detected using fluorescence [15]. In the last 20 years, CE/UV has undergone advancements primarily related to enantiomer separation procedures. Chen *et al* [16,17] proposed the use of Cu(II)-L-phenylalaninamide and Cu(II)-L-alaninamide followed by Cu(II)-L-prolinamides as chiral selector (CS) molecules for separating DL-AAs by ligand exchange CE. Zn(II)-L- phenylalaninamide [18] and a mixture of Zn(II)-L-4-hydroxyproline and γ-CD [19] have also been used. Similarly, L-Ala–derivatized amino acid ionic liquids have been synthesized, which led to [1-butyl-3-methylimidazolium][L-Ala] formation. When associated with Mn(II) and β-CD, it facilitated the effective separation of proteinogenic AAs (except Gly). However, the fact that the enantioseparation of DL-Cys and DL-Lys has not been reported is a pertinent issue, whereas DL-ornithine (Orn) has been resolved using this method [20]. The detection of biogenic amines and AAs using CE/UV with dansylation has been compared to that using CE/laser-induced fluorescence (LIF) after labeling with fluorescein isothiocyanate (FITC). The selectivity and sensitivity of fluorescence detection was observed to be suitable for the quantitation of these compounds [21].

Terguride-based CS molecules were developed and used with polyacrylamide-coated capillaries, wherein the aim was to separate D-Ser (after dansylation) in samples derived from the mammalian body. 1-Allyl-5S,8R,10S-terguride was shown to be the best CS for separating 0.01% D-Ser from 99.99% L-Ser [22]. Usually, the enantioselectivity of dansylated AAs has been studied using a combination of β-CD and tetraalkylammonium Arg ionic liquids in nonaqueous CE using N-methylformamide. The results have shown that the resolution between enantiomers is above 2 (Trp, Phe, His, Cys, and Ala were tested) [23].

The Folin's reagent, 1,2-naphthoquinone-4-sulfonate, is a common reagent used for measuring the levels of primary amines [24], has also been used for resolution. Under the selected

separation conditions, Leu, Ile, and Phe peaks were partially resolved, and His and Leu were observed to comigrate. The lack of selectivity was overcome using the spectral and electrophoretic differences of analytes to recover their pure electrophoretic and spectral profiles. Each compound could be effectively quantitated [25,26]. Additionally, this dye has been used for in-capillary labeling via the sandwich configuration, in which reactive/sample/reactive zones are used for derivatization. Trp, Phe, Met Thr, Pro, and Ala could be effectively separated using stacking with large-volume samples (of low conductivity), with an LOD of 0.4 µM (Trp) to 1.4 µM (Phe) achieved for standard AAs [27].

Zhang and Gomez [28] demonstrated in-column derivatization using phthalic anhydride (in acetonitrile) injection after the application of the AA sample (composed of standard His, Trp, Leu, Met, Thr, Ser, and Gly (also diluted in acetonitrile)), followed by electrophoresis. The differential migration velocities allowed the two zones to penetrate each other in the electric field. In a review on on-capillary derivatization, it was shown that the technique enhances sensitivity; in particular, the author focused on the methodologies that are used for reactant mixing in the capillary [29]. Ptolemy and Britz-McKibbin [30] reviewed the application of on-line sample preconcentration with chemical derivatization and reported its on-line use for derivatization. Following this, the authors described the in-capillary derivatization of phospho-AAs with 9-fluorenylmethyloxycarbonyl chloride (FMOC) using CE/UV analysis. In this method, the analytes were focused using a dynamic pH junction, and FMOC labeling was influenced by buffer pH, ionic strength, sample injection length, and dye concentration. The LODs achieved were ~0.1 µM [31].

Terabe's lab [32] suggested the use of a capillary with an internal diameter (ID) of 100 µm packed with 5-µm C18-coated particles (basic-pH compatible). The capillary was filled with a running buffer containing a derivatization reagent, *o*-phthalaldehyde (OPA)/β-mercaptoethanol (BME), and borate buffer (pH 10). After the electrokinetic injection of a mixture of biogenic amines (histamine, serotonin, tyramine, putrescine, and cadaverine) or AAs, only free biogenic amines entered the anodic site of the capillary and travel along the column, where the analytes reacted with OPA/BME and were separated, and were then detected by measuring absorbance at 340 nm. In a mixture consisting of these biogenic amines and 17 AAs, the biogenic amines were selectively separated and detected based on their absorbance at 340 nm. Similar, Koval *et al* [33] proposed the use of in-capillary derivatization with OPA/BME separated in an alkaline BGE using 2-hydroxypropyl-γ-CD as a CS. First, two hydrodynamic injections of an AA sample (negatively charged) were administered, followed by the injection of an OPA/BME mixture (neutral). Next, an electric field was applied to facilitate merging of

the two zones, derivatization, and separation of the derivatives. UV absorption detection at 230 nm yielded an LOD of 3 µM. Baseline resolution of D- and L-serine derivatives could be achieved in less than 10 min. The tertiary amino function of ofloxacin acyl chloride is charged in acidic and neutral media and can be used to label AAs. Amantadine (amino drug), tranexamic acid (nonproteinogenic AA), Gly, and Met have been analyzed by this method using CE/UV at 300 nm. The LODs ranged from 1.0–2.5 µM. An application of tranexamic acid analysis to plasma samples has been demonstrated earlier [34].

2.2. CE/UV without AA derivatization

Procedures for CE without derivatization have also been designed. Direct UV detection can be used for the determination of proteinogenic and non-proteinogenic AAs [35], which is a process that only works on standards. Indirect UV detection was performed for the identification of 3 phospho-AAs in phosvitin hydrolysate using AMP (with 2.5% Brij 35, pH 7.5), as UV-absorbing constituents of the BGE [36]. Zunic *et al* [37] reported the separation and quantification of 30 underivatized physiological AAs and peptides using *p*-aminosalicylic acid buffered with sodium carbonate at pH 10.2 (Fig. 2). The LODs ranged from 2 µM (Glu) to 20 µM (Gly). This analytical procedure was successfully performed for studying plasma and a macrophage culture supernatant, for which the sample preparation procedures only involved protein precipitation and dilution steps. The use of indirect UV detection (215 nm) of gabapentin (using Glu as an internal standard) in a bulk drug and capsules over a concentration range of 20–200 $\mu g \cdot mL^{-1}$ was developed as a pharmaceutical application. The analytes were separated using 5 mM 5-sulfosalicylic acid and 0.5 mM cetyltrimethylammonium bromide (CTAB) at pH 11 [38]. The CE conditions were improved for the separation of AAs in blood and/or plasma samples [39]. The method involved direct detection using a BGE containing disodium monophosphate for detection of compounds with absorbance in the UV region. Conversely, detection by indirect absorbance using *p*-amino salicylic acid facilitated the quantification of 30 underivatized physiological AAs and peptides. A preconcentration method combining large-sample injection based on a dynamic pH junction with a sweeping process was designed by Xu *et al* [40]. The sweeping process involved indirect UV detection (with 20 mM benzoic acid used as the chromophore) using 10 mM β-CD and 6% (v/v) methanol within the sample matrix (3 mM H_3PO_4). The LOD ranged from 0.85 µM (Glu) to 0.4 µM (Asp). AAs in human serum samples have been analyzed by adding a mixture of acetonitrile and methanol to precipitate proteins. Transient isotachophoresis (NaCl in the sample and HEPES in the BGE)

for the on-line preconcentration of high-salinity samples was used for 3-nitrotyrosine quantitation in atherosclerosis and other inflammatory diseases. The analyte was quantitated by UV detection using MEKC [41].

A simple 30 mM phosphate buffer (pH 9.25) for Arg, choline, and allantoin detection was described by Zhang *et al* [42], and UV absorbance was measured at 200 nm. Derivatization or indirect UV detection were not necessary. The LODs ranged from 2.0 µM (Arg) to 0.4 µM (choline). Lys, Met, Thr, and cystine were detected in fish flour using borate buffer. The LOD ranged from 20 µM (Cys-Cys) to 140 µM (Lys). The on-line sweeping preconcentration technique was combined with the coordination interactions between AAs and Cu^{2+} ions to improve CE/UV detection sensitivity and to analyze AAs in human saliva and green tea samples. The LOD for the seven separated AAs ranged from 0.1 µM (Leu) to 0.5 µM (Phe) [43]. Phe and Tyr in urine have been analyzed using pH junction preconcentration [44]. Before sample injection, a plug containing NH_4OH solution was injected, following which the urine sample was mixed in a 1:1 (v/v) ratio with a BGE (1 M formic acid (FA)). For analysis, 1.7 nL of 12.5% NH_4OH solution was injected first, followed by 196 nL of urine. The LODs were in the 0.01 µM range.

N-acyl derivatives of 2,6-diaminopimelic acid are considered possible inhibitors of N-succinyl-L,L-diaminopimelic acid desuccinylase. The amide function shows absorbance at 206 nm. Besides, these compounds can be easily detected using CZE or MEKC (with SDS or cetyl trimethyl amine bromide). Eight separation conditions were tested at acidic or basic pH to determine the degrees of purity of 13 mono-N-acyl derivatives of 2,6-diaminopimelic acid [45].

An interesting study was performed for comparing the efficacy of CE/UV (195 nm) and C^4D in determining the dissociation constants (pKa) of 20 proteogenic AAs using 22 buffers with pH ranging between 1.5 and 12.0. A short-end injection method was developed to reduce the effective length (8 cm) of the capillary. Consequently, the analysis time per AA was less than 2 h when the 22 buffers were used [46]. This study reported the pKa values of 11 AAs as well as the corresponding electrophoretic mobility rates deduced using eight buffers at different pH levels [47].

CE/UV with derivatization is easy to perform because the labeling reactions are identical to the ones used in liquid chromatography (LC). Although fluorescamine, FMOC, and dansyl chloride can be used, the sensitivity is observed to be limited to micromolar concentrations when these are used, and selectivity could be limited owing to the matrix effect. A study, possibly the most notable one on this topic, showed the effective separation of phospho-AAs

labeled with FMOC with an LOD of 0.1 µM [31]. Owing to their negative charge, phospho-AAs were effectively separated from non-phosphorylated AAs, and an LOD of 0.1 µM was achieved using capillary labeling along with a dynamic pH junction. The non-labeling methods are limited to the identification of aromatic AAs.

3. CE/C^4D

The use of C^4D for CE-based detection was proposed more than 20 years ago by Zeman *et al* [48] and Fracassi da Silva [49]. They suggested using two cylindrical electrodes placed at a distance of several millimeters around the capillary, forming a cylindrical capacitor. Electric conductivity of the electrolyte in the gap is measured by a function generator, which applies a sinusoidal signal to the first cylinder. The second cylinder is connected to a current-to-voltage converter. The rectified signal is proportional to the conductivity of the inner solution in the gap.

Kuban and Hauser [50] recently published a review article outlining the developments in C^4D for CE in 20 years. They mentioned that the effectiveness of this method is indicated by the fact that there were 1200 articles published on the topic, and that C^4D is a commercialized detection method; furthermore, they also mentioned that this equipment could be connected to all CE instruments owing to its compactness. An advantage of C^4D is that it can be used for the detection of all small inorganic ions and organic compounds. The LOD usually lies in the micromolar range. Table 2 summarizes the basic analytical conditions in the studies discussed in this chapter.

Coufal *et al* [51] were the first to propose the separation of 20 underivatized proteinogenic AAs using a simple BGE composed of 2.3 M acetic acid and 0.1% w/w hydroxyethylcellulose. The LOD of these AAs ranged between 9 µM (Lys) and 29 µM (Asp). The separation was realized in 32 min. The results could be improved using 6 mM lactic acid as the BGE. This modification helped achieve LODs of 0.2 µM for Arg and 0.4 µM for His, while the LODs ranged from 0.5 to 50 µM for the other nine AAs tested. The basic reaction environment at pH 10–11 established using a mixture of 2-amino-2-methyl-1-propanol and CAPS facilitated the separation of the 20 AAs in less than 9 min, where only Trp, Leu, Met, and Gln were observed to comigrate [52]. Three AAs and four monosaccharides were also separated using a basic buffer (10 mM NaOH, 4.5 mM Na_2HPO_4, 1 mM CTAB, pH > 12) [53].

Samcova and Tuma [54] reported the separation of 18 proteinogenic AAs, creatinine, 1-Me-His, 3-Me-His, Orn, and citrulline. Only the two Me-His comigrated with the BGE

containing 1.7 M acetic acid and 0.1% hydroxyethylcellulose (HEC); however, the separation time was 48 min, which was considerably high. This separation protocol was applied on plasma samples (deproteinized using acetone/water at 1:1 ratio). The LODs reported ranged from 4.3 µM (Arg) to 42.9 µM (Cys). 3-Me-His, 1-Me-His, and His were resolved using a BGE containing ammonia (0.5 M acetic acid, 0.1 % HEC, 20 mM NH_4OH); however, in this case, apart from the 19 proteinogenic AAs, no other components were separated [55].

Twenty-eight AAs were analyzed using a capillary with an effective length of 18 cm, and 14 of them were completely resolved. The short separation pathway decreased the separation time of AAs (below 6.5 min), and the LODs also reduced to a submicromolar range (Lys: 0.1 µM, Asp: 1.7 µM) [56]. Pormsila *et al* [57] reported the quantitation of carnitine and six acylcarnitines in plasma and urine samples using CE/C^4D with 0.5 M acetic acid and 0.05% Tween 20. In a notable study, choline, creatinine, Orn, Lys, Arg, His, Gly, Ala, Val, Ile, Leu, Ser, Thr, Gln, Glu, Phe, Tyr, and Pro were separated in a dried blood spot (DBS) after elution using 20 µL of methanol/water (1:1, v/v) in a BGE containing 1.6 M acetic acid, 1 mM (+)-(18-crown-6)-2,3,11,12-tetracarboxylic acid (18C6H4), and 0.1 % (v/v) Tween 20. Phe concentration was detected to be 61.3 µM [58]. Fig. 3 shows the electropherograms obtained for DBS from five patients.

AAs from ocean water samples have also been quantitated, taking into account the challenges posed by the high salinity of water. In the absence of sample dilution, 5 M acetic acid with 10 mM 18C6H4 and 10% acetonitrile were shown to be necessary to separate β-Ala, His, γ-aminobutyric acid (GABA), Gly, Ala, 2-aminoisobutyric acid, Val, Ser, isovaline (with the isomers of Val not separated), Leu, Glu, and Asp [59].

Chiral separation was also performed using 18C6H4 in a BGE containing 10 mM citric acid/Tris at pH 2.2. An LOD of 2.5 to 20 µM was achieved for DL-Arg, DL-Val, DL-Ser, DL-Phe, DL-Tyr, and DL-Asp, and migration durations less than 28 min were obtained [60]. Of note, *cis*/*trans*-amines were also effectively separated using a cyclic ether [61]. Elsewhere, DL-Asp and DL-Glu were enantioseparated using 5 mM vancomycin at pH 7.35 in a BGE containing 10 mM Tris, 4.4 mM maleic acid, and 0.03 mM CTAB. Experiments in which Tween 20 was used have also been reported [62].

Samples used in neuroscience studies, such as microdialysates, have also been analyzed using C^4D; however, it is necessary to preconcentrate them owing to the lack of sensitivity in this detection method. Microdialysates of periaqueductal gray matter were preconcentrated by filling 25% of the capillary with the microdialysate sample diluted in acetonitrile (1:3, v/v) [63], followed by focusing of the ions in the sample using an electric field while simultaneously

forcing the acetonitrile zone out of the capillary by increasing the pressure in the cathodic vial. The researchers could easily identify GABA, Glu, and Gly among several other components. When a microdialysate was used, several ions from Ringer's perfusate were visible in the electropherograms. The concentrations of these AAs in the periaqueductal gray matter of rats were monitored after treatment with 1% m/v carrageenan for induction of hyperalgesia, followed by administration of 300 $mg \cdot kg^{-1}$ paracetamol after 60 min of dialysis. The LODs improved to 29 nM (GABA and Gly) and 37 nM (Glu) using this stacking method. Asp was not quantitated [64]. Val, Ile, and Leu were also quantitated in a microdialysate using 2.1 M acetic acid in 20% (v/v) MeOH + 1% (v/v) INST (a coating solution used for the elimination of EOF in CE [Biotaq, Gaithersburg, USA]). The microdialysates were diluted four-fold with acetonitrile acidified using 0.01 M HCl to attain the best sensitivity and resolution. The LOD for these AAs was 0.1 µM [65]. This coating method has been compared to a covalent one implemented after a reaction with poly(acrylamide-co-(3-acrylamidopropyl)trimethylammonium chloride) containing 1% m/m of (3-acrylamidopropyl) trimethylammonium chloride. This coating reversed the flow (direct polarity is maintained) and yielded the best results at 14.4 cm effective length during the high-performance separation of Ala, Val, Ile, Leu, Ser, Gln, and Glu from rat plasma in less than 5 min with a buffer containing 3.2 M acetic acid and 20% methanol [66]. Food chemical analyses were also performed using this method. Lys, Ala, Pro Glu, and Asp in royal jelly supplements were quantitated using 2 M lactic acid as the BGE [67]. Taurine, choline, and niacin were separated in two capillaries, each containing a buffer selective for taurine (150 mM Tris/lactic acid, pH 8.96) and another selective for choline and niacin (150 mM Tris/acetic acid, pH 9.5). The contents of these compounds in energy drinks were quantitated [68].

Theoretical studies have also been performed using such detection methods. The effective mobility rates of free AA^{+} and AA^{2+} have been determined using CZE with a laboratory-made contactless conductivity detector and a double detection cell (1 cm and 1.442 cm distance between the two detection cells). The acidic BGE (chloroacetic acid lithium hydroxide mixtures at pH ranging between 2.0 and 3.2) at constant equal ionic strength (10 mM) allowed the measurement of the effective mobility of the cations. The data were fitted to the regression functions depending on the pH of the electrolytes. pKa values were obtained using the Onsager theory and McInnes approximation [69]. A similar study was conducted at a lower acidic pH (1.6–2.6, to ensure a higher degree of AA protonation), with poly(vinyl alcohol) added to the BGE to prevent adsorption on the capillary wall [70].

Table 2 shows that 0.5–4.0 M acetic acid is a common buffer that can be supplemented with 18C6H4 (as a CS) or hydroxycellulose for better stacking. For most applications to AAs, this is the simplest and most efficient detection method for AA quantitation at a submicromolar concentration. C^4D is considered a universal detection method for AA quantitation using CE, either in an acidic or basic BGE. This method may soon be used by companies employing CE for routine clinical applications. This is primarily because in contrast to CE/UV, this method does not require derivatization, and sensitivity is sufficient for the clinical analyses of AAs.

4. Developments in CE/fluorescence

The use of fluorescence detection of AAs in conjunction with chromatographic and electrophoretic separation procedures was first reported in the 1980s [15], and has since been reported in multiple original articles [71,72]. Marina and Castro-Puyana provided an overview of the derivatization methods used for CE applications by reviewing previous reports [73]. Unfortunately, most AAs do not emit fluorescence intrinsically. Similar to the issue experience with UV absorption, researchers have attempted to develop efficient methods for labeling these molecules for fluorescence detection. The reports on derivatization relevant for UV detection can be consulted herein [11,12]; these extensive studies have also been reviewed recently [74]. LIF- or light-emitting diode (LED)-induced fluorescence (LEDIF) detection is limited by the wavelengths of lasers or LEDs available and the restricted number of fluorophores that allow the excitation of an AA at different available wavelengths after derivatization. Table 3 outlines the basic analytical conditions in the articles that are reviewed in this chapter.

4.1. Native fluorescence

Two notable reviews have been published that have showcased the developments in native UV fluorescence detectors and discussed multiple articles on aromatic-AA separation procedures [75,76]. The use of native fluorescence to detect aromatic AAs is no longer restricted to owners of expensive UV lasers. Chang *et al* [77] reported the application of a low-cost diode frequency quadrupled pulsed laser with emission at 266 nm. Bayle *et al* [78] detailed the determination of Tyr and Trp in cerebrospinal fluid (CSF) after 1:20 dilution in water using a pulsed laser (Fig. 4). Trp was detected at a concentration of 0.15 nM, indicating that the process was 105-fold more sensitive than UV absorbance. Zhang and Sweedler described an improved inexpensive "turnkey" NeCu laser operating at 248.6 nm and interfaced with a sheath flow-based CE system; this setup performed similarly to an expensive large-frame frequency-

doubled Ar ion laser at 257 nm. The LODs for serotonin, dopamine, and Trp (27 nM, and 8 µM, and 63 nM, respectively) were within the range of those achieved using a frequency-doubled Ar ion laser at 257 nm (21 nM, 8 µM, and 2 nM, respectively) [79].

A 266-nm diode-pumped laser with a 10 ps duration pulse and a repetition rate of 40 MHz was used with a time-correlated single-photon counting device to detect DL-Trp. The chiral separation of DL-Trp was performed using CD, sulfated CD, and highly sulfated γ-CD at different pH values. Highly sulfated γ-CD (0.35 %, pH 2.5) was found to be the most effective CS. The LOD for Trp was 65 pM [80]. Beyreiss *et al* [81] have described a similar UV-LIF detector based on lifetime detection. The abovementioned 266-nm laser was used for excitation, and the process was also coupled with time-correlated single-photon counting detection. The average fluorescence lifetimes were independently determined for Trp, Ser, propranolol, and 3-phenoxy-1,2-propanediol. Using lifetime measurements, a better discrimination of background fluorescence and a better signal-to-noise (S/N) ratio were obtained. These methods can be applied to protein analysis.

In an interesting attempt first made by Park *et al* [82], they suggested the use of a wavelength-resolved electropherogram of AAs with single-cell injection of an individual cerebral ganglion neuron. The natively fluorescent AAs and biogenic amines were detected after excitation with a 257-nm Ar laser, and fluorescence detection was implemented using a charge-coupled device (CCD) spectrometer. The resulting fluorescence spectrum ranged between 260 and 710 nm. This UV-LIF detector could detect Trp, Tyr, Phe, and dopamine in an individually injected neuron. Conversely, in a standard solution of tryptamine, serotonin, norepinephrine, octopamine, N-acetylserotonin, dopamine, epinephrine, Trp, Tyr, Phe, and 3,4-dihydroxyphenylalanine administered by electrokinetic injection, the LOD varied from 3.9 µM for norepinephrine to 4.8 nM for tryptamine.

Nanomolar LODs were achieved using a capillary containing a bubble cell for detection and a pulsed 266-nm LIF detector, which increased the sensitivity by a factor of 3 for Trp and 5 for atenolol. The increase was limited by photodegradation, which could be attenuated by adjusting the laser power in the bubble cell [83]. The values last reported were well below those mentioned in a previous report on UV-LIF detection [78] or Hg-lamp fluorescence detection [84].

When a 224-nm pulsed He-Ag metal vapor laser (low-cost but low-lifetime laser) or a 264-nm expensive Ar ion laser was used, detection at variable emission wavelengths allowed the quantification of Trp, Tyr, and their related metabolites. The optimal detection wavelength

for these analytes was determined by scanning the fluorescence emission using an automated CCD device. The LOD obtained using the wavelength-resolved system was 1 nM for serotonin and 88 nM for Tyr [85]. The LODs of these aromatic AAs and amines could be improved using a deep UV laser and two-photon excitation to quantitate Phe, Tyr, and Trp. The LODs of these AAs added as residues in a polypeptide chain reached 15 amol [86].

As the optical gating of fluorophore-labeled analytes facilitates the use of shorter injection lengths and rapid separation procedures and offers the highest separation efficiency, a UV-LED array (900 mW, 365 nm) was designed [87]. On-line photolytic injection of caged 5-carboxyfluorescein-bis-(5-carboxymethoxy-2-nitrobenzyl)-ether-alanine-carboxamide-succinimidyl ester derivatives was performed. Photolytic optical gating involves the use of a caged fluorophore with a low fluorescence quantum yield prior to photolysis by UV radiation. In this method, the samples were injected upon transient exposure to UV radiation via photolytic uncaging of the fluorophore to generate highly fluorescent sample plugs. Photolytic optical gating offered good sensitivity by providing a low-background signal and reduced noise. The uncaged derivatives were detected at 496 nm (using an Ar laser). Studies on the applications of this technique with labeled citrulline and Arg have been published, wherein a nanomolar LOD was achieved [87].

Several studies published prior to the time period considered in this review for UV-LIF experiments used considerably expensive UV lasers. These developments may be considered "dated" at present; however, they reflect interesting approaches that facilitated the quantitation of aromatic AAs and amines in neurochemical applications. Presently, some researchers use a 266-nm pulsed laser to detect these AAs. The LOD can be considerably improved using an efficient stacking process, as proposed by Hsieh and Chang [88]. The authors in this study described a pH and viscosity stacking process between a sample zone at acidic pH and a viscous separation buffer at higher or lower pH, using which they achieved an LOD of 0.3 nM for tryptamine and epinephrine.

Photodegradation serves as a limitation in this type of pulsed diode laser for aromatic-AA detection, which limits sensitivity [89] and prevents the construction of linear quantitative curves [90].

266-nm pulsed lasers are readily available and are useful for the determination of AAs with native fluorescence using UV-LIF detection, with LODs achieved in the nanomolar range (for Trp, Tyr, and their metabolites). Serotonin can be detected in microdialysates using a highly efficient stacking process in CE. While UV-LIF detection has shown considerable promise, it

remains a relatively expensive process (€10000 for a laser), and the use of pulsed lasers limits sensitivity owing to photodegradation. The attempts to use a time-correlated single-photon counting device have also been promising; however, since only laboratory-made detectors were used, the process faced certain limitations. Therefore, CE UV-LIF is a simple technique for the quantitation of highly fluorescent AAs and their derivatives present at nanomolar concentrations.

4.2. Visible LIF or LEDIF detection

Using visible-range lasers or LEDs, AAs can be detected after a derivatization step. Different applications have been described using 2,3-naphthalene dialdehyde (NDA). This fluorogenic dye has largely been employed in neurochemical applications, where several technical advances have been made that are relevant to the topic at hand.

4.2.1. NDA

The use of NDA, a fluorogenic dye specific for primary amines, was extensively described by Rammouz *et al* [91]. It has been used in multiple studies on the quantitation of AAs in microdialysates for neurochemical applications, as NDA reacts rapidly with the primary amine in AAs in the presence of KCN. A 457-nm Ar laser was first used to excite NDA derivatives of AAs in hydrolysates of peptides and proteins [92]. Ar lasers are more stable than HeCd lasers (442 nm), even though 457 nm is not the optimal wavelength for detection of the obtained 1-cyano-2-benz[f]isoindole derivatives (440, 420, and 405 nm are the optimal excitation wavelengths). Robert *et al* demonstrated the detection of dopamine and norepinephrine present at nanomolar concentrations in microdialysates, and monitored their concentrations in rat brain [93]. Conversely, Glu, Asp, and phosphoethanolamine [94] were quantitated by adding NDA to a well-adapted reactor for on-line labeling of AAs in microdialysates. Six neuroactive compounds (Gly, Glu, Asp, GABA, dopamine, and noradrenaline) were labeled with NDA, separated, and quantitated using MEKC and lithium dodecyl sulfate, with an LOD lower than that achieved with SDS [95]. In the mentioned study, the method used was compared to HPLC fluorescence analysis of NDA derivatives. Better results were obtained with MEKC/LIF (HeCd laser, 442 nm). Moreover, the authors reported differences in derivatization rates (dopamine is labeled five-fold more rapidly than Gly), and molar UV absorption coefficients (Gly has an absorbance 2.5-fold greater than that of Asp) of

the NDA derivatives. They highlighted the fact that all NDA derivatives do not have the same absorption maximum (λ_{max}); for example, the λ_{max} value for Lys is 460 nm, while it is 442 nm for the other AAs studied.

At present, it is difficult to purchase HeCd lasers as they are manufactured by a limited number of suppliers. Therefore, it is necessary to use other light sources. In this respect, LED or mercury lamps are suitable as excitation sources. Melanson and Lucy [96] demonstrated the analysis of NDA derivatives using an LED (405 nm) source expected to have a lifetime of 50,000 h, which was 10-fold greater than that of Ar or HeCd lasers. Moreover, their costs are considerably lower. With excitation at 457 nm, the LODs achieved were reported to be 40-fold higher than those achieved using the 442-nm HeCd laser. Using a similar LED source (405 nm) and an electrolyte containing poly(ethylene oxide) (PEO) and CTAB, Chen *et al* [97] achieved an LOD ranging from 9.5 nM (GABA) to 50.5 nM (Thr) for a mixture of 14 AAs or primary amines. In the presence of CTAB and acetonitrile, the adsorption of PEO on the capillary wall was suppressed, which led to the formation of a rapid and more reproducible EOF and enabled separation in less than 4 min. Branched-chain AA determination in ascites was performed using PEO-containing buffers (1.5% m/v PEO) with 5-s gravimetric injection (height difference: 30 cm), and an LOD of 10 nM was achieved [98]. The reaction with NDA and CE of NDA derivatives (excited using 405-nm LED) using PEO 8,000,000 improved the separation, as stated by Hsieh and Chang [99]. The use of PEO 8,000,000 for increasing the resolution and speed could be optimized by varying capillary length, separation voltage, buffer composition, pH, and ionic strength, and a low matrix effect was observed when this polymer was used. Moreover, intensive sample stacking could be employed. NDA has also been utilized for Arg, monomethylarginine, asymmetric dimethylarginine (ADMA), and symmetric dimethylarginine (SDMA) determination by CE as well as glass microchip CE with a 14-cm separation channel [99]. In both cases, 5 mM sulfobutylether-β-CD was added.

In addition, NDA was used with a fluorescence detector equipped with a 100-W high-pressure mercury lamp for excitation radiation, an excitation filter of 400–490 nm, and a dichroic mirror at 510 nm to detect histamine and His. The derivatization conditions and separation parameters, including pH and concentration, were optimized. The optimal derivatization reaction was performed using 1.0 mM NDA and 20 mM NaCN (pH 9.1) for 15 min, while the separation of NDA-labeled histamine and His could be achieved in less than 200 s using 40 mM phosphate buffer (pH 5.8). The LODs for histamine and His were 5.5 and 3.8 nM, respectively. The method was successfully applied to the analysis of these molecules in

P815 mastocytoma cells and in beer samples [100]. The same method was also applied successfully for the baseline separation of phosphothreonine, phosphotyrosine, and phosphoserine (LOD = 7.0, 5.6, and 7.2 nM, respectively) within 180 s and for validation using a β-casein hydrolysate [101].

In-capillary derivatization electrophoresis using electrophoretically mediated microanalysis (EMMA) is a useful technique for derivatization with NDA/NaCN. In EMMA, reactants are injected in an ascending order corresponding to their electrophoretic mobility rates. The reactants migrating most rapidly merge with the slowly migrating reactants [102]. Fig. 5A shows the injection/derivatization scheme. The separation of standard AAs is illustrated in Fig. 5B. Plasma and culture medium samples are subjected to protein precipitation by the addition of a mixture of MeOH and propanoic acid (4:1) at 100-fold dilution. EMMA has been applied to metabolomic studies on human embryos to find a correlation between the developmental potential of an embryo and AA turnover. Optimized EMMA was compared to the transverse diffusion of laminar flow profiles [103].

NDA and BME were used in a post-column reactor in coaxial-gap mode, where a thin polyimide sleeve with a length of 10 mm was used to align the separation and reaction capillaries with a 20-μm gap. Owing to gravitational pull, NDA and BME were transferred into the reaction capillary through a 20-μm annulus between the separation and reaction capillaries, with a 5-mm reaction distance from the annulus to the LIF detector (473 nm). The liquid level difference between the NDA/BME solution and outlet buffer as well as the annulus dimensions and reaction distance were adjusted, which helped achieve an LOD ranging from 80 to 1000 nM with a separation efficiency ~1.4×10^5 theoretical plates. This post-column reactor was optimized and yielded better results (1000-fold more sensitive) when the flow rate of the derivatization solution and the reaction distance were increased [104]. The primary issue with NDA derivatization using BME is the instability of the obtained fluorescent compounds, which become non-fluorescent [105].

An in-column fiber-optic LIF detector was evaluated using a 457-nm diode-laser. An optical fiber was inserted into the capillary and positioned in the detection window. Fluorescence emission was recorded using a 40× microscope objective (focused on a spatial filter) and passed through a band pass filter; the photomultiplier tube (PMT) measured the obtained signal. NDA-derivatized D-penicillamine was quantified with an LOD of 0.8 nM [106]. One of the most important limitations of this optical detection scheme is the photodegradation of the compounds of interest owing to irradiation for a longer period than that

required in a conventional detector. A similar optical arrangement was used for AAs labeled off-line with NDA or FITC, using violet (425 nm) and blue (480 nm) LEDs (a single LED has the ability to emit at these two wavelengths). AAs labeled with NDA or FITC were monitored, and the LODs achieved ranged from 17 to 23 nM for NDA derivatives and from 8 to 12 nM for FITC derivatives [107].

A 25-mW diode laser (well adapted for such applications) was used at 445 nm with a 25 µm ID capillary (effective length: 20 cm) to achieve the rapid separation of Glu and Asp labeled with NDA. The separation was performed in a highly diluted buffer (10 mM sodium phosphate pH 7.5) to ensure migration times between 51 and 56 s with resolution above 2 and an LOD of ~300 nM (100 picomole/planarian). This approach has been tested for quantitation of these AAs in *Planaria*, which are free-living flatworms serving as a model organism for studies on primitive central nervous systems [108].

The rapid kinetics of the reaction with NDA/CN- makes CE/LIF suitable for the detection of AAs (except Pro) in the nanomolar range. The dye is fluorogenic, and because excitation can be achieved using an LED with emission at 405 nm, LEDIF detection is selective. EMMA can help achieve efficient separation, and even with an unadapted 488-nm laser (available with the majority of LIF detectors), nanomolar concentrations can be detected.

4.2.2. Other aromatic dialdehydes (3-(4-carboxy-benzoyl)-2-quinolinecarboxaldehyde [CBQCA], 3-(2-furoyl)quinoline-2-carboxaldehyde [FQ], and OPA)

There are other compounds that act as fluorogenic dyes specific for primary amines. A pioneering study on AAs was performed by Liu *et al* [109] using CE/LIF at 488 nm (with an Ar laser), in which they synthesized CBQCA. In presence of KCN, the reagent reacted with primary amines to generate highly fluorescent isoindole derivatives, which could be excited using the classic 488-nm Ar laser (as well as a 480-nm LED). Additionally, the isoindole nucleus contained a negatively charged carboxylic function. Bergquist *et al* [72] reported the use of CBQCA for the analysis of ten AAs (Arg, Gln, Thr, Val, GABA, Ser, Ala, Gly, Glu, and Asp) in CSF. The separation procedures were performed at pH > 9. The CBQCA derivatives should have a single negative charge for Lys and Arg, double negative charge for neutral AAs, and triple negative charge for acidic AAs (Asp and Glu). We recently demonstrated that, when derivatives (synthetized in D_2O) are analyzed using negative-ion electrospray ionization (ESI) high-resolution MS (HRMS), the carboxylate function of the AA is eliminated, and Trp is

considerably difficult to identify owing to the decrease in fluorescence sensitivity (100-fold less fluorescence than that emitted by Leu). Possibly, intramolecular quenching occurs due to the proximity of the indole and isoindole nucleus of the Trp to quinolone moieties [109]. Lastly, we compared the feasibility of quantifying Trp in mouse plasma using CE/LEDIF (480 nm) with CBQCA derivatization and using CE/C^4D without derivatization. Quantitation was only feasible using C^4D detection [110]. Boulat *et al* used CBQCA with a greater number of AAs and amines (29 compounds) [111] and achieved remarkable separation in less than 55 min using MEKC in the presence of SDS and γ-cyclodextrin (γ-CD). The S-S dimer of homocysteine (Hcy) could be detected; however, neither free Cys nor free Hcy could be detected (owing to the intramolecular reaction of the thiol group with the CBQCA nucleus instead of CN^-), and neither could Trp be detected. Arriaga *et al* showed that the Arg derivative shows a good fluorescence yield allowing detection even at zeptomolar levels; however, the authors were unable to label this AA when it was present at levels less than 0.1 μM [112]. In addition, CBQCA was used to detect considerably low levels of AAs in a study where the analytical parameters, including sodium borate concentration, buffer pH, operating voltage, and operating temperature, were extensively monitored. The rate of derivatization, stability of the labeled AAs, and AA quantitation varied for each amine. The authors claimed to have detected these derivatives at 17 pM (Met) to 383 pM (Glu). Interestingly, they could detect Pro, the only secondary-amine-containing AA, which would not have been labeled. A bacterial AA in a chemically defined medium was successfully detected using this method [113]. Recently, it was shown that CBQCA could be used for AA detection in mouse tear fluid (70 ± 25 nL, collected via phenol red thread). The levels of Arg, Ala, Asp, Glu, His, and taurine were in the micromolar range [114].

FQ is another fluorogenic dye that reacts with primary amines (in the presence of CN^- ions) and can be excited at 488 nm. It has been used for the detection of AAs. Although it is considerably similar to CBQCA, it is uncharged. Ehlen *et al* [115] used factorial analysis as an efficient technique to correlate the variables of the separation conditions (pH and concentration of borate buffer, β-CD, and SDS) and to optimize the analysis, since these conditions depend on analytes, sample composition, and the sample matrix. Nine buffering conditions were studied, and microdialysates collected from near the suprachiasmatic nucleus of male hamsters were analyzed. An LOD of 8 nM was achieved for GABA, 110 nM for Glu, and 25 nM for Asp. FQ was also utilized for the in-capillary derivatization of AAs present in pharmaceutical formulations [116]. The development of other quinolone carboxaldehydes has been performed.

For example, 3-(4-bromobenzoyl)-2-quinolinecarboxaldehyde was synthesized, and its derivatization was optimized (pH 8, 55 °C, 50 min, 30:1 reagent/amine, 15:1 KCN/amine) using an optimal running buffer containing 120 mM boric acid (pH 9.1), 38.5 mM SDS, and 19% acetonitrile (v/v) with a 75 µm ID 60.5/50 cm capillary and a 22.5-kV 488-nm laser. Samples containing Asn, His, Met, Gln (unseparated), Ser, Thr, Tyr, Gly, Glu, Asp, Ala, taurine, GABA, norepinephrine, Val, dopamine, Ile, Leu, Phe, and Arg were analyzed. The LODs for AAs ranged from 0.65–5.00 nM, while for catecholamines, the LODs ranged from 58–73 nM. Human plasma and vitreous perfusate samples treated or untreated with medication after intraocular hypertension were studied [116]. Another quinolone carboxaldehyde, 3-(4-chlorobenzoyl)-2-quinolinecarboxaldehyde, was reported to react in the same manner. It has been used in CE/LIF (488 nm) experiments to detect AAs and catecholamines in HEK293 and PC12 cell samples under optimized MEKC conditions. LODs ranging from 1.4 to 100 nM were achieved, which was twice higher than that achieved using the brominated compound, and had a nanomolar range (barring the LODs for norepinephrine and dopamine: 60 nM with 3-(4-bromobenzoyl)-2-quinolinecarboxaldehyde) [117].

OPA/BME derivatives are commonly used in HPLC fluorescence assays for amine detection [118]. If the derivatives are not adequately stable, the reaction is rapid and can be performed to label primary amines on-line at the output of a chromatographic column. Nonetheless, OPA has rarely been used in CE owing to the lack of an available laser wavelength. HeCd (325 nm) could be used, but it is expensive and has a short lifetime. However, a 100-mW 365-nm UV LED (expensive, with short lifetime) was used effectively to excite Glu and Asp OPA derivatives (which are formed off-line), and an LOD of 47 nM was attained for each [119]. The authors described an on-line labeling method that involved the introduction of both the sample and derivatization reagents (OPA/BME) into a mixing tee at a rate of 1.2 µL/min using a syringe pump. The outlet of the reaction tee was connected to a 100 µm ID capillary. The reaction time (dependent on the length, flow rate, and capillary ID) was 70 s. The reaction capillary was interfaced with the separation capillary (25 µm ID, 8 cm effective length) through a flow-gating interface, where a crossflow (1 mL/min) of separation buffer was continuously applied across the gap to prevent analyte transfer between the two capillaries. The sample was injected into the separation capillary via temporary disruption of the crossflow; meanwhile the separation capillary was maintained at constant high voltage. The reported LOD was approximately 7 nM for these two AAs (Fig. 6). The use of a laser-drilled capillary has been described as well, where an aperture created using laser ablation was used

for mixing OPA/BME with free Lys Arg, Glu, and Asp separated by CE; micromolar LODs were achieved [120]. 3-mercaptopropionic acid, N-acetyl-l-cysteine (NAC), and N-isobutyryl-l-cysteine were used instead of BME for OPA in-column derivatization, as these form more stable derivatives. In addition, NAC and N-isobutyryl-l-cysteine have an asymmetric carbon, which forms diastereoisomers after derivatization of a mixture of enantiomers, which can be separated using CE. The use of NAC and γ-CD enabled the most effective indirect enantioseparation of 16 AAs with resolution above 2.6. In this case, the derivatization occurred within the capillary through "sandwich injection": the derivatization solution was injected sequentially before and after the sample [121]. The selective enrichment of aminothiols labeled with OPA and BME using Tween 20-capped gold nanoparticles prior to CE-LIF analysis (with the instrument equipped with a 355-nm diode-pumped solid-state laser) yielded an LOD of 4 nM for Hcy, which was equivalent to an eleven-fold improvement in sensitivity [122].

2-((5-fluoresceinyl)aminocarbonyl)ethyl mercaptan, which emits fluorescence at 488 nm, is also used along with OPA for AA detection; 2-((5-fluoresceinyl)aminocarbonyl)ethyl mercaptan replaces the conventional thiol used for OPA derivatization. The presence of Tris(2-carboxyethyl)phosphine prevents thiol loss resulting from S-S bridge formation. Owing to the reactivity of OPA, the reaction is considerably rapid (<30 s). The LODs achieved for dopamine, norepinephrine, Glu, and Asp were shown to be below 0.5 nM [123].

OPA is highly suitable for LIF detection when on-line labeling can be performed. However, the requirement of a UV light source limits its use. CBQCA is suitable for the detection of most AAs and their metabolites (except Pro and Trp); the sensitivity achieved is in the nanomolar range, and the separation procedures are effective at resolving most AAs. Although it is more expensive than NDA, it can be excited at 488 nm, which is useful because most instruments available exhibit emission at this wavelength.

4.2.3. Fluorescein-based dyes

Fluorescein-based dyes are widely used in studies with CE/LIF experiments. For example, FITC has been used for almost 50 years to label the amino functions of AAs and proteins [124]. These dyes are used because they have a high fluorescence yield (significantly higher than that of previously described reagents). Cheng and Dovichi were the first to use these in CE/LIF studies [125]. These have been used in several technical advances in fluorescence detectors.

4.2.3.1. Fluorescence detector optimization using an FITC-labeled AA

Jong and Lucy [126] were pioneers in the designing of LEDIF experiments using FITC derivatives. A 470-nm LED was focused on a capillary with a lens obtained from a discarded DVD-ROM. The fluorescence was recorded at 45° through an ocular obtained from a pen microscope and was passed through a band-pass filter to a photodiode. Using this simple device, the LOD obtained (which was above the micromolar range) for FITC-labeled AAs was higher than that obtained using an LIF detector [127]. Understandably, the device in question was less sensitive than a commercial instrument; however, the estimated cost of the detector was claimed to be approximately $50. To enhance light transmission in a LEDIF detector, glycerol was used to optimize i) irradiation using a 470-nm LED in the optic fiber illuminating the capillary and ii) measurement of fluorescence between the capillary and the collecting optical fiber. Glycerol was employed to reduce the refractive index discontinuities in the silica/air interfaces. This led to a 2.8-fold improvement in the S/N ratio. The LOD for FITC-labeled AAs (Lys, Trp, and Phe) was between 10.9 and 4.8 nM [128]. Of note, glycerol is relatively volatile, which may have affected the stability of detection.

The construction of a miniaturized liquid core waveguide-CE system and a LEDIF system (470 nm) was reported [129]. The system consisted of a Teflon AF-coated silica capillary, which served both as the separation channel and as a transversely illuminated liquid core waveguide. This device took advantage of flow injection-based split-flow sample introduction through a falling-drop interface. The Teflon AF separation capillary was fixed on a glass slide. The inlet reservoir also served as the falling-drop interface for coupling with the flow injection system. A 478-nm LED served as an excitation source near the outlet of the capillary. At this outlet, a buffer reservoir containing a large-core optical fiber aligned with the capillary channelized the emitted fluorescence (trapped in the Teflon AF capillary) into a PMT. No focusing arrangement was employed. AAs labeled using FITC have also been studied. A total of 144 samples/h could be analyzed with precision using the continuous flow injection of a series of samples (30 µL each). Baseline separation was achieved for FITC-labeled Arg, Phe, and Gly. The LOD ranged from 1.3 µM (Arg) to 1.9 µM (Phe, Gly). Kostal *et al* [130] described a similar miniaturized fluorimetric detection cell, where the excitation wavelength was 488 nm and a compact CCD spectrometer was connected to the detection optical fiber for detecting the fluorescence signal. This detection cell was used with off-line labeling (with FITC and iodoacetamidofluorescein [IAF]) to detect fluorescein-labeled AAs in plasma. The levels measured in healthy volunteers were compared to those measured in patients with inherited

metabolic disorders. The LODs were better than those achieved using a conventional LIF detector.

Using a confocal microscope, Zhu *et al* [131] attempted to determine why the best LIF sensitivity is obtained in CE when the laser does not illuminate the capillary along the axis used in fluorescence collection. A shift of 20 µm from the axis of the capillary helped reduce the noise and increase the S/N ratio (×8.3). Separation of FITC-labeled Arg, Phe, Gly, and Glu at 100 pM was presented. Additionally, a compact handheld quasi-confocal LIF detector (9.1 × 6.2 × 4.1 cm, weighing 350 g) with a 450-nm laser diode was also constructed. Arg, Phe, Ala, Gly, Glu, and Asp labeled with FITC were separated with an LOD of approximately 0.4 nM [132], which indicated good sensitivity.

4.2.3.2. The use of FITC in CE/fluorescence

Even though FITC is largely used for testing new detectors and instrument arrangements, its reaction with an amine aqueous medium generates a high number of impurities that are responsible for numerous parasitic peaks in electropherograms. FITC is not fluorogenic, and its peaks are considerably high compared to those of AAs owing to its high abundance in the reaction mixture, along with that of its degradation products. However, as its derivatives are highly fluorescent, the sample obtained after derivatization can be diluted, and adequate separation can be achieved with considerably high sensitivity. The fluorescein nucleus can be excited using a 488-nm Ar laser, with its fluorescence yield depending strongly on the pH of the separation buffer [133], which must be above 9.0–9.6 (pKa of the phenolic function) to generate the dianion form [134]. Lalljie and Sandra [135] stated that it is difficult to label AAs at a concentration below 0.1 µM if quantitative results are to be obtained. Therefore, FITC finds application in several biochemical studies. For example, it has been applied to AA determination in cerebrospinal fluid [136] and wine [137], where AAs are present at concentrations above the micromolar range, but the samples are diluted 1000- or 2000-fold prior to injection to obtain the best resolution and the lowest influence of the sample matrix on the separation process. Compared to UV absorption, the detection process is significantly more selective [137]. FITC has been used widely for AA quantitation (at concentrations above 0.1 µM) [138]; however, its reaction time is high at ambient temperature. Zinellu *et al* [139] devised a 20-min derivatization procedure at 100 °C using a 200 mM Na_2HPO_4 (pH 9.5) buffer; 12-min AA separation procedures were performed using an 18 mM phosphate running buffer (pH 11.6), and several biological samples (cultured cells, CSF, saliva, and vitreous humor) were studied

to determine the limits of quantitation (approximately 0.2 μM) (S/N ratio = 10). In addition to these developments with FITC, the migration time reproducibility rates of PITC-, FITC-, and tetramethyl rhodamine isothiocyanate–labeled AAs have been investigated. Several methods to improve the procedures have also been suggested [140].

Tan *et al* [98] described a combined detection system based on C^4D and fluorescent detection for CE in a common cell. A blue LED (470 nm) served as the excitation source, and an optical fiber was employed to measure fluorescence. Inorganic ions (K^+, Li^+, Mg^{2+}, Ca^{2+}, and Ba^{2+}), FITC-labeled AAs (Trp, Phe, Lys, and Gly), and a small peptide were separated and detected using the combined system, with LODs ranging from 0.8 to 2.5 μM for AAs. Electropherograms with good resolution were presented by superimposing the signals of the conductometer for inorganics and the fluorometer for AAs, both in the same run.

A capillary array electrophoresis system with a rotary confocal fluorescence scanner has been described [141], in which a high-speed direct-current rotary motor, combined with a rotary encoder and a reflection mirror, directed the excitation laser beam precisely onto an array of capillaries, which were symmetrically distributed around the motor. The separation and LIF detection (488 nm) of enantiomers of Glu, Met, and Trp labeled with FITC were also described.

Three different LEDs (430, 450, and 480 nm) were collimated into a single-mode optical fiber for fluorescence detection using the same in-column fiberoptic LIF detector. This excitation source allowed the simultaneous determination of FITC-labeled L-Asn (480 nm), 4-fluoro-7-nitro-2,1,3-benzoxadiazole–labeled (NBD-F) epinephrine (450 nm), and CBQCA-labeled L-Leu (430 nm). The LODs attained were 0.8, 120, and 40 nM, respectively. Fluorescence was detected using a PMT, which measured the emission wavelength of the three dyes. Migration was implemented using a 75 μm ID capillary. After single-LED excitation (corresponding to one of the three dyes) for analyzing the mixture of the three labeled molecules, the electropherograms showed two main peaks (for the dye and the corresponding labeled AA accurately excited at the given wavelength) and a small peak corresponding to other weakly excited dyes. Therefore, at 430 nm, CBQCA-Leu was primarily detected, whereas a short peak of FITC was observed. At 450 nm, NBD-F- and NBD-labeled epinephrines were primarily detected along with FITC. At 480 nm, FITC and FITC-Asp were detected while a short peak of NBD-F was recorded. The authors claimed that the performance of the newly developed multi-wavelength LED excitation source was superior to that of the single-wavelength LED [142].

A coated capillary with a buffer containing hexadimethrine bromide and 20% isopropyl alcohol was used for the analysis of FITC-labeled AAs in beer using a 470-nm LED or a 488-nm Ar laser [143]. The resolution achieved with the laboratory-made instrument was significantly poorer than that achieved using the commercial device, because the light beam of the LED was ~3-fold wider than the laser beam. In addition, the LODs of the FITC-labeled compounds were approximately 1.8-fold poorer than those obtained with the conventional fluorescence system when the LED was used.

Multiphotonic excitation fluorescence (MPEF) using a diode laser (808 nm, 1 W) was described by Chen *et al* [144]. The separation of off-line FITC-labeled AAs was demonstrated using CZE and MEKC. Although the LODs of AAs were not specified by the authors, the one for Rhodamine B was reported to be 1.2 µM, which is considerably high. The effectiveness of MPEF detection and classic fluorescence detection (at 488 nm) were compared using six FITC-labeled biogenic amines (histamine, spermidine, cadaverine, putrescine, phenylethylamine, and spermine). MPEF was reported to show superior electrophoretic resolution with detection volume in the attoliter range. The quantitative analysis of varying concentrations of biogenic-amine species seemed to indicate that this approach may help obtain a yoctomolar LOD. MPEF coupled with MEKC has been used to determine the biogenic-amine profile of decayed oriental crucian, wherein LIF detection was found to be considerably more sensitive than MPEF [145].

In conclusion, FITC offers the key advantages of high fluorescence yield; good reactivity with an amine group facilitating derivatization at submicromolar concentrations; ability to derivatize primary and secondary amines; and ability to be doubly charged, which results in compounds bearing three negative charges. However, it is not fluorogenic, and its purity is ~90 %, which makes the identification of unknown compounds difficult, because numerous FITC peaks are formed.

FITC is the most sensitive dye for LIF detection, as the LODs obtained are in the picomolar range. Moreover, its reaction rate is considerably lower (than that of the above mentioned dye), and can extend to several hours at ambient temperature. It is difficult to identify some AAs when they are present at low concentrations, because they migrate at the same migration rate as FITC and its degradation byproducts. Furthermore, FITC is reported to ineffective as a labeling agent at concentrations lower than the micromolar range. It can only be used to label AAs present at micromolar concentrations, that too, primarily acidic and basic ones, which migrate behind or ahead of FITC and its byproducts.

836

837 **4.2.4. Other fluorescein-based reagents**

838 Dichlorotriazinylaminofluorescein (DTAF) has also been used for LIF detection
839 coupled with CE. It appears to be more reactive at lower concentrations than FITC, which leads
840 to the quantitation of AAs even at lower levels (10 nM) [135]. DTAF has been used in the
841 quantitation of phospho-AAs using MEKC. Different variables affecting the derivatization
842 (DTAF concentration, pH, temperature, and time) and separation (surfactant type, pH, and
843 buffer concentration) have been studied. In one study, baseline separation of three phospho-
844 AAs was achieved in less than 11 min with good reproducibility. The LODs ranged from 0.5–
845 1.0 nM. The method was used to detect phospho-AAs in hydrolyzed phosphorylated-protein
846 samples [146]. Molina and Silva [147] proposed the use of in-capillary derivatization with
847 DTAF; they emphasized that the success of the in-capillary reaction of analytes by LIF detection
848 hinges on the "excellent" labeling chemistry of the reagent. The optimization of the
849 electrophoretic conditions and mixing step in this protocol allowed the determination of AAs,
850 biogenic amines, and phospho-AA herbicides with LODs in the $\mu g \cdot L^{-1}$ range and relative
851 standard deviations ranging from 3.5% to 5.8%. Phospho-AAs have also been derivatized using
852 N-hydroxysuccinimidyl fluorescein-O-acetate at 40 °C for 40 min in borate buffer (pH 8.5).
853 Fluorescein-O-acetate fluoresces at 488 nm, and LODs in the nanomolar range can be achieved
854 [148]. 5-carboxyfluorescein-N-succinimidyl ester has been used with CE/LIF (488 nm) for the
855 quantitation of Asp and Glu in rat periaqueductal gray matter. The LODs were reported to be
856 0.69 and 0.81 nM, respectively [149]. 6-carboxyfluorescein-N-succinimidyl ester has been used
857 for precolumn derivatization of gabapentin in plasma. Optimal separation and detection were
858 achieved in an electrophoretic buffer containing 50 mM sodium borate (pH 9.5) using an Ar
859 laser (488 nm). The calibration curve, ranging from 0.3 to 150 µM, was linear, and the LOD in
860 plasma was 60 nM [150].

861 The analytical potential of synthetic 6-oxy-(N-succinimidyl acetate)-9-(2′-
862 methoxycarbonyl) fluorescein has been investigated using CE-LIF. Derivatization was
863 performed at 30 °C for 6 min in boric acid buffer (pH 8.0). The derivatives were baseline-
864 separated in 15 min using a 25-mM boric acid running buffer (pH 9.0) containing 24 mM SDS
865 and 12.5% (v/v) acetonitrile. The LOD attained for biogenic amines was 80 pM (S/N ratio = 3).
866 The optimal results obtained using the running buffer indicated that a weak acidic BGE offers
867 better separation than a basic one. Several fluorescein-based probes for amino compounds were

compared. This dye has been reported to exhibit excellent photostability and pH-independent fluorescence (pH 4–9). This method was applied to the detection of biogenic amines in three different beer samples [151].

In the chapter on medical applications, we will present the use of IAF, which has largely been employed for the selective identification of thiol-containing AAs and glutathione (GSH)-derived peptides [152]. Maleinimide fluorescein has been used as well. Diastereoisomers can be obtained with the latter, as the reaction between the thiol group and maleinimide leads to the formation of an asymmetric carbon [153]. Though less popular, 5-(bromomethyl)fluorescein can also be utilized to selectively detect thiol AAs and GSH. Of note, this molecule can react with the carboxylic function as well. The separation of Hcy, Cys, GSH, Cys-Gly, Glu-Cys, cysteamine, penicillamine, mercaptopropionylglycine, and mercaptoacetic acid (internal standard) was successfully performed using this reagent, with LODs achieved between 61 nM (Hcy) and 183 nM (penicillamine) [154].

DTAF has been described as a better nonfluorogenic dye than FITC, and its reactivity allows the labeling of all AAs at low concentrations; the LODs are in the nanomolar to picomolar range. The reaction rate is identical to that of FITC (several hours at ambient temperature). IAF is highly suited for the detection of thiols; it has been used extensively in several applications owing to its high fluorescence, selectivity for the -SH function, and capacity for excitation with the 488-nm line of an Ar laser or a 480-nm LED.

4.2.5. Other amine reagents

Fluorescamine is another dye that is widely used for labeling AAs [155]. Nonetheless, in CE, its use is restricted by the lack of an available laser or diode that can generate excitation at 360–390 nm. However, an AA mixture, after derivatization with fluorescamine, was analyzed using a 355-nm pulsed laser, with LODs obtained in the nanomolar range [77]. Fluorescamine has been used to separate enantiomers using MEKC with hydroxypropyl-β-CD [156]. This has led to the development of one of the most remarkable applications of CE/LIF—the Mars Organic Analyzer [157]. This is a microfabricated CE instrument for sensitive AA biomarker detection. It consists of a four-wafer sandwich combining glass CE separation channels, microfabricated pneumatic membrane valves and pumps, and a nanoliter fluidic network. It allows the analysis of AAs at concentrations ranging from 1 µM to 0.1 nM. The Mars Organic Analyzer was first used to analyze soil extracts from the Atacama Desert (Chile), and could detect AAs present at 70 parts per trillion to 100 parts per billion in jarosite, which is a sulfate-

rich mineral associated with the liquid water that was recently detected on Mars. Kang *et al* [158] developed an in-column derivatization method for a fully automated assay of Hcy and other thiols. It involved the direct injection of a sample containing Hcy and 4-aminosulfonyl-7-fluoro-2,1,3-benzoxadizole, which reacted for 10 min at 50 °C. Hcy was detected within 7 min, and the LOD obtained for Hcy with LIF detection was 5 nM; this decreased to 2.5 nM with precolumn LIF detection.

Based on a report by Ruyters and de Wal [159], NBD-F has been used regularly in analytical studies, similar to 4-chloro-7-nitro-2,1,3-benzoxadiazole [160]. The NBD nucleus can be excited at 470–490 nm. The reactivity of these dyes was studied 40 years ago by Imai and Watanabe [161]. Zhang *et al* [162] used NBD-F for in-capillary derivatization. The best NBD-F/sample molar ratio was found to be 215, and the injection process, spanning 4 s for the sample and 2 s for the NBD-F solution, was performed in a capillary whose temperature was maintained at 45 °C. The LOD was ~100 nM for Ala and 600 nM for Asp. With off-line labeling, the separation of DL-Ser was studied using 40 mM hydroxypropyl-β-CD and implemented in the rat brain tissues for the detection of D-Ser, with an LOD of 300 nM [163]. However, the major issue with this dye is that its fluorescence yield is highly sensitive to the polarity of the separation buffer, and highest fluorescence is obtained in a low-polarity solvent [164]. EMMA was also used with NBD-F, and the ratio of the dye to AA was studied. The LODs obtained were in the nanomolar range [165]. R(−)-4-(3-isothiocyanatopyrrolidin-1-yl)-7-(N,N-dimethylamino sulfonyl)-2,1,3-benzoxadiazole was synthesized for enantiomeric separation using fiberoptic LEDIF and CE, and an LOD of ~3 µM was achieved for DL-Tyr derivatives [166].

Maleinimide eosin has been used to study thiols. We have previously indicated that diastereoisomers are obtained as the reaction of the thiol residue with maleinimide results in the formation of an asymmetric carbon. In a study, an inexpensive, 515-nm diode laser was used as the source [167]. The LOD obtained for GSH was 0.18 nM, and the derivatization conditions were optimized.

NBD-F is certainly a popular dye for AA labeling. Micromolar concentrations of AAs can be detected, and the labeling rate appears to be higher than that of FITC or DTAF but lower than that of NDA or CBQCA. The 7-nitro-2,1,3-benzoxadiazole nucleus is highly sensitive to electrolyte polarity; this poses a limitation when data are adjusted for evaluating migration.

In summary, NDA- and CBQCA-labeled AAs are largely used to quantitate AAs in the presence of KCN; their reactivity levels are good, as are their fluorescence yields. Nevertheless, these dyes cannot be used to label secondary amines. Trp is considerably difficult to detect in most such studies. For the selective detection of thiols, IAF is also commonly used. While attempts at derivatization with other derivatives are documented, only a few studies have described the process, as these ragents are not commercially available or as the resultant sensitivity may be insufficient. FITC has been widely used; it has several advantages (a high fluorescence yield and a charge); however, it is not fluorogenic, and only low purity FITC (90%) is available commercially. It can be used when AAs present at micromolar concentrations are to be detected. Additionally, 1000–2000-fold dilution of the sample in water prior to injection is necessary to ensure effective separation.

5. CE/MS

ESI MS allows the determination of the m/z values of $[M+H]^+$ ions of each AA and the recording of electropherograms for the m/z values. Therefore, using this method, an AA can be characterized based on its m/z value and migration time. In contrast, in other detection methods, different AAs are only characterized based on their migration time. Moreover, in ESI/MS/MS, the $[M+H]^+$ ions of the AA can be fragmented into smaller ions, and the m/z values of the molecular ion(s) F^+ is characteristic for each AA. Therefore, for each AA, if we consider its diagnostic fragmentation $[M+H]^+ \rightarrow F^+$, we introduce a supplementary parameter that increases the selectivity of detection. Consequently, the AA will be characterized based on its migration time, the m/z value of $[M+H]^+$, and the specific m/z value of F^+. Precise determination of the m/z value of $[M+H]^+$ using HRMS helps determine the chemical formula of the compounds, based on which researchers can detect several hundred nonproteinogenic AAs.

Fanali *et al* [168] and Ferré *et al* [169] recently published review articles on CE/MS and its state-of-the-art applications; among them, some applications are discussed. CE-ESI/MS is now popularly used for the detection of AAs after pioneering developments by Soga and Heiger [170]. Since 2000, numerous authors have described CE/MS applications where AAs are detectable even when their identification is challenging owing to low molecular mass [171,172]. Table 4 summarizes the analytical conditions of the studies reviewed.

5.1. General CE/MS studies

Soga and Heiger [170] used simple conditions for AA separation [1 M FA and a sheath flow of 10 µL/min of 5 mM ammonium acetate in 50% (v/v) methanol–water in a 100 cm long 50 µm ID capillary] using Agilent CE and a quadrupole MS instrument. They selected the multiple-reaction monitoring mode (MRM) to study nine free AAs and monitored protonated $[M+H]^+$ ions for AA detection, with a sampling time of 44 ms for each. At an m/z value of 132, isobaric ions of Leu, Ile, and hydroxy-Pro were found to be well separated. The LODs ranged from 0.3–11.0 µM. Around the same time, Klampfl and Ahrer [173] reported a study in which CE/MS was used to quantify free AAs in infant food samples using a sheath flow interface (4 µL/min). Based on the zwitterionic nature of the analytes, two different modes of separation and detection were tested: a basic electrolyte (established using a 100-mM triethylamine electrolyte) with negative-ion MS analysis and a highly acidic carrier electrolyte (300 mM FA) with MS detection in positive-ion mode. The latter was found to be the optimal solution. Free AAs in different infant food preparations were analyzed without sample pretreatment.

DL-2-amino-2-methyl-3-(3,4-dihydroxyphenyl) propanoic acid (MDOPA) and DL-2-amino-3-(3,4-dihydroxyphenyl) propanoic acid (DOPA) enantiomers were separated and identified using electrokinetic chromatography coupled with ESI^+ MS [174]. A double-junction CE/MS interface was used to maintain the separation efficiency and alleviate ion suppression from sulfated β-CD. The double-junction interface consisted of an inlet reservoir connected to a separation capillary leading to a liquid junction reservoir and a capillary of 5 cm/50 µm (ID) adjoining the separation capillary. The other end of the connecting tube was adjusted in the sheath liquid reservoir of the ESI emitter. At an S-β-CD concentration of 2%, the CDs acted as carriers of the positively charged molecules DOPA and MDOPA. During separation (reverse polarity), the S-β-CD anions carried cationic analytes from the inlet reservoir toward the junction reservoir. By controlling the polarity of the connecting column, the CD anions were retained in the junction reservoir, whereas the positively charged analytes continued to migrate to the ESI source for detection. S-β-CD was prevented from entering the ESI source, and ion suppression was avoided. In this arrangement, all enantiomers of DOPA and MDOPA were separated and detected efficiently with LODs in the range of 0.5 µM in MRM, and the repeatability of migration times and peak areas ranged from 2.5%–8.0% (RSD%, N = 3) and 10.9%–19.5% (RSD%, N = 3), respectively. This method was used for analyzing methyl-DOPA tablets [174].

Sheathless CE/ESI^+ MS is highly sensitive owing to the low CE flow rates (nL/min); a split-flow technique [175] for interfacing CE with MS was used for the detection of

underivatized AAs for separating D/L-enantiomers. The AAs were separated and detected at low-femtomole levels using a fused-silica capillary with length 130 cm and ID 20 µm modified using 1 M FA and a 30 mM 18C6H4 solution as the BGE. The same was also used for the separation of L-Arg and L-canavanine (an analog of Arg) in a complex mixture containing all standard proteinogenic AAs. In a study on blood samples, two metabolic diseases (phenylketonuria and tyrosinemia) were diagnosed [176].

The last study mentioned has launched a debate between researchers who favor the sheath flow and sheathless methods.

A third interface was devised by Wojcik *et al* and commercialized by CMP Scientific. This interface used an electrokinetically driven sheath flow (and not mechanically pumped sheath flow) to generate a stable nanospray [177]. The generation of negative ions during electrospray requires the application of a negative potential to the emitter. To attain a stable flow and the best sensitivity, the surface chemistry of the emitter can be manipulated. An amino-coated borosilicate glass emitter with a positively charged surface and a negatively charged double layer was prepared, and the separation capillary was threaded into the emitter tip. The emitter preparation procedure had sufficient reproducibility. Detection of the metabolites extracted from stage 1 *Xenopus laevis* embryos facilitated the manual identification of over 100 features [178].

As described above, MS helps increase both the sensitivity and selectivity of CE. Mamani-Huanca *et al* [179] suggested the use of in-source fragmentation of 57 AAs to identify the mechanisms underlying major fragmentation reactions observed for diagnostic ions generated in ESI^+ HRMS. The in-house library of diagnostic ions was used to establish a workflow for the targeted extraction of AAs that are not easily identifiable. Therefore, the authors showed that fragmentation mechanisms constitute an informative reference for accurate molecular identification.

5.2. Developments in sheath flow CE/MS (CE/SF-ESI-MS)

Soga *et al* [180] proposed a method for AA separation using CE under acidic conditions (1 M FA as a BGE) and detection using tandem MS (MS/MS). Using a sheath flow (5 mM ammonium acetate in 50% [v/v] methanol–water) of 10 µL/min, they found that the position of the electrospray probe is a factor that affected sensitivity. Through MRM detection for increasing selectivity and sensitivity, they showed that the LODs for the 32 free AAs studied

ranged between 0.1 and 14 µM, which was adequately sensitive for AA detection in urine samples. Because AAs yield characteristic MS/MS spectra, the MRM approach is selective, quantitative, and reproducible; however, it does not permit the detection of unknown compounds. The use of CE/ESI-MS and CE/ESI-MS/MS for the detection of nonproteinogenic AAs helped identify the oxidation and nitrosation products of N^g-hydroxy-L-Arg. Citrulline, cyano-Orn, and N^g-nitroso-arginine could be identified using the standard [181].

To determine the exact mass and achieve high sensitivity at low m/z values, Hirayama and Soga [182] proposed the use of two lock masses (the ^{13}C isotope ion of the methanol dimer with m/z = 66.0632, and a [hexakis(2,2-difluoroethoxy)phosphazene] protonated ion with m/z = 622.0290). High mass-spectrometric resolution helped obtain resolved electrophoretic peaks using single ion monitoring (SIM). Most LODs ranged from100–300 nM.

In transient-isotachophoresis using a pH junction in a stacking process with CE/MS, AAs present at nanomolar concentrations were detected in samples with AAs diluted in ammonium acetate buffer, where a 1 M FA solution served as the BGE. The migration behavior of charged metabolites was modeled (for assessing the role of absolute mobility and pKa) to support MS characterization in a multiplexed approach for studying the selective nutrient uptake behavior of *Escherichia coli*. Computer simulations in Simul 5.0 [183] facilitated the *de novo* identification of unknown nutrients [184].

CE/ESI^- MS has also been used for detecting anionic metabolites in urine. Among nucleosides, carboxylic acids, and phosphorylated species, Pro and pyroglutamic acid were detected in the micromolar range using different water/methanol (1:1, v/v) solutions containing 25 mM triethylamine or ammonium acetate at pH 11.7 or 9.0, and a sheath liquid containing one of them at 5 mM concentration. A study using human urine samples led to the identification of an average of 231 molecular features [185].

HRMS increases the selectivity of MS, which helps improve metabolite detection. The use of CE/HRMS has been suggested for fluxomic studies, in which AA detection using ^{13}C labeling is conducted for carbon flow calculation. ^{13}C labeling analyses usually involve conventional gas chromatography (GC)/electron ionization (EI)-MS after AA derivatization for isolation of N,O-*tert*-butyldimethylsilyl derivatives. Using CE-SF-ESI/HRMS, the same treatment used in GC/MS was used for flax (*Linum usitatissimum* L.) embryos. Nonetheless, no derivatization was performed to volatilize them. The water-solubilized and lyophilized AA extract was directly injected into a CE instrument. It was shown that Val, Leu, and Ala were not synthesized from the same pyruvate pool during the accumulation of reserves in flax seeds

[186]. A grounded nebulizer of the CE/SF-ESI-MS source was constructed to measure the concentrations of 28 AAs using ESI^+ and 6 organic acids using ESI^- HRMS; this approach helped distinguish between homoarginine (m/z 189.1346) and N^6-trimethyl-Lys (m/z 189.1598), which have the exact same migration time in CE. The significant improvement in a high-resolution setup enabled researchers to identify 270 metabolites [187] (Fig. 7).

Neonatal screening for inborn defects of metabolism was realized using CE/MS detection of AAs and acylcarnitines in DBS samples. On-line sample preconcentration and desalting steps helped improve the sensitivity and limit the ionization suppression or interferences caused by the presence of isomers and isobars. During these steps, an acidic BGE was used, whereas the sample was buffered with ammonium acetate. The buffer discontinuity enabled the electrokinetic focusing of AAs and acylcarnitines; meanwhile, strong electrolyte salts (Na^+ and NH_4^+) present in the sample migrated ahead of the analytes. The linearity of twenty target metabolites was determined in five replicates at five different concentrations over a 90-fold concentration range for most AAs. A 200-fold concentration range was used for Arg and 4-OH-Pro. Interday precision of quantitation was reported to be below 11% [188].

A multivariate strategy for *de novo* quantification of AAs and other cationic metabolites was designed using CE-ESI-MS. Multivariate calibration was implemented between the measured relative response factor of polar molecules and the physicochemical parameters associated with ion evaporation in ESI-MS: the octanol–water distribution coefficient (log D), absolute mobility, molecular volume, and effective charge. It was revealed that a limited set of properties can be analyzed to predict the relative response factor of various classes of molecules, provided that an appropriate training set is validated and ion responses are normalized to an internal standard. Micromolar levels of metabolites added into red blood cell lysates were quantified using CE-ESI-MS in this model. The authors claimed that the study demonstrated the feasibility of virtual quantification of low-abundance metabolites in real-world samples based on physicochemical properties estimated using computer modeling. This method also helped obtain a wider view of the disparities in solute responses during ESI-MS. The predicted ionization efficiency may enable the rapid and semiquantitative analysis of a newly discovered chemical when standards are unavailable [189].

An assay using 1 M FA buffer was developed by Wakayama *et al* [190], who analyzed 34 amines and AAs simultaneously with 12 organic acids without derivatization. The LODs ranged from 2.5 µM in the ESI^+ mode to 5 µM in the ESI^- mode. In cases in which the total ion electropherogram was difficult to interpret, the electropherograms were used to identify each

AA with ease. The technique was applied to the metabolomic analysis of diurnal changes in pineapple leaves, in which changes in Asp, Asn, and citrate concentrations were measured. Butylation of the carboxylic function of AAs has been reported to improve ionization efficiency rates and detection sensitivity. In addition, the esters formed have higher masses and ensure better mass selectivity. Sanchez-Hernandez *et al* [191] added butanol at 80 °C to a dry residue of AAs (Orn, β-Ala, GABA, alloisoleucine, citrulline, and pyroglutamic acid) extracted from vegetable oils in a 30-min reaction. Under acidic migration conditions and with ESI/MS/MS detection, they achieved LODs between 0.04 and 0.19 ng/g.

AA fingerprints from index, middle, and ring fingers were investigated for the improvement of existing fingerprint enhancement techniques using an optimized CE/ESI$^+$-MS method. Using full mass spectra and extracted ion electropherograms, nine underivatized AAs were quantitated in a fingerprint sample (Orn, Lys, His, Gly, Ala, Val, Ser, Pro, and Asp). Gly and Ser were found to be the most abundant AAs. Ile/Leu (unseparated) and Glu were only detected and not quantified, as they were present at concentrations below the quantitation limit. Overall, 17 AAs yielded calibration data with a quantitation limit ranging from 20 ng (Lys) to 180 ng (Met) when deposited on a Mylar film used for AA fingerprint collection. MS/MS fragmentation experiments were conducted for additional identity confirmation (except for Gly, which does not fragment). The authors mentioned that the migration times had appropriate CV% (between 9.6% and 14.6%), with the MS technique being adequately selective for confirming the identity of the compound migrating between 12.9 min (Arg) and 29.3 min (trans-4-hydroxyproline) [192].

The kynurenine pathway of Trp catabolism has been studied using CE/ESI$^-$-MS. Three specific metabolites, 3-hydroxyanthranilic acid, quinolinic acid, and picolinic acid, were quantitated without any isotopic internal standard. A covalently coated sulfonated capillary was prepared, and different separation and ionization parameters (such as pH, the type of BGE, and the type of organic modifier) and the optimization of ESI$^{+/-}$-MS modes were tested [193]. The separation time was less than 10 min. The authors reported the migration profile of the initial substrate, 3-hydroxyanthranilic acid, as well as the formation of picolinic acid and quinolinic acid after the double-enzymatic reaction of 3-hydroxyanthranilate-3,4-dioxygenase and α-amino-β-carboxymuconate-ε-semialdehyde decarboxylase.

Chirality has also been studied effectively using CE/MS; recently, Lee *et al* [194] proposed the use of a partial-filling technique to reduce contamination of the ESI source by the CS, *i.e.*, 18C6H4, which is nonvolatile. In this partial-filling experiment, the capillary contained two electrolytes: one on the injection side and another one on the MS side. Here, the length of

the separation zone (on the injection side) was adjusted to 70% of the capillary, and the zone was filled with 30 mM 18C6H4 in water, and the other 30% (on the MS side) was filled with 1 M FA. The complex AA/18C6H4 ions could not be observed, whereas the $(AA+H)^+$ ions were predominant. The enantiomers of the isobaric ions (DL-alloisoleucine, DL-Ile, and DL-Leu) were successfully separated using CE. LODs ranging from 13 µM (Gly) to 0.5 µM (Phe) were achieved. A derivatization protocol was also designed to separate the D/L enantiomers of Ser, Asn, Asp, Gln, and Glu using (+)-1-(9-fluorenyl)ethyl chloroformate. The resultant separation of diastereoisomers was found to be dependent on the pH of the BGE (150 mM acetic acid adjusted to pH 3.7 using NH_4OH). Submicromolar concentrations were detected, and the method was evaluated for CSF analysis. It was concluded that the matrix effect was marginal, and the recovery rates ranged from 46% to 92% [195].

FITC has been used to derivatize Orn to facilitate the separation of D/L enantiomers, and the derivative has been studied using CE-ESI^+/MS/MS. The $[M+2H]^{2+}$ ion was the ion detected predominantly (m/z 456, doubly labeled Orn); it fragmented at m/z 522 (singly protonated FITC-Orn) and 390 (singly protonated FITC). The m/z 456 $\rightarrow$ m/z 390 transition has been used for Orn determination in beer. The optimized CE buffer contained 0.75 mM γ-CD. The LOD obtained using CE/MS/MS was 2.5 nM, whereas resolution between the two enantiomers was ~2.5. The migration durations were ~28 min, as the authors employed a long capillary [196]. The use of 6-deoxy-6-(1-(2-amino)ethylamino)-beta-CD, 6-deoxy-6-(N-(2-methylamino)pyridine))-beta-CD, and 3-mono-deoxy-3-monoamino-beta-CD as CS molecules for CE-ESI^+-MS and CE-LIF experiments has been investigated for the enantioseparation of FITC-labeled Asp, Glu, Ala, Asn, and Arg. The presence of electrical charges in the CD is usually advantageous because it can induce additional ionic interactions with the analyte and can be used at a low concentrations compatible with ESI^+. CE/LIF experiments with 0.5 mM 3-mono-deoxy-3-monoamino-β-CD at pH 8 yielded better resolution (up to 16 for DL-Asp) between different enantiomers, with the LODs ranging from 40 to 90 nM. In CE-MS, the resolution values ranged from 0.9 (DL-Arg) to 4 (DL-Asp), and the LODs ranged from 68 to 1870 nM when these AAs were assayed in vinegar and soya [197].

An original study on metal (M = Zn, Cu, Mn, and Fe) complexes with Gly, known as glycinates $(M(Gly)_x(H_2O)_y(SO_4)_z)_n$, was performed using CE/induced coupled plasma (ICP)-MS and CE/ESI-MS/MS. The buffers used were 20 mM ammonium acetate (pH 7.4) for CE/ICP-MS experiments and 50 mM ammonium acetate (pH 7.4) for CE/ESI-MS/MS. The compounds were identified and quantitated, and the authors showed that glycinate integrity was

preserved under the conditions employed. The LODs in CE-ICP/MS for ZnGly, CuGly, and MnGly were ~0.8–4.0 µM, which allowed glycinate detection in premixes or feed samples [198].

CE-SF-ICP-MS and CE-SF-ESI-MS/MS have been applied for the identification of Zn^{2+}-binding ligands in Goji berry extracts [199] using 20 mM ammonium formate (pH 9) as a BGE. Electrophoretic peaks corresponding to Zn^{2+} were identified. $ESI^{+/-}$MS/MS assays of molecules containing the two most abundant isotopes of Zn revealed fragments that did not contain the Zn^{2+} ion. Nine different complexes were identified; among them, $Zn(Gly)^{+}$ and $Zn(Met + 2H_2O + OH^{-})^{+}$ were detected.

In conclusion, several studies on CE/MS with a sheath flow interface have been published in which the flow rate ranged between 5 and 10 µL/min with a composition primarily based on FA (a certain quantity of MeOH or propanol may have been added). The sheath flow helps ensure good stability and tolerance to changes in BGE composition; however, spatial dilution at the interface capillary/sheath flow and greater noise can limit its utility for the detection of AAs, which have low m/z values. Based on this, few authors have reported the need for derivatization to increase the mass of the molecules. Nonetheless, sensitivity in such studies is not considerably better than that in studies involving free-AA determination. The commercial CE/MS interfaces [mostly obtained from Agilent (Walbron, Germany), and from Analis (Namur, Belgium) at times] are robust and easy to use with all CE instruments. Sensitivity in the micromolar range has been reported in most studies. Because the interface is robust and not as expensive (less than €5000), and requires a simple fused silica capillary, its use has facilitated the rapid growth of CE/MS applications in the field of AA determination. In the chapters on the applications of these methods, it has been shown that these methods are most commonly applied in metabolomic studies, and only a few laboratories worldwide use CE/MS in AA assays.

5.3. Sheathless CE/MS (CE/SL-ESI-MS)

For a sheathless setup, a porous tip at the end of the capillary is formed by removing 25–40 mm of the polyimide coating of the capillary and etching this section with a 49% HF solution. The electrical connection to the capillary outlet is implemented by simply inserting the capillary outlet containing the porous tip into the metal ESI needle and filling it with the BGE. To test the utility of this tip, an assay was performed using 17 AAs. An FA/18C6H4 solution served as a complexation reagent to enhance the sensitivity of AA detection. It was

noted that the complex increased the apparent masses of the AAs. The results obtained with the porous tip were similar to those obtained using a conventional interface design. It was noted that bubble formation due to redox reactions of water at the high-voltage electrode occurred outside the separation capillary and did not affect the separation or MS performance [200]. Age estimation of silk textiles on the basis of AA racemization rates was realized based on the 2500-year L-to-D conversion half-life of aspartic acid in silk. The analysis required only 100 μg of silk fiber [201]. Moini has published a detailed review article on the uses of the porous tip interface [202]. Recently, SL-ESI-MS using a commercial porous tip emitter was reported by Zhang *et al* [203], with 10% acetic acid solution used as the BGE. The authors obtained a nanomolar LOD (1–92 nM) and identified AAs and biogenic amines in a methanol/water extract from 500 HepG2 cells. Ramautar published a precise description of the CE-SF-ESI$^{+/-}$MS protocol for analyzing amines and AAs (positive ions) as effectively as acidic molecules (phosphoesters) [204].

Because metabolomic studies lead to the identification of molecules containing acid, alcohol, or amine functions, which can be identified using either negative or positive ESI, Huang *et al* [205] proposed an original two-step labeling method for identifying organic acids, amines, and AAs using ESI^{+}. In this method, 300 mM 3-(diethylamino)propanoylchloride was added to a dried sample extract to obtain an ester with alcohol and an amide with amines. Next, N-[(dimethylamino)-1H-1,2,3-triazolo-[4,5-b]pyridin-1-ylmethylene]-N-methylmethanaminium hexafluorophosphate-N-oxide (1 M) was reacted with N,N-diethylethylenediamine and the abovementioned derivatized sample to convert the acid group into an amide one. Finally, all chemical functions were converted into esters or amides using an NN-dimethyl amine nucleus, which could be protonated easily. Even though Leu/Ile were not separated, LODs in the nanomolar range were obtained, and 17 AAs and 5 organic acids were identified.

A sheathless interface was designed using an ionophore membrane-packed electroconduction channel to prepare a “durable” interface that functioned well with a volatile alkaline BGE and enabled short analysis duration (<15 min). The MRM mode and electrokinetic injections yielded LODs as low as 0.05–0.81 μM, whereas the RSDs of intraday and interday repeatability were less than 3%. The determination of free AAs from serum using isotope dilution mass spectrometry (IDMS) resulted in recovery rates of 96.3%–101.8%. The concentrations of Ala, Phe, Pro, Leu/Ile (not separated), Tyr, and Val in serum (after simple

filtration through a filter with a molecular weight cutoff of 10,000) were measured in both HPLC-IDMS and CE/IDMS experiments. The two techniques yielded similar results [206].

Metabolomics is currently being applied in an increasing number of functions and represents the most important research topic in CE/MS.

At present, only a few studies have been published that have used a sheathless interface. The two primary reasons for the same are as follows: Sciex is the major supplier of the instrument, and the interface has been commercialized for less than 6 years; the capillaries with porous tips are considerably expensive, and therefore, have limited use. A study comparing sheathless and sheath flow interfaces was published a few years back (2014). Bonvin [207] demonstrated that the ionization efficiency of the sheathless interface for small molecules was 20–40-fold higher (at submicromolar concentrations); the LODs reported in the latest AA studies were mostly in the nanomolar range. The efficiency rates achieved were also better when the sheathless technology was used, which is more important for lower-electrophoretic-mobility compounds. This could be attributed to the absence of the nebulizing gas and sheath liquid, as these exert a suction effect that broadens the peaks. Therefore, the sheathless technology is easier to use, and the installation step is simpler. In both cases, the buffer composition is a major limitation in CE/MS experiments; the components must be volatile, and ammonium formate or acetate are mostly used. The addition of 18C6H4 helps separate D/L AAs. For major AA applications, the determination of AAs at nanomolar concentrations is not particularly useful; at present, the (cost per analysis)/(high sensitivity usefulness) ratio for sheath flow interface in AA determination is more favorable.

5.4. CE-MS as a metabolomic tool: diverse horizons

The field of metabolomics has seen considerable contributions in the last decade. In particular, CE-MS coupling for accessing metabolomics data has undergone significant advancement. Consequently, the emphasis has been placed on human and animal fluids and on plants. There has been specific interest regarding cell or tissue metabolomics, often related to cancer and other pathologies. Recently, Hirayama *et al* [208] published a detailed study about the use of this technique for tissue analysis in the MRM mode. Rodriguez *et al* [209,210] have published a simple and well-described CE/SF-ESI$^+$/MS method for the quantitative determination of 27 AAs (including Leu, Ile, alloisoleucine, Orn, citrulline, GABA, carnosine, and hydroxyproline) in urine within 30 min. The BGE used was 0.80 M FA and 15% methanol, and the pH-stacking procedure involved the injection of 12.5% NH_4OH solution at 0.5 psi at 9

s prior to sample injection. The LODs ranged from 0.63 to 29 μM. Urine samples were collected from children with vesicoureteral reflux.

The generation of unidentified peaks in CE-MS analysis is a major obstacle that is yet to be overcome in metabolomic studies. A novel metabolomics-based chemoinformatic approach has been designed for ranking candidate structures. The approach utilizes information about known metabolites detected in samples containing unidentified peaks and involves three discrete steps: i) identification of the "precursor/product metabolites" as potential reactants or products derived from the unidentified peaks; ii) search for candidate structures for an unidentified peak against the PubChem database using a molecular formula, which are then ranked by structural similarity against precursor/product metabolites and candidate structures; iii) prediction of the migration time for refining candidate structures. To initiate the validation of this "proof-of-concept tool" for the 20 proteinogenic AAs represented by the pseudo-unidentified peaks, the authors identified precursor/product metabolites of 18 of the 20 AAs, with Arg and Trp being the only exceptions. The authors also proposed the analysis of two unidentified peaks in a urine sample, which were shown to correspond to glycocyamidine and *N*-acetylglycine [211]. This method and its further development may help metabolomists optimize their findings.

5.4.1. Application in cancer

The use of CE/MS in metabolomic applications involving small molecules has been developed and reviewed extensively [204,212], and the importance of its use is particularly well evaluated. Here, we summarize and discuss new developments reported in the most recent articles.

A deeper understanding of the metabolomics of cancer cells has driven specific therapeutic advances. The tumor microenvironment has been studied in surgically resected tissues from lung and prostate tumors. CE-MS detection of AAs has revealed widely different profiles between normal tissues and tumors, with the AA content significantly higher in tumors. Squamous cell carcinoma and other types of lung cancer can be distinguished using CE-MS, and the elevated phosphorylation levels of pyruvate kinase and phosphofructokinase in tumor tissues indicate hyperactive glycolysis [213]. Investigation of the oral squamous cell carcinoma (OSCC) metabolic system has revealed glucose consumption associated with lactate production (Warburg effect), which is concomitant with a higher rate of glutaminolysis [214]. The decarboxylation of isocitrate to α-ketoglutarate has been demonstrated in gliomas and acute

myeloid leukemias. In one mutant (IDH1), higher transformation of α-ketoglutarate to D-2-hydroxyglutarate was documented. Consequently, D-2-hydroxyglutarate was suggested to act as an oncometabolite. Glutaminolysis has also been shown to be activated in gliomas [215]. Serum samples from patients with chronic hepatitis C receiving pegylated-interferon or ribavirin therapy showed higher Trp levels than those collected from healthy controls [216].

Saliva has been found to be a useful biofluid well-suited for the diagnosis of a wide range of diseases, including cancers. A metabolite assay of saliva samples obtained from 215 individuals (including 69 patients with oral, 18 with pancreatic, and 30 with breast cancer; 11 patients with periodontal disease; and 87 healthy controls) was performed using CE/MS. The obtained results indicated that 57 principal metabolites could be used as predictors of these diseases. Higher concentrations of most metabolites were detected in all three cancer types, with salivary metabolites forming a cancer-specific signature. Most of the AAs were included in these 57 metabolites, along with several biogenic amines (*e.g.*, putrescine, cadaverine, piperidine, and burimamide) and unidentified molecules (with only their chemical formulae known) [217]. OSCC has also been studied using saliva samples. A study on twenty-two Japanese patients with OSCC and 21 healthy controls led to the identification and quantitation of 499 metabolites. Only 25 metabolites were shown to constitute a molecular signature of OSCC. These included amines (choline and cadaverine), acids (*p*-hydroxyphenylacetic acid, and 2-hydroxy-4-methylvaleric acid [$P < 0.001$], 3-phenyllactic acid, hexanoic acid, octanoic acid, terephthalic acid, 3-(4-hydroxyphenyl)propionic acid [$P < 0.01$], among others), proteinogenic AAs (Val, Leu, Ile, Trp, and Ala), and non-proteinogenic AAs (γ-butyrobetaine, N^6,N^6,N^6-trimethyllysine, taurine, among others) [218].

Esophageal cancer has been studied using paired tumor tissues (Ts) and nontumor esophageal tissues (NTs). In one study, the Ts and surrounding NTs were surgically excised pairwise from 35 patients with esophageal cancer. One hundred and ten compounds could be quantified using CE/MS. The concentrations of the metabolites between Ts and NTs, between stage pT1 or pT2 (pT1-2) and stage pT3 or pT4 (pT3-4), and between node-negative (pN-) and node-positive (pN+) cases were compared by principal component analysis and hierarchical clustering analysis. These statistical methods revealed specific metabolomic differences. The concentrations of most AAs (except Gln) were higher in Ts than in NTs. The authors inferred that metabolomic characteristics differ significantly between tumor and nontumor tissues, which may help implement personalized medicine [219].

CE-SF-ESI^+ MS was used for targeted (MRM mode) and untargeted (full scan mode) analyses of the sub-5 kDa urine metabolome of patients with prostate cancer [220]. The

capillary was coated with trimethoxysilylpropyl polyethyleneimine-HCl (a cationic polymer), using a buffer composed of 0.5% (v/v) FA and 50% (v/v) methanol. It was possible to separate Ala from sarcosine (N-methyl-Gly), its isomer [221]. In a targeted experiment, sarcosine, Pro, Cys, Leu, Glu, and kynurenine were quantitated in four patients and in pooled urine sample collected from healthy volunteers. Untargeted analysis (full scan: m/z 50 to 850) of patient urine also led to the identification of over 400 compounds per patient. The authors stated that the introduction of urine sample collection into the surgery workflow would be a promising strategy for the construction of an abaque (or "nomogram") for proper adjustment of cancer treatment. A small plug of ammonia/water injection before sample injection facilitates the on-line concentration of urine in CE. Urinary metabolic changes (indicated by AA and organic acid contents) in breast cancer after chemotherapy were assessed using CE-MS via a similar concentration method. Both negative and positive ionization modes were employed to analyze the two types of compounds. After chemotherapy, Gly, Cys, His, Trp, and cystine levels were found to decrease in chemotherapy-sensitive patients.

5.4.2. Other human pathologies

Subsequent studies have focused on obesity, particularly on metabolically healthy patients with obesity who do not exhibit insulin deficiency or altered lipid profile that could be used to distinguish them from non-healthy patients. Serum samples were analyzed using GC-MS and CE-MS, and gene expression in adipose tissue were studied in parallel. The combination of collected data indicated that branched-AA catabolism and tricarboxylic acid cycle (TCAC) are less downregulated in healthy patients [222]. Multisegment injection CE/MS has been used to study the effect of high-intensity training (6 weeks for cardiorespiratory fitness enhancement) on glucose tolerance. Aromatic- and branched-chain-AA downregulation in plasma was monitored after oral glucose loading. Such studies assist the designing of personalized lifestyle improvement programs [223]. Ra *et al* primarily focused on fitness in their study on fatigue symptoms in soccer players [224]. CE-MS analyses were performed using saliva samples obtained from athletes after three consecutive days of intense sport activity. The levels of 3-methyl-His, taurine, and some other AAs increased significantly with fatigue. To optimize heart examination and health, it is important to understand cardiac metabolomics. As the energy content in cardiac muscles depends on fatty acid oxidation, and the two ventricles of the heart work under different pressures, it would be interesting to determine the metabolic profiles of arteries and ventricles. Using CE-MS, the levels of nucleotides and AAs (Pro, Ile,

Trp, Phe, Gly, Asp, Ala, Met, Glu, Arg, Lys, His, Gln, and Asn) were measured. These were found to be present at similar concentrations in the two ventricles; however, the levels of lactate, acetyl-coenzyme A, and TCAC metabolites were higher, and the phosphate pool was more enriched in the ventricular tissues than in the atrial tissues [225].

A search for biomarkers as early indicators of nephrotoxicity resulting from drug absorption was performed using plasma samples from rats. CE-MS was used successfully to select 3 metabolites (among the 169 identified) as potential biomarkers: 3-methyl-His, 3-indoxyl sulfate, and guanidoacetate [226]. CE-MS was also applied in studies on the urine metabolic profile of rats fed bisphenol A for 45 days to evaluate its toxicity. The results indicated perturbations in Val, Leu, and Ile biosynthesis and in Gln/Glu metabolism. The levels of neurotransmitters (Glu, GABA, and norleucine) and related metabolites were found to be altered, suggesting the toxic effects of bisphenol A even when administered at levels lower than 50 $mg \cdot (kg \cdot day)^{-1}$ [227].

Leishmania, the trypanosome that causes leishmaniasis, has gradually gained resistance to classic antimonial treatments. Information regarding the development of resistance is important owing to the small number of treatment options available. GC, LC, and CE-MS have been used to analyze the metabolic changes in the parasite during resistance development. An increase in the level of free AAs was observed in resistant parasites [228].

Piestansky *et al* [229] reported a CE/SF-ESI^+MS study where they reoptimized CE conditions to separate Leu and Ile. They proposed the use of 0.5 M FA to achieve optimal resolution of the two AAs. They obtained the highest sensitivity in MRM mode with LODs in the range of 1 µM. Urine samples from patients with Crohn's disease treated with azathioprine were diluted 10-fold using water, passed through disposable membrane filters (pore size 0.22 µm), and immediately injected into the CE/MS instrument.

Balderas *et al* [230] analyzed plasma and urine samples from children with type I diabetes mellitus for evaluating the effect of insulin therapy on glycemic control. Even though no remarkable difference was noted between healthy volunteers and patients with diabetes, specific changes were detected, particularly in the levels of proteins, AAs (Ser, Asp, Lys, Val, Leu/Ile, Phe, and Cys in urine), glucose, and hemoglobin glycosylation. Cultured HK-2 proximal tubular cells were used to study diabetic nephropathy. High-glucose level-induced metabolic alterations in HK-2 cells were monitored using three culture treatments: 25 mM glucose (high-glucose group), 5.5 mM glucose (normal-glucose group), and 5.5 mM glucose and 19.5 mM mannitol (osmotic control group). Extra- and intracellular media were studied, and 11 AAs were identified. In the high-glucose group, the major changes were observed in the

extracellular medium, where increased levels of Ala, Pro, Glu, and Cys were detected, along with Amadori products [231].

CE/MS metabolomic analysis was performed for quantifying 60 metabolites in 32 plasma samples collected from male patients exhibiting lower urinary tract symptoms; a multivariate analysis revealed that an increase in the level of Glu and decrease in the levels of Arg, Asp, and inosine monophosphate were statistically significant compare to a control group [232].

Changes in the metabolite levels in plasma samples collected from 33 medication-free patients (who were subsequently treated for 8 weeks) with major depressive disorder (MDD) and 33 non-psychiatric control subjects were investigated in another study. The levels of 33 metabolites differed between the medication-free MDD patients and the control subjects. Several ratios, including kynurenine/Trp, Gln/Glu, and Met/methionine sulfoxide, differed significantly between the two groups. After treatment, the first two ratios normalized, which indicated the mechanism underlying the action of antidepressant agents in MDD [233].

Mutations in glycine cleavage system genes may be associated with schizophrenia. To investigate this, a metabolomic study using five plasma samples from patients harboring glycine cleavage system (CGS) variants and five controls was performed using CE/MS. The PyroGlu, Asp, and Glu levels were found to change, and the Asp levels showed negative correlation with negative symptoms [234].

The global metabolomic alterations associated with the onset of schizophrenia are well recognized. A CE-SF-ESI-MS study on 30 patients with first-episode schizophrenia, 38 healthy controls, and 15 individuals with autism spectrum disorders revealed increased levels of creatine and decreased levels of N,N,N-trimethyl-Gly (betaine), nonanoic acid, benzoic acid, and perillic acid. These changes indicated the abnormalities in Hcy metabolism, hyperCKemia, and oxidative stress [235].

Alteration in the plasma levels of Hcy, Cys, Met, and Glu is a common symptom of amyotrophic lateral sclerosis (ALS). A CE-MS/MS method was validated and yielded RSD values below 6% and 11% for intraday and interday repeats, respectively [236]. In a study on samples from 20 healthy subjects (controls) and 39 patients with ALS, a quantitative comparison of these AAs revealed significantly elevated concentrations of Glu ($p = 0.004$) and Cys ($p = 0.0006$) in the plasma of patients with ALS; however, Met and Hcy concentrations did not differ significantly between the controls and patients.

Identification of metabolites in the sweat of screen-positive infants with cystic fibrosis was performed [237]. Such studies may involve the conventional sweat chloride test [238].

Nontargeted metabolite profiling was performed by multisegment injection-CE-MS [239] as a high-throughput method for the detection of polar/ionic metabolites in sweat samples available in small quantities. Asn and Gln were found to be the two endogenous sweat metabolites associated with asymptomatic affected infants [237].

The metabolomic profiles of feces, urine, and plasma samples from mice with adenine-induced renal failure and control mice housed under germ-free or specific pathogen-free (SPF) conditions were studied. Using CE/MS, the authors evaluated the influence of gut microbiota on the retention of uremic toxins during chronic kidney disease in mice. A total of 183 molecules were quantitated, and the plasma levels of 11 of these molecules were found to be significantly lower in germ-free mice than in SPF mice with renal failure. Microbiota-derived short-chain fatty acids and efficient AA utilization may have exerted a renoprotective effect, and the loss of these factors may have exacerbated renal damage in germ-free mice with renal failure [240].

Homozygous Watanabe heritable hyperlipidemic (WHHL) rabbits have specific symptoms of familial hypercholesterolemia and are model organisms for certain human cardiac pathologies. Using CE-SF-ESI MS, 230 metabolites were analyzed in plasma and tissue samples collected from the liver, aorta, cardiac muscles, and brain of affected and control rabbits. N,N,N-trimethyl-Gly, N,N-dimethyl-Gly, and N-methyl-Gly were found to accumulate in the analyzed tissues (lipid metabolism). 3-methyl-His downregulation was observed in the liver and cardiac muscle, whereas citrulline downregulation was observed in the cardiac muscle and brain. Homoserine, O-acetylserine, and homocarnosine levels were affected as well. When the rabbits were treated with simvastatin, only negligible differences were observed in AA concentrations between the controls and the WHHL group [241].

5.4.3. Metabolomics in food

Diet exerts significant effects on human health. The complete profile of metabolites present in foods, as well as the influence of food production and processing systems (which could alter the metabolome) are unknown. Certain metabolomic studies have been designed to measure the impact of agricultural practices, processing, and storage on global chemical composition of food to identify novel bioactive compounds. This approach could be also used for the authentication and region-of-origin classification [242].

Rice is a common and widely studied plant model. Kusano *et al* [243] published a review summarizing current knowledge on rice metabolites, including sugars, AAs, aromatic

compounds, organic acids, and phytohormones, as analyzed using CE-MS, LC, or GC. In C3 plants, an increase in CO_2 partial pressure enhances photosynthesis, whereas nitrate assimilation and nitrogenated molecule synthesis are inhibited. CE-MS revealed that plants overexpressing NAD kinase 2 show a primary metabolite profile different from that in wild-type plants when CO_2 partial pressure is increased. This could be attributed to the increase in the concentrations of Asn, Gln, Arg, and Lys [244].

Soybean is also a relevant crop in this respect. The metabolite profiles of aphids growing on leaves of resistant and susceptible soybean strains were analyzed using CE-MS. The levels of specific AAs, TCAC components, and glucose-6-phosphate were similar between aphids cultured on Tohoku149 (an aphid-resistant soybean strain) leaves and those cultured under starvation. Two methylated metabolites, S-methyl-Met and trigonelline, were undetectable or present at a lower level in the aphids cultured on Tohoku149 plants. These metabolites are a sulfur carrier and an osmoprotectant, respectively [245].

Root exudates improve nutrient acquisition by plants. Metabolites present in a common bean root exudate were analyzed at different phosphate concentrations. The levels of organic acids and AAs (such as Orn, Arg, Asp, among others) were found to be higher in the exudates of plants grown in the absence of phosphate [246].

Differences in the metabolite profile of two strains of maitake mushrooms (*Grifola frondosa* [Dicks.] Gray) under different conditions of culture on sawdust substrate from trees were studied by Sato *et al* [247] using CE-SF-ESI/MS. The authors conducted a metabolomic study of strains Gf433 and Mori52 by culturing them on sawdust substrate from *Betula ermanii* (birch), and then analyzed the Gf433 strain cultured on sawdust substrate from *Betula ermanii* mixed with sawdust from *Larix leptolepis* (larch). They reported that the AA and organic acid contents in Gf433 were not affected by the type of sawdust. They found that the strain Mori52 contained more AAs, particularly Glu and Orn, than the strain Gf433 did.

Metabolic profiling has also been applied to food quality control. Storage of porcine meat for long durations reduces its quality. CE-MS metabolic profiling has indicated that the levels of glycolytic compounds (and related AAs, *i.e.*, Phe and Tyr), ATP degradation products, and protein hydrolysis products (Met and Tyr) increase with storage time [248]. A similar CE-MS approach was applied in studies on the foot muscle and gills of brackish water clams collected from different areas. Although no metabolite could be used to distinguish between male and female specimens, the β-Ala, choline, GABA, Orn, Gly, and betaine levels were found to vary based on water salinity [249].

5.4.4. Miscellaneous metabolomic studies

Ohashi *et al* [250] introduced sonication treatments during the methanol extraction of metabolites from His-auxotrophic *E. coli* cells. They mentioned that this approach improved the extraction of phosphate-containing molecules. The authors identified 375 charged hydrophilic metabolites, and provided quantitative data on 198 molecules to evaluate the changes in response to His starvation. The intracellular levels of His synthesis intermediates rapidly increased in response to the drop in His levels. TCAC, glycolysis, AA biosynthesis, and nucleotide biosynthesis may be independently activated under conditions of starvation.

The metabolomic profile of *Synechocystis* (a cyanobacterium) has been studied under nitrogen starvation, as nitrogen availability is crucial for the survival of these aquatic and photosynthetic bacteria [251].

The metabolomic profile of dried *Orostachys japonicus* A. Berger, a perennial medicinal herb, has been compared with that of *O. japonicus* fermented with *Lactobacillus plantarum* to elucidate the metabolomic changes induced by the fermentation process. A total of 144 cationic metabolites and 86 anionic ones were identified, and the relative peak areas were determined. Monitoring of the TCAC metabolites (Arg, Glu, Asp, and 2-oxoglutaric acid) revealed that their levels were altered by the fermentation process, which was also observed for components of the urea cycle, as indicated by the significant increase in histamine concentration [252].

An original study combining the advantages of matrix-assisted laser desorption ionization (MALDI) and CE/ESI-MS was performed to study single cells from pancreatic islets. Optically-guided MALDI MS facilitates the high-throughput identification of cellular lipids and peptides; however, it is not quantitative and cannot detect several low-mass metabolites owing MALDI matrix interferences. CE/ESI-MS allows the quantitation of cellular metabolites and offers increased analyte coverage; however, it has a low throughput. A custom liquid microjunction surface sampling device mounted on an xyz translational stage offered 90.6% ± 0.6% analyte removal efficiency. The microjunction component was composed of two concentric capillaries. The outer one delivered an analyte solution for extraction (1:1 methanol/water, 0.5% acetic acid [v/v]), while the inner one aspirated the liquid droplets at the end of the outer capillary. When the microjunction came in contact with a cell, it extracted molecules with a spatial accuracy of 42.8 ± 2.3 μm. The analyte extraction footprint was represented by an elliptical area with the longest diameter of 422 ± 21 μm. Single rat pancreatic islet cells were first analyzed using optically-guided MALDI MS to classify cells into established cell types (α_i, β_i) based on their peptide content. Following this, microjunction

extraction coupled with CE/ESI-MS helped collect qualitative information on metabolites (AAs and dopamine) [253].

6. Medical applications

Some of the most critical studies in the field of AA medical applications involve total Hcy measurement. Researchers have been encouraged by the significant importance of this compound in the diagnosis of cardiovascular diseases. Most published studies have used LIF detection owing to its sensitivity, since Hcy is present at micromolar concentrations in plasma. Although UV detection has also been used, it is either non-sensitive or lacks sufficient selectivity. However, it is considerably less expensive, and sample processing is not mandatory. A number of studies have characterized thiols in biological samples [254].

6.1. Hcy and aminothiols

6.1.1. Laser-induced fluorescence detection

Several strategies to analyze these molecules using CE/LIF have been implemented. Carboxylic function labeling with 5-(bromomethyl) fluorescein reduced the analysis time to less than 2 min, and the resulting sensitivity was better than 0.19 µM for all analyzed compounds. The usefulness of carboxylate derivatization for diagnostic purposes was confirmed in a study on 91 patients (79 with cystinuria and 12 with homocystinuria) [154]. The amine group can also be modified [255] with FITC to study the plasma samples from patients. Nonetheless, these two methods detect all the AAs and lack selectivity. The thiol group was successfully derivatized using fluorescein-5-maleimide, and Cys, Hcy, and GSH could be selectively detected [153]. However, this approach gave rise to two peaks for each thiol owing to the presence of diastereoisomers after derivatization.

The most commonly used reactant of thiols is 5-IAF [256,257]. Preanalytical conditions were studied [258], and multicenter comparisons between CE-LIF studies and other techniques were also performed [259,260]. An ultrarapid CE-LIF method for the quantitation of total thiols in plasma was reported by Zinellu *et al* [261]; this method involved the use of 75 mM N-methyl-D-glucamine buffer (pH 11). The thiols reduced by tri-n-butylphosphine reacted with 5-IAF, and the baseline separation of total plasma Cys-Gly, Hcy, Cys, and GSH required 5 min. The same authors have published several articles on assays of thiols in biological media and described the quantification of reduced and total forms of thiols in erythrocytes. To minimize

the oxidation of reduced thiols, the erythrocytes were lysed in water (15 min at 4 °C), following which protein precipitation was performed using acetonitrile. The supernatant was rapidly derivatized with 5-IAF to minimize auto-oxidation. Under these conditions, Cys-Gly, Cys, GSH, and γ-glutamylcysteine (Glu-Cys) were separated within 4 min. The influence of the acidic precipitation on intracellular thiol concentration was investigated, and the data suggested that sample acidification modified the measured redox thiol status owing to the establishment of a pro-oxidant environment. Similarly, the thiol redox status of erythrocytes was evaluated in 22 healthy volunteers [262]. The thiol-containing AAs linked by disulfide bonds to low-density lipoprotein (LDL) were also quantitated [263], and the levels of Hcy linked to LDL were measured in 16 patients with acute myocardial infarction and 32 healthy volunteers [264]. In the subjects with acute myocardial infarction, an increase in the levels of apo-B Hcy and Cys linked to LDL was observed. This finding suggests that LDL S-homocysteinylation may serve as a marker for cardiovascular-risk evaluation. In a study on 104 healthy patients, Hcy, Cys, Cys-Gly, Glu-Cys, and GSH bound to LDL were quantitated. The study showed that among the thiol-containing AAs, only the total plasma Hcy content was related to apoB-Hcy concentrations [265]. The same separation method was used to quantitate Cys and Hcy in 124 healthy patients (44 women and 80 men, age: 50 ± 10 years). The mean levels of Hcy and Cys were ~11 and 284 μM, respectively. To be precise, 90% subjects in this group had Hcy levels <15 μM, as the samples were obtained from a healthy population. Univariate Pearson's analysis revealed a correlation between the white blood cell count and serum Hcy and Cys levels in healthy subjects [266]. Similarly, Pinna *et al* [267] measured the plasma levels of Hcy and Cys in healthy subjects and patients with retinal vein occlusion. The mean plasma concentration of Cys was significantly higher in patients with retinal vein occlusion. Hypercysteinemia may have contributed to the pathogenesis of this disorder. Furthermore, using the same method, the levels of intracellular thiols in human umbilical vein endothelial cells, ECV304 cells, and R1 stem cells were investigated [268], and an increase in the injection volume was observed to be necessary.

Total, reduced, and free (of protein) thiols, and for comparison, protein-bound plasma thiols, were quantified by varying the order of disulfide reduction and protein precipitation. After derivatization with 5-IAF, CE/LIF (at 488 nm) was performed to measure the total and oxidized Hcy, Cys, Cys-Gly, Glu-Cys, and GSH levels. More than of 50% of these thiols were shown to be protein-bound, except GSH (30%). It was found that 3% Hcy and 4.5% Cys molecules were in the reduced form (Fig. 8) [269].

N-acetyl-L-cysteine (NAC), a widely used mucolytic agent, may alter the plasma levels of some low-molecular-mass thiols. Zinellu *et al* [270] described a CE method using which NAC was baseline-separated from other physiological thiols. The suggested method was used to measure the levels of this drug and those of Hcy, Cys, Cys-Gly, Glu-Cys, and GSH in NAC-treated patients with chronic obstructive bronchopneumopathy. There was no evidence of the effect of NAC on the concentration of plasma thiols.

Other studies have also addressed this topic: in-column derivatization was designed for a fully automated assay of Hcy and other thiols. The method involved the direct injection of a sample containing Hcy and 4-aminosulfonyl-7-fluoro-2,1,3-benzoxadizole, which reacted for 10 min at 50 °C. Hcy was detected within 7 min, and the LOD achieved for Hcy with LIF detection was 5.0 nM, as compared to 2.5 nM obtained using precolumn LIF detection [158].

6.1.2. UV absorbance detection

Zinellu *et al* [271] reported an original application for the quantitation of biological thiols, including Cys, Hcy, cysteine, Hcy-thiolactone, and Hcy-cysteine. These molecules were reduced using $CuSO_4$, with thiolactone serving as an internal standard. CE/UV detection (at 190 and 232 nm) was performed in 40 mM Tris solution (pH 1.6), and an overpressure of 0.1 psi was applied from the inlet to the outlet. The LOD obtained was ~1 µM. Furmaniak *et al* [272] analyzed Hcy-thiolactone in urine using CE/UV (at 240 nm). This molecule was found to be an efficient predictor of mortality of cardiovascular patients. Field-amplified sample injection and sweeping MEKC were performed for this application. The stacking method required two different BGE systems (including one with SDS).

Zinellu *et al* [273] also published a method for detecting Met in samples where analyte derivatization should be avoided owing to low sample concentration. Met was detected by UV absorbance (204 nm) using an acidic Tris-phosphate buffer. The performance of the assay was evaluated by measuring Met concentrations in patients with retinal venous occlusion.

UV absorbance was also used with 2,2′-dipyridyl disulfide for Hcy detection. Reaction with Hcy induced the equimolar formation of 2-thiopyridone, which was separated using MEKC and detected at 343 nm. The concentration of Hcy could be calculated from the result of 2-thiopyridone detection [274].

Kubalczyk *et al* [275] proposed the derivatization of thiols using 2-chloro-1-methylquinolinium tetrafluoroborate and the separation (from plasma) and detection of a Hcy-2-S-quinolinium derivative using CE/UV with acetonitrile stacking. Zhang *et al* [276] reported

a CE/UV method without Hcy derivatization. Significantly higher Hcy concentrations were detected in patients with Alzheimer's disease than in controls. The elevated plasma Hcy levels could be attributed to environmental factors than genetic ones, such as mutations in N^5,N^{10}-methylenetetrahydrofolate reductase or cystathionine β-synthase genes.

6.2. Studies on dimethylarginines and other methylated species

Dimethylarginines are potent endogenous inhibitors of nitric oxide synthase (NOS) and accumulate in the plasma of patients with renal failure, peripheral arterial occlusive disease, or clinically asymptomatic hypercholesterolemia. These have been studied using CE/LIF, CE/UV, and CE/C^4D.

As Arg and its derivatives are basic molecules, they migrate more rapidly than most other AAs. This property is important because it facilitates their separation. Caussé *et al* reported a method for the separation of symmetric and asymmetric dimethylarginine (SDMA and ADMA), N^G-monomethyl-L-arginine, and Arg in a simple boric acid/CAPS buffer (pH 10) using homoarginine as an internal standard after derivatization with FITC (with LIF detection at 488 nm). The variation in ADMA levels was compared between serum samples collected from healthy subjects and subjects undergoing hemodialysis [277]. In another study, the separation of mixtures containing SDMA, ADMA, N^G-monomethyl-L-arginine, Arg, homoarginine, Orn, and L-citrulline, labeled as 4-fluoro-7-nitrobenzofurazan derivatives, was accomplished [278] using borate/deoxycholic acid at pH 9.4 as the BGE. ADMA levels were measured in plasma at 0.125 µM using LIF (at 488 nm).

Zinellu *et al* [279] measured the ADMA, SDMA, and Arg concentrations in human plasma using CE/UV (200 nm, no derivatization) after acetonitrile/ammonia (90:10) protein precipitation, centrifugation, and filtration on a microconcentrator. The sample was evaporated and diluted in water prior to CE. A water plug was injected for 1 s (0.5 psi), followed by sample injection for 10 s (0.5 psi). Separation was performed in Tris-phosphate buffer. The recovery rates of plasma ADMA were between 101% and 104%.

Methylarginines are potent vasoconstrictors present at elevated concentrations in the blood of patients with cardiovascular diseases, and must be rapidly quantified in serum. For this purpose, samples are rapidly heated (at 100 °C for 1.5 min) and NDA/CN-derivatized before separation by CE-LIF (using a 445-nm diode laser) [280].

A CE technique was designed by Tuma *et al* [55] for assaying urinary methylhistidine (MH). 3-MH, 1-MH, and His were separated in both acidic and alkaline media, where these AAs form cations and anions, respectively. The effective mobility of all ionic forms was measured over a broad pH range (1.67–11.80). 3-MH and 1-MH were quantified along with creatinine in untreated urine samples with LODs of 2.4 and 3.0 μM, respectively. Separation was performed using an acetic acid/Tris/hydroxyethyl cellulose electrolyte. The analysis revealed differences between healthy individuals and patients, with more extensive degradation of muscle proteins observed in the second group.

6.3. Other clinical studies

6.3.1. CE/LIF studies

CE is also typically used for separating, characterizing, and quantifying AAs in inflammation. For instance, CE-LIF of NBD derivatives (488 nm) was performed to quantify Lys and cadaverine in dental and tongue biofilms and saliva before and after oral hygiene restriction [281,282]. NBD-F-derivatized GABA was quantitated in the CSF of 24 neuropediatric patients receiving different antiepileptic treatments; the data were compared with those obtained from 55 healthy individuals. The investigators noticed an increase in GABA concentration when CSF was maintained at room temperature for 0.5 to 5 h. They established reference values for children of different age groups at less than or above 6 months of age: 48 and 66 nM respectively. Higher concentrations were recorded in neuropediatric patients undergoing antiepileptic treatments [283].

Sbrana *et al* [284] optimized a CE/LIF (He-Cd laser, 325 nm) method for the measurement of the ratio between S-adenosyl-L-Hcy and S-adenosyl-L-methionine, which can be used to assess antiviral potency *in vivo*. After chloroacetaldehyde derivatization, the separation and quantitation of S-adenosyl-L-Hcy and S-adenosyl-L-methionine in human plasma were achieved in less than 1 min. The same group of researchers also showed that in patients infected with human immunodeficiency virus (HIV), disease progression is associated with a decrease in GSH and Cys levels [285].

Two sensitive and reproducible CE/LIF (488 nm) and HPLC-fluorescence procedures were designed for the quantitative detection of L-ergothioneine. Patients affected by autoimmune disorders such as rheumatoid arthritis and Crohn’s disease present with high levels of L-ergothioneine in blood. In one study, 5-IAF was used for L-ergothioneine quantitation by

precolumn derivatization in plasma, and an LOD of 0.27 μM was recorded [286]. Serum L-ergothioneine, taurine, Hcy, Cys, GSH, Cys-Gly, and Glu-Cys were quantitated in 439 subjects using the method mentioned last. The reference range of L-ergothioneine was established (0.36 to 3.08 μM in healthy subjects), and the authors showed that age and plasma Glu-Cys levels are independent factors negatively associated with L-ergothioneine concentration [287].

Bipolar disorder (BD) is a common psychiatric disorder. Literature data show that patients with BD have higher plasma concentrations of Glu, Gln, and Gly, and these AAs act as possible biomarkers of this pathology. A CE method was designed for measuring the levels of AAs in patients with BD and to monitor the effects of medical treatment. CE/LIF (488 nm) of NBD-F–derivatized plasma was performed for separating D-Ser, L-Ser, and nine other AAs. The method was successfully used for the diagnosis of BD and its progression [288].

CE/LIF (488 nm) of CBQCA-labeled AAs from plasma (using a 488-nm Ar ion laser) of patients with phenylketonuria, tyrosinemia, maple syrup urinary disease, hyperornithinemia, or citrullinemia was performed in a study [111]. Twenty-nine AAs (barring Trp) were detected and could be reproducibly separated in 70 min. Existing literature shows that Trp is difficult to identify using CBQCA derivatization owing to its poor fluorescence properties [289]. The use of NDA was also proposed for the separation of 21 AAs using CE/LEDIF (405 nm) in plasma [290]. The authors used 5% polyvinylpyrrolidone as a sieving medium with acetonitrile and SDS in the BGE. Tyr and Trp have also been quantified using CE/UV-LIF (266 nm) in CSF [78]; native fluorescence can serve as an alternative to visible LIF for aromatic-AA detection. In a study, CE-LIF and a near-infrared laser (785 nm) were used to analyze Tyr and nitrotyrosine in biological media. A near-infrared dye was used to label these compounds and was compared to FITC and NBD-F (both using a 488-nm laser). Micromolar concentrations of the AAs were detected in sinus washes [291]. Inborn errors of metabolism were diagnosed using urine samples from children, as the early detection of the AAs implicated in metabolic diseases enables early initiation of compensatory therapies. In a CE/LIF (488 nm) experiment for the separation and quantification of FITC-labeled pyroglutamic acid, Tyr, Phe, Val, Pro, Gly, and sarcosine, 130 mM 18C6H4 was used as the BGE [292].

D-AAs play an important physiological role; as reviewed above, they have rarely been assayed in clinical studies. Yet, in rats, the concentration of D-Ala in the anterior pituitary and islets of Langerhans increased in response to glucose stimulation. NDA-labeled D-AAs were chirally separated and quantified using CE-LIF (440 nm, diode laser) in a formamide-based electrolyte containing hydroxypropyl γ-CD (nonaqueous CE separation); however, a D-amino

acid oxidase pretreatment and preconcentration step was required [293]. CE-LIF has also been used to quantitate L-Met, L-Cys, taurine, and GSH in the livers of male and female rats to test whether the glutamyl cycle is gender-specific [294].

6.3.2. CE/UV

2,4-Dinitrofluorobenzene, a AA reactant, has been used for the complete separation of 16 AAs and D-norleucine within 8 min. The running buffer contained 30 mM sodium tetraborate (pH 9.8), isopropyl alcohol, and 30% Brij 35 (825:150:25, v/v/v), and UV detection was performed at 360 nm. The AA concentration was measured in the sera of 32 patients with chronic renal failure. Among them, the levels of Ser, Ile, and Val were significantly lower than those in healthy volunteers ($P < 0.01$), whereas the levels of cystine, Trp, and Phe were significantly higher ($P < 0.01$) [295]. A CE/UV method (not described in the article) helped evaluate the effect of a high-fat meal, orange juice, and antacids (which neutralize stomach acidity) on the absorption of a single oral dose of cycloserine and estimate its pharmacokinetic properties. The pharmacokinetic parameters were found to be minimally affected by orange juice and antacid intake, whereas the high-fat meal delayed the absorption. The administration of cycloserine without a high-fat meal prevented potential alterations in the pattern of absorption [296]. By the simultaneous quantification of multiple markers, better diagnostic value can be achieved for multiple renal function markers in human urine samples. The successful high-throughput separation of creatinine, creatine, uric acid, and *p*-aminohippuric acid was performed using CE/UV. *p*-Aminohippuric acid had an LOD of 1.5 µM and a linear detection range of 1.5–250 µM [297]. Another interesting approach involved the analysis of mixtures containing aminolevulinic acid, porphobilinogen, levulinic acid, and Gly. These compounds were separated at pH 9.3–9.4 and detected using UV spectrophotometry at 205 nm. The method was applied to the culture broth of *Rhodopseudomonas sphaeroides* [298].

Among other studies related to clinical studies, tryptophan derivatives were selectively separated from 24 types of nutraceuticals. A pretreatment system involving a combination of homogeneous liquid-liquid extraction and a sweeping method has been used to separate and quantitate four types of Trp derivatives: 5-hydroxy L-tryptophan, 5-methyl L-tryptophan, 1-methyl L-tryptophan, and L-tryptophan. The LODs following complete separation of the Trp derivatives were at 10-nM levels when UV detection was used [299]. Aromatic AAs (Phe, Tyr, and Trp) are indicative of liver and kidney function. Twenty patients with chronic kidney

disease were shown to have decreased plasma Tyr concentration, with the Phe levels being normal or marginally increased. This simultaneous quantification was realized using CE/UV (200 nm; Fig. 9) [300].

Zinellu *et al* [301] studied the development of a simple free-zone CE method for the simultaneous measurement of creatinine and creatine levels in human plasma. The effects of analytical parameters, such as concentration and pH of Tris-phosphate running buffer and cartridge temperature, on resolution, migration time, peak areas, and separation efficiency were investigated. Effective separation using CE/UV (190 nm) was achieved in less than 8 min. The plasma creatinine levels in 120 healthy subjects were assayed, with marginal changes observed in plasma creatinine and creatine levels after moderate physical exercise. Guanidinoacetic acid, creatinine, and creatine in plasma and urine were quantitated in less than 7.5 min using CE/UV (190 nm) with a BGE with acidic pH in 32 patients, using these molecules as markers of renal function [302]. Guanidinoacetic acid and creatine were quantified using CE/UV (190 nm), whereas total and reduced Hcy were quantified using CE/LIF (after derivatization with 5-IAF and detection at 488 nm) in 16 young volunteers categorized as sedentary individuals and athletes. It was shown that after exercise, the levels of reduced Hcy decreased, total Hcy levels remained unchanged, and the creatine concentration increased [303]. Transient isotachophoresis using MEKC for 3-nitro-tyrosine detection in urine was performed with an LOD of 70 nM; this experiment on AA detection was performed in biological media in one study [304].

6.3.3. CE/C^{4}D

CE/C^{4}D was used by Tuma *et al* for the detection of free AAs in amniotic fluid [54]. Twenty proteinogenic AAs and 12 other biogenic compounds, including ethanolamine, choline, Ala, 2-aminobutyric acid, GABA, creatinine, Orn, carnitine, citrulline, 4-hydroxyproline, 1-MH, and 3-MH, were identified in a separation run of 65 min. Acetic acid and hydroxyethylcellulose served as the running electrolyte. Addition of acetonitrile to the samples improved the separation of AAs. The LODs ranged between 1.5 µM (Arg) and 6.7 µM (Asp). The method was later applied to clinical assays of amniotic fluid samples collected from 20 pregnant women aged above 35 years and 24 pregnant women in whom abnormal fetus development was suspected. The second group of women was found to show systematically enhanced amniotic levels of most AAs studied. More rapid separation was realized using 20% MeOH in the separation buffer, which led to the separation of four branched AAs from seven

other AAs in less than 3 min [305,306]. Venous-arterial differences in Val, Ile, Leu, Ala, and Gln levels in skeletal muscles have also been evaluated [66].

The detection of cystine using capillary isotachophoresis with on-line isotachophoresis sample pretreatment and conductivity detection was performed for monitoring cystine levels in urine samples without sample preparation [307].

We believe that even though the importance of this detection technique is relatively low in clinical studies at present, the studies presented here show how it could be useful for the detection of some AAs associated with clinical diagnostics.

7. AAs in neurochemistry applications

Because microdialysis can be performed on live and freely moving animals, it allows us to collect information regarding the chemical changes that occur in the region of the brain where the microdialysis probe is implanted during specific activities of the animal. As Ringer buffer flows in the probe at a flow rate of several µL/min, and consequently collects the neurotransmitter molecules, the small volumes to be analyzed are well suitable for CE. Accordingly, CE/LIF holds promise as an effective tool in neuroscience, and its applications in various subfields of neuroscience are of interest. In the 1990s, Hernandez *et al* [308] proposed the use microdialysis coupled with CE/LIF for monitoring the increase of Glu and Asp concentrations. The method gained significant and rapid popularity. The authors used NDA and claimed to quantitate AAs at ranges between 10 and 0.01 µM. The approach was then improved by Robert *et al* [309], who analyzed dopamine and noradrenaline in microdialysates using NDA derivatization and measured the basal level of noradrenaline (5 nM) in the rat medial frontal cortex. This was soon followed by the on-line derivatization of 0.5-µL volumes of microdialysates for detecting NDA derivatives of catecholamines, along with Asp and Glu. Using microdialysis, the temporal resolution of 2-min fractions was achieved for the simultaneous monitoring of noradrenaline and Glu concentrations in rat brain cortex microdialysates [310]. Several authors have devised on-line derivatization systems, including the above-mentioned one, in which OPA and BME were used [311,312], as well as another one in which NDA and KCN were used [313], the latter obviating the need for an expensive UV LED source. Using the OPA/BME system, Glu and Asp were assayed in the striatum of anesthetized rats during acute electrical stimulation in the rat brain; the temporal resolution (*i.e.*, the interval between two consecutive collections of a microdialysate) achieved was 12 s, with

an LOD of 200 nM recorded [311]. Using MEKC analysis, Asp, Glu, Ile, Leu, Lys, Met, Phe, taurine, Tyr, and Val were detected at basal concentrations ranging from 1.9 µM (Asp) to 5.3 µM (Val), with a temporal resolution of 3 min. The concentrations of these AAs in the striatum were monitored after K^+ depolarization [312]. In another study, the concentrations of Glu and Asp were measured at 5-s intervals in the striatum of chloral hydrate–anesthetized rats after depolarizing electrical pulses were administered to the prefrontal cortex, followed by injections of tetrodotoxin or depletion of extracellular Ca^{2+}, or after infusion of L-trans-pyrrolidine-2,4-dicarboxylic acid using the dialysis probe [314].

The extracellular concentrations of Glu, Asp, and *O*-phosphoethanolamine have also been analyzed in hippocampal slice cultures and in the striatum of anesthetized rats treated by perfusion with a solution with high K^+ levels or containing a Glu uptake inhibitor. With NDA labeling, basal concentrations of 33 nM for *O*-phosphoethanolamine, 4.4 µM for Glu, and 210 nM for Asp were recorded.

The primary aim in these studies was to initiate microdialysate experiments using the CE/LIF technique, as it can be easily adapted to small sample volumes and low concentrations [315]. However, this idea has certain commercial limitations, as insufficient progress has been made in this area of research compared to that in LC/electrochemical detection. Yet, significant research advances have been realized in various subfields of neuroscience using CE, as recently reviewed by Lapainis and Sweedler [316]. Here, we shall primarily focus on microdialysis assays.

Since the 2000s, state-of-the-art methods have been designed by Parrot *et al* [317] and Nandy and Lunte [318]. Some important studies have been discussed below.

After MEKC optimization and pH adjustment for the separation of Glu, Asp, and GABA labeled with NDA, a dual-probe microdialysis system was used in the striatum of mice to detect nanomolar concentrations of AAs [319]. Two laboratory-made concentric microdialysis probes were glued together (spaced at 0.5 mm). Vigabatrin, an antiepileptic drug, was perfused through the "delivery probe", and then diffused into the extracellular space. The effluent of this probe was directed toward waste. The second probe was continuously infused with artificial CSF collecting vigabatrin, Asp, Glu, GABA, and cysteic acid present in the extracellular space, which were then off-line-labeled with NDA. The authors mentioned that vigabatrin induces alterations in Glu and GABA levels in a drug concentration–dependent manner at the site of biochemical changes; these finding may help develop a better understanding of the mechanism underlying the action of the drug [320].

Five neurotransmitters—dopamine, noradrenaline, GABA, Glu, and Asp—were labeled with NDA/KCN through direct mixing in a collection tube. The authors observed that the sampling time was limited by the minimal volume (5 μL) required for analysis using the automated CE system. The neurotransmitters could be assayed in 667-nL dialysates (collection time: 20 s). The LODs in the dialysis probe were between 1 nM (noradrenaline) and 420 nM (Glu). Temporal resolution enabled the simultaneous monitoring of these molecules in rats, which revealed the increase in GABA concentrations concomitant with seizures, as indicated by the combined electroencephalographic recordings [321].

To achieve better on-line derivatization of microdialysates and to prevent off-line derivatization during in-capillary derivatization, the samples were sandwiched between two plugs (at a reagent-to-sample plug length ratio of 4) of a reagent mixture (NDA/NaCN at 1:1 ratio) at the capillary inlet and then separated. The initial electrophoretic mixing was followed by a zero-potential reaction step before the application of separation voltage. The LODs were found to be identical to those obtained with off-line derivatization, and Asp and Glu were identified in brain microdialysates [322].

Kaul *et al* [323] monitored the levels of carbamathione (a partial noncompetitive inhibitor of N-methyl-D-aspartic acid glutamate receptor), GABA, and Glu in brain microdialysis samples collected from the nucleus accumbens. After the administration of an intravenous dose of carbamathione (200 $mg \cdot kg^{-1}$), a change was observed in the GABA and Glu levels.

On-line derivatization of a microdialysate using OPA/BME was performed using a large-sized and expensive Ar laser functional at 351 nm, and CE separation was performed using hydroxypropyl γ-CD in the BGE. O'Brien *et al* [324] demonstrated the contrasting changes in striatal GABA and D-serine neurotransmitter levels in mice with hyperglutamatergic Tourette's syndrome and obsessive-compulsive disorder–like pathology. This was followed by measurement of the changes in extracellular D-Ser concentrations in the rat striatum in response to stimulation with glutamate agonists and antagonists [325]. In the same manner, on-line microdialysis-CE-LIF analysis was performed with OPA/BME on-line derivatization of the supernatant across an intact larval tiger salamander retina to quantitate D-Ser (Fig. 10) [326].

Li *et al* [327] used a similar on-line derivatization protocol by inserting microdialysis probes into the nucleus accumbens core of rats and achieved 15-s temporal resolution of the AAs in microdialysates. The researchers trained Sprague–Dawley rats to self-administer either 10% ethanol-containing gelatin or nonalcoholic gelatin. An increase in taurine concentration

correlated with the quantity of ethanol consumed ($R^2 = 0.81$), whereas no concentration changes were detectable in the rats that consumed the nonalcoholic gel. A considerable increase in Gly concentration in both groups correlated with the quantity of gel consumed. The highest increase in Gly concentration was observed during the longest time-out period after each delivery of the gel. The anticipation of reinforcement correlated with an increase in Gly levels in the nucleus accumbens. Kasper *et al* [328] performed the microdialysis of the nucleus accumbens core under basal conditions and after potassium stimulation, in response to a novel candidate drug, 4-phenyl-2-N,N-dimethylaminotetralin, and other modulators of 5-HT2C receptor, which were administered by reverse dialysis. The GABA concentrations were measured. The authors stated that the 5-HT2C receptor agonists specifically attenuated a stimulated GABA release in the nucleus accumbens core, whereas 5-HT2C antagonists or inverse agonists did not exert any effect. Under the same conditions but with LIF with a 351-nm diode-pumped solid-state laser, the changes in the time course of the detection of AAs and a neurotransmitter in the rat nucleus accumbens were investigated by Venton *et al* [329]. They showed that following exposure to a predator odor, a rapid and transient increase in the levels of AA neurotransmitters (Glu, Asp, GABA, Gly, and Taurine) correlated with behavioral reactivity to salient stimuli.

NBD-F has been used for the on-line labeling of Ile, Leu, Val, Ala, Gln, and Glu as important indicators of adipocyte lipogenesis. Microdialysis was performed to assess metabolism dynamics of 3T3-L1 cells. The LODs achieved were 400, 200, and 100 nM for Ile, Leu, and Val, respectively [330]. Arg, Lys, Ile, Leu, Met, Phe, Val, GABA, Gln, Ala, Gly, and taurine were studied under the same conditions, and the on-line derivatization was implemented in a 66-cm portion of the capillary (75 µm ID) heated at 80 °C (resulting in a reaction time of 5 min). The separation was realized in a short portion of the capillary in less than 16 s. In this case, the LODs ranged between 0.7 µM (Val) and 6.5 µM (Gln). The microdialysis probes were implanted into the inguinal adipose tissue depot of C57BL/6 mice to record dynamic *in vivo* changes under insulin stimulation via tail vein injection. In this case, the Val, Ala, and taurine concentrations increased by 37%–46% [331].

Microdialysis sampling of cells (with temporal resolution of 20 s) from an immortalized astrocytic cell line (C8-D1A) cultured in direct contact with a porous probe was performed to measure the release of small AAs and amines (labeled with NBD-F) from astrocytes after on-line derivatization. The basal release of Phe, taurine, DL-serine, and Glu was evaluated. Upon stimulation with KCl, the levels of Gly, taurine, and DL-Ser increased drastically by 700%,

185%, and 215%, respectively, whereas the levels of Phe and Val were unaffected. The results of microdialysis were compared with data from the traditional collection of aliquots from cultured cells, which are suitable for measuring static concentrations. While the data were in agreement, the higher temporal resolution of *in vitro* microdialysis-CE enabled measurements that better reflected the dynamic changes in the cells [332].

A mixture of 8 mM heptakis(2,6-di-O-methyl)-β-cyclodextrin and 5 mM 6-monodeoxy-6-mono(3-hydroxy)propylamino-β-cyclo-dextrin was used as a CS to separate L-Glu, D-Asp, and L-Asp. D-Asp is of interest because it modulates adult neural plasticity and embryonic brain development. The extracellular concentrations of these AAs were measured in microdialysis samples from freely moving chicks. The D-Asp concentration decreased during the first week after birth. The potassium-evoked release of D-Asp was observed. D-Asp constituted a greater percentage of total Asp in the extracellular space than in whole-tissue extracts; therefore, the bulk of D-Asp detected in tissues was from the extracellular space [333].

Some of the studies performed in this field were based on the strategy devised by Hernandez *et al* 30 years ago using FITC as a labeling dye [308]. Intracerebral microdialysis in the hippocampus can be used to measure variations in agmatine concentration in the extracellular environment. Even though detectable quantities of this amine were found in the dialysates from probes located in the hippocampus, it was not found in the probes located in the lateral ventricle. The extracellular agmatine levels were shown to be calcium- and impulse-dependent, and eventually, the depolarization of hippocampal neurons was shown to lead to an increase in the extracellular agmatine concentration [334]. Skirezwski *et al* [335] investigated the role of ventral pallidum GABAergic terminals in rats with depressive-like behavior induced by the forced swim test. Changes in GABA levels were monitored in the ventral pallidum during the test. The GABA levels increased significantly during days 1 and 2 during swimming and returned to pre-swimming levels after the test ended. In another study, the GABA, Glu, and agmatine levels in the hippocampus were measured in rats subjected to a ketogenic diet for 2 weeks and were compared to the levels in rats fed a normal rat chow diet. The GABA and agmatine levels were found to increase, whereas there were no changes in Glu levels. The authors concluded that the ketogenic diet altered the levels of various transmitters by favoring inhibitory over excitatory neurotransmitters [336]. Putrescine is another molecule whose concentration was measured in blood droplets collected from patients with Parkinson's disease. A statistically significant increase in erythrocyte putrescine concentration was detected with a

nonsignificant increase in its plasma concentration. This leads us to the following question: Is putrescine causally involved in the pathophysiology of Parkinson's disease [337]?

The levels of FITC-labeled Arg and Glu in gingival crevicular fluid collected from adult patients with chronic periodontitis (versus periodontally healthy controls) were measured using two types of microdialysis probes (normal and U-shaped probes). The two probes yielded the same results, and the increase in Arg and decrease in Glu concentrations were associated with periodontitis [338]. Microdialysis in the medial striatum of young post-hatch domestic chicks suggested that Asp is co-released with Glu and may play a substantial role (distinct from that of Glu) in the striatum [339]. These data indicate that FITC derivatization can be suitable for microdialysate analysis after off-line derivatization, and even though FITC contains several impurities and has relatively low reactivity, it can be used to analyze AAs or biogenic amines present at nanomolar concentrations.

DTAF derivatization has also been applied to investigate focal cerebral ischemia and reperfusion induced by middle cerebral artery occlusion. Microdialysis in the hypothalamus of rats was performed to investigate the dynamic changes in the levels of 14 AAs (Arg, Lys, Trp, Phe, Gln, GABA, Asn, Pro, Ser, Ala, Tau, Gly, Glu, and Asp) during cerebral ischemia/reperfusion. Middle cerebral artery occlusion and reperfusion led to a significant increase in the extracellular levels of these AAs [340]. Additionally, this strategy was adapted to quantitate Arg, Lys, Trp, GABA, l-Ser, Ala, Tau, Gly, Glu, Asp, dopamine, and the neuromodulators D-Ser and *O*-phosphoethanolamine. The levels of neurotransmitters and neuromodulators were observed to be elevated during cerebral ischemia/reperfusion [341].

5-carboxyfluorescein N-succinimidyl ester was used for Glu and Asp quantitation in the microdialysates of rat periaqueductal gray matter. The LODs obtained were below 1 nM, and the basal concentrations of the AAs were measured in the microdialysates and after formalin injection [342].

FQ has also been suggested for this application. Wu *et al* [343] monitored its reaction rates with five neurotransmitters (Ala, taurine, GABA, Gln, and Glu) in artificial CSF. The LODs ranged from 1 to 10 nM. FQ was also used in a study on microdialysates and brain homogenates from rats [344].

In a particular study, microdialysis involving UV-LIF (266 nm) was performed for the detection of fluorescent molecules such as serotonin with pH-mediated in-capillary

preconcentration of samples and a buffer consisting of 80 mM citrate (pH 2.5) and 20 mM hydroxypropyl-β-CD. The reported LOD was 0.25 nM [345].

MS with ESI has also been used to analyze neurotransmitters in microdialysates. This approach was first proposed 25 years ago by Takada *et al* [346], and was developed recently for a crustacean model, *Cancer borealis*. In an attempt to combine CE with MALDI, a simple tool was devised, named pressure-assisted capillary electrophoresis-mass spectrometric imaging platform, in which CE flow and matrix flow (α-cyano-4-hydroxycinnamic acid) from a second capillary were mixed at the tips [347–349] . The resulting flow gently touched the MALDI plate surface, which was controlled mechanically, and moved along the long axis of the plate. A straight and uniform trace was deposited on the MALDI plate and was analyzed using MALDI MS imaging. MALDI imaging of the eluent migrating off the capillary was performed, similar to the process used in CE-ion mobility-MS experiments. The obtained results were compared with LC/MS data. Seventy-one compounds were selectively detected using CE/MALDI [350].

Over the past 20 years, the progress in CE techniques performed using detectors of different types has improved our understanding of the functioning of the brain in animals and humans. Intensive research aimed at identifying and quantifying neurotransmitters associated with the studied functions is conducted almost exclusively through on-line derivatization using microdialysis-CE-LIF devices. However, the popularity of these important studies seems to be transient, as in recent times, virtually no new applications have been reported in neurochemistry.

8. Food analyses

AAs are essential nutritional components in a balanced diet and are present in food either as free AAs or AA residues in proteins. Furthermore, they can help elucidate the origin of a food product. Enantiomeric separation, a single procedure for a complex mixture, rapidity, sensitivity, and repeatability are helpful qualities for identity control and quality control techniques for foods and plants. Enantiomeric separation procedures help determine the impact, if any, of the chiral composition of dietary components on health.

Unfortunately, food product analysis requires the release of AAs from a complex matrix, separation of individual AAs, and AA quantification using calibration standards. Even if the principle remains unchanged, each step has to be adapted to the specifics of the sample at hand.

Owing to this, publications on the development of electrophoretic methods for applications in the food industry have rarely gained ground. Following a spike in the number of publications in 2010, fewer than five studies have been published per year.

Technical developments are mostly related to sample preparation, and in recent years, to the introduction of "omics" tools (CE-MS for food).

Surprisingly, the number of reviews (not focused on the subject but addressing it) is comparatively high. The first review on the use of CE-MS for the determination of AAs in food was published in 2005 by Simo *et al* [351]. In 2007, a review was published that focused on the applications of CE to the analysis of small molecules (free AAs, carbohydrates, organic acids, vitamins, and a variety of antioxidants) in foods [352], which helped establish CE as a useful alternative to chromatographic methods such as HPLC and GC in this field. In 2010, a review focusing on grape-derived products was published, in which different chromatographic methodologies (including CE) as well as several derivatizing reagents used for enological purposes [353] were compared [354]. In the same year, enantiomeric CE separation methods for characterizing AAs, pesticides, and phenols in foods and beverages were studied [355]. A review with a special focus on electromigration methods for the analysis of food constituents, including AAs and biogenic amines, was also published [356]. In 2014, a review was published on CE-based assays (electromigration, microchips, CE/MS, and chiral CE) of biomolecules present in food and beverages [357]. The evolution of AA, protein, lipid, and carbohydrate analyses of food samples using electromigration techniques over a period of 20 years [358] and the use of CE for the analysis of nonproteinogenic AAs [359] were also reviewed.

Last year, there was significant interest regarding methods for assessing food quality and authenticity based on AA determination [360]. Assays on nonproteinogenic AA determination were also reviewed for the period spanning 2015–2018 [361], while three detailed examples of enantioseparation were described by Castro-Puyana and Marina [362].

8.1. AAs in beverages

Most studies on CE for analysis of food products have focused on beverages, and more specifically on fruit juice, tea, beer, and wine.

8.1.1. Juices

The simultaneous analysis of citrus juice components using CE was integrated into a single procedure using a BGE containing 5% of acetonitrile. Biogenic amines, flavonoids, and

aromatic AAs (Trp, Phe, and Tyr) in citrus juice can be used to assess the quality, freshness, and possible adulteration of these products. Simo *et al* [363] successfully differentiated between three types of commercial orange juice (*i.e.*, nectars, orange juice reconstituted from concentrates, and pasteurized orange juices not manufactured using concentrates) by quantitating FITC-labeled L- and D-AAs using MEKC-LIF and β-CD. In addition, the authors also described a new coaxial chiral CE-MS coupling method for separating D- and L-AAs [364]. β-CD was used with a BGE with a coated capillary (ethylpyrrolidine methacrylate-N,N-dimethylacrylamide, a copolymer), which prevented contamination of the electrospray [365]. Under optimum CE-MS conditions, the MS sensitivity levels obtained for FITC- and dansyl-AAs are similar, whereas chiral resolution is more suitable for FITC-AAs. Chiral CE-MS allows the detection of D/L-Asp, -Glu, -Ser, -Asn, -Ala, -Pro, -Arg, and GABA in commercial orange juices (Fig. 11).

A rapid CE separation method was designed to analyze S-adenosyl-L-methionine in fruits and fruit juices without a pre-purification step; this method was found to be 50% more rapid and sensitive than the conventional HPLC technique [366].

Cys and GSH were also quantified in orange juices and soft drinks at micromolar levels using a disulfide reduction step followed by quinolinium derivatization of thiols and separation using CE with acetonitrile stacking [367].

8.1.2. Soft drinks

A rapid CE method was designed for the simultaneous detection of AAs within 17 min in several beverages using 1,2-naphthoquinone-4-sulfonate derivatives ; The LOD obtained for all AAs was 1 $mg \cdot L^{-1}$ [368].

In a particular study, a PMMA chip was used to quantitatively analyze AAs in sports beverages, jelly-form beverages, and tablet-form functional foods. MEKC was coupled with LEDIF detection, and the sample labeling and analysis required less than 10 min [369].

8.1.3. Tea

Seventeen NDA-AA derivatives were quantitatively analyzed within 16 min in tea (*Camellia sinensis*) leaves and beverages using CE/LEDIF (410 nm) [370].

To decrease matrix interference, a methodology was published for the improved analysis of tea samples without pre-purification and pre-concentration. An in-capillary OPA/BME

derivatization procedure combined with stacking CE was used to implement the analytical process at a subnanomolar detection level [371].

Aroma is an essential factor that affects tea quality. Using CE, it was discovered that dark storage significantly raises the levels of most AAs, including L-Phe, a key precursor of phenylpropanoids/benzenoids [372].

In a study, CE was coupled with evaporative light scattering detection. This was combined with a step for sample cleanup using carboxylated single-walled carbon nanotubes. The method was applied to white tea samples [373]. This technique is claimed to have an LOD in the micromolar range; however, a CE system based on this technique is not yet commercially available, nor are the carbon nanotubes.

8.1.4. Beer and wine

Nine AAs, along with serotonin, were detected in wine samples of different origins and vintage using rapid CE/LIF. In the study, DTAF microwave-assisted derivatization was performed, and a direct hydrodynamic injection was applied to commercial Italian wines [374]. An ionic liquid with β-CD and SDS was added to the BGE for a CE assay of AAs with in-capillary OPA/BME labeling of beer samples. Eleven AAs were detected and quantified, indicating the valuable potential applications of this method in food analysis [375].

Saccharomyces cerevisiae growth is known to decrease significantly under acidic conditions. A metabolomics approach was adopted to understand this phenomenon [376]. *S. cerevisiae* was cultured in a lactic acid–containing medium (pH 2.5). The addition of Pro to the culture medium protected the proliferating cells from acid stress. A separation method based on CE/LIF was developed to evaluate AA consumption by yeast during beer fermentation [377].

Trp detection in beer was performed using an isotachophoretic CE process between the leading electrolyte comprising 10 mM HCl, 1% HEC, 20 mM 1,3-bis[tris(hydroxymethyl)methylamino]propane, and 10 mM 6-aminocaproic acid, and the terminating electrolyte, which was 20 mM 2-amino-2-methyl-1,3-propanediol. An LOD of 2.6 $mg \cdot L^{-1}$ was achieved. The results were found to be comparable to those obtained using HPLC [378].

8.1.5. Other beverages

Chiral ligand exchange CE with UV detection has been used for the selection of aromatic D- or L-AAs in rice-brewed suspensions (Laozao) using a Zn(II) complex as a chiral selection agent [379]. Baseline separation of DL-aromatic AAs and partial separation of some 9-fluorenylmethoxycarbonyl–labeled nonaromatic AAs were achieved. Aromatic AAs were found to be present in the millimolar range in Laozao from four different brands.

Jayarajah *et al* [380] devised a portable microCE instrument that could detect biogenic amines with fluorescamine-labeled primary amino groups in fermented beverages within only 120 s using a glass CE device containing 21.4 cm long separation channels.

N-phenylpropenoyl-l-amino acids are important contributors to the astringent taste of cocoa. Crude extracts of defatted seeds were analyzed using CE in less than 30 min [381]. A CE-LIF (488 nm) assay for FITC-labeled Arg, Val, Trp, folic acid, and niacinamide, plus riboflavin (natively fluorescent) in roasted cocoa beans was reported and applied to four health drink samples [382].

In a study, on-line coupling between liquid–liquid extraction and CE/C^4D was tested on complex food matrices with high sodium contents. The sample was prepared in a dextran-rich phase (8% w/v 500 kDa Dextran), and 5.0 M acetic acid with 6% w/v of 6-kDa PEG (the second phase) was used as the BGE. Glu could be quantitated in soy sauces, and Lys, His, Arg, Gly, Ala, Ser, Val, Leu, Asn, Thr, Trp, Met, Tyr, Pro, and Cys could be detected in less than 12.5 min. The LOD for Glu was ~10 µM [383].

An interesting approach was designed using a portable battery-operated CE instrument. The instrument had two capillaries, each equipped with a C^4D detector and different buffers to quantify taurine, niacin (vitamin B3), and choline in energy drinks, fresh and powdered milk, and probiotic green rice. LODs of ~2 µM were achieved [384,385].

In a study, baseline separation of the enantiomers of 11 DL-AAs, detectable as $[AA+18C6H4+H]^+$ ions (*i.e.*, complexed with 18C6H4) was performed successfully using CE-MS, whereas five other AAs were only partially separated. The identification of several D enantiomers in balsamic and red vinegars correlates with fermentation during the manufacturing process. The taste quality of fermented foods can be assessed based on the concentration of D-AAs [386]. Similarly, a CE/MS approach was used successfully to distinguish between low- and high-quality Japanese Ginjo sake [387].

8.2. Milk products

The detection of furosine (ε-N-2-furoylmethyl-L-lysine) in food using CE has been optimized for analyses of pasteurized milk and Mozzarella cheese [388]. Later, a CE method for assaying AAs was developed and validated. The method enabled the separation and detection of important metabolic acids and AAs in yogurt and commercial cheeses. Using this method, 10 AAs were resolved, with an LOD of 2 mM achieved for Gly [389]. A CE/MS metabolomic approach was used to compare a type strain of *Lactococcus lactis* and a GABA-producing strain, *L. lactis* 01-7 [390]. This approach showed that the GABA content was higher in *L. lactis* 01-7–fermented milk. Furthermore, the study also revealed that the Orn levels were 27-fold higher than those in control milk.

AAs from alternative nutritive sources are of interest to some authors. A cheap method was proposed for analyzing FITC-labeled AAs based on CE/LEDIF in Cucurbitaceae milk from Sub-Saharan Africa. Six essential AAs (Phe, Thr, Val, Trp, Ile, and Leu) were detected in the extracts; however, lysine was not detected [391]. *Lathyrus* plants, also known as peavines, represent an alternative protein source; however, excess consumption of these can lead to lathyrism caused by β-N-oxalyl-L-α,β-diaminopropionic acid. A relevant CE/UV (195 nm) detection method was published for its analysis [392].

8.3. Miscellaneous

1-aminocyclopropane-1-carboxylic acid present in apple tissues was detected using MEKC/LIF [393], in which the compound was baseline-separated from other AAs. An LOD of 10 nM was documented without extra purification and enrichment procedures.

MEKC/UV (265 nm) detection of S-alk(en)ylcysteine-S-oxides in 12 commonly consumed alliaceous and cruciferous vegetables (*e.g.*, garlic, onion, leek, chive, cabbage, radish, cauliflower, and broccoli) was developed using FMOC derivatization [394]. The total content of these oxides in the analyzed *Allium* species varied between 0.59 and 12.3 $mg \cdot g^{-1}$ fresh weight.

Cereals are major sources of Phe. A MEKC/UV (200 nm) method was devised to assess the Phe content in cereals [395]. The obtained selectivity and accuracy were found to be comparable with those of an LC-MS/MS method, and the new method could be applied to some cereal products.

A CE/C^4D technique was used to detect free AAs in *Nicotiana tabacum* leaves [396]. Although LODs in the lower micromolar range for the 20 proteinogenic AAs made this system suitable for metabolic studies, Met and Cys could not be detected using this method. In another

study, LC-MS, CE-MS, and GC-MS were utilized for metabolomic analysis of tobacco leaves [397]. Leaf aging clearly led to reduced AA concentrations, especially for Gln or Asn. A similar approach was adopted to investigate the interactions between carbon and nitrogen metabolic pathways in mature tobacco leaves [398].

A metabolomic investigation was performed to analyze glucosinolates, isothiocyanates, sugars, and AAs along with the bacterial loads in rocket salad [399]. CE/MS was employed to simultaneously assay the effects of carbon dioxide supply, nutrient formulation, and LED irradiation on head lettuce production [400].

A novel method for furosine detection in food products using CE-MS/MS was optimized and validated. Solid-phase extraction treatment was applied to different flours and different food products (pasta, milk). Appropriate LOD, recovery, and intraday repeatability values were obtained [401].

A CE-MS/MS method was developed to detect seed-oil adulteration in extra virgin olive oils. This approach enabled the determination of Orn, β-Ala, GABA, alloisoleucine, citrulline, and pyroglutamic acid levels [191]. The suggested method was validated and applied to the identification of the selected nonproteinogenic AAs in various oils. The method was also used for analyzing olive oil adulteration with soybean oil.

The presence of AAs in fermented soy sauce was investigated with a focus on food safety [402] using a Förster resonance energy transfer detection approach with OPA/BME derivatives. Trp concentration was selectively determined, because Trp decomposes when soy is treated by acidic hydrolysis instead of natural fermentation. A sensitivity of approximately 10 nM was achieved for Trp.

9. Conclusion

In conclusion, the most pertinent question is why CE is used instead of LC. The limitations of CE concerning the repeatability are well known. They can be due to the buffering capacities of the electrolyte and to the buffer replenishment. The capillary cutting, the precision of the injection volume and the rinsing steps are also very important. The temperature needs also to be controlled. The commercial instruments, especially those coupled to MS, have cooling capacities for an optimized temperature regulation. When controlling these different parameters, CE will have repeatabilities comparable to LC. Then, CE is more compatible with lower sample volumes than usual LC (few nL vs. few µL). Moreover, it may also be argued that the working cost of a CE run is considerably lower than that of an LC run, in particular because of low buffer volumes (few mL per day for CE vs. few hundred mL for LC). Additionally, in most studies, a simple fused silica capillary is used in CE (costing 10€/m),

which is considerably less expensive than an LC column. Enantiomers are also easier to separate using CE than LC. Lastly, by coupling CE with C^4D detection, the analysis and quantification of AAs in the µM range (and at times in the sub-µM range) can be realized without derivatization, whereas LC-UV requires a derivatization step.

We would like to focus on the learnings from this review. A significant body of research exists on the determination of AAs using CE. Several authors have investigated different means of separation and various method of detection of AAs, using UV, LIF or LEDIF, C^4D, or MS. Therefore, researchers who wish to use CE for AA determination will have access to a lot of information, maybe even excess. This review was our attempt to assist future users of CE in the selection of an appropriate CE method.

For detection of molecules at nanomolar concentrations using CE, CE/LEDIF should be used, and based on the excitation wavelength, one has to select the suitable dye from different dyes, which have also been discussed in this review. Moreover, specificity for the target AA should be considered during selection. Some of these AAs are difficult to detect (*e.g.*, Trp). If AA concentrations are in the micromolar range, C^4D is considerably effective and has been proved to be the best detection method candidate, as the method does not require derivatization and the sample preparation process is simple. The buffers used primarily contain acetic acid at high concentrations with different adjuvants to improve separation. Several other weakly charged molecules, including lactic acid, citric acid, Tris, Ches, MES, and CAPS, can also be used in BGEs for CE-C^4D. In the near future, this detection technique will assist AA applications in clinical biochemistry laboratories. As for CE/UV, its major limitation is the necessity for derivatization, which is not a prerequisite for CE/C^4D. This makes CE/C^4D the preferred method.

When AAs and other small-molecule compounds in micromolar and submicromolar ranges are to be detected using CE, MS is the detection method of choice owing to its selectivity and mass measurement resolution, even though the choice of volatile buffers available is considerably limited. Sensitivity, selectivity, and easily operable devices make MS an impressive detection method even for small ions from AAs. In studies on metabolomics, the use of CE/MS is usually discussed passively. Analytical conditions are usually not presented, and this technique is gradually becoming redundant, even though the impressive results obtained using this method are well-reported.

10. References

[1] V. Poinsot, M.A. Carpéné, J. Bouajila, P. Gavard, B. Feurer, F. Couderc, Recent advances in amino acid analysis by capillary electrophoresis, Electrophoresis. 33 (2012) 14–35. https://doi.org/10.1002/elps.201100360.

[2] V. Poinsot, V. Ong-Meang, A. Ric, P. Gavard, L. Perquis, F. Couderc, Recent advances in amino acid analysis by capillary electromigration methods: June 2015–May 2017, Electrophoresis. 39 (2018) 190–208. https://doi.org/10.1002/elps.201700270.

[3] V. Poinsot, V. Ong-Meang, P. Gavard, F. Couderc, Recent advances in amino acid analysis by capillary electromigration methods, 2013-2015, Electrophoresis. 37 (2016) 142–161. https://doi.org/10.1002/elps.201500302.

[4] V. Poinsot, V. Ong-Meang, P. Gavard, F. Couderc, Recent advances in amino acid analysis by capillary electromigration methods, 2011-2013, Electrophoresis. 35 (2014) 50–68. https://doi.org/10.1002/elps.201300306.

[5] V. Poinsot, P. Gavard, B. Feurer, F. Couderc, Recent advances in amino acid analysis by CE, Electrophoresis. 31 (2010) 105–121. https://doi.org/10.1002/elps.200900399.

[6] V. Poinsot, M. Lacroix, D. Maury, G. Chataigne, B. Feurer, F. Couderc, Recent advances in amino acid analysis by capillary electrophoresis, Electrophoresis. 27 (2006) 176–194. https://doi.org/10.1002/elps.200500512.

[7] V. Poinsot, C. Bayle, F. Couderc, Recent advances in amino acid analysis by capillary electrophoresis, Electrophoresis. 24 (2003) 4047–4062. https://doi.org/10.1002/elps.200305692.

[8] V. Poinsot, A. Rodat, P. Gavard, B. Feurer, F. Couderc, Recent advances in amino acid analysis by CE, Electrophoresis. 29 (2008) 207–223. https://doi.org/10.1002/elps.200700482.

[9] L. Denoroy, S. Parrot, Analysis of Amino Acids and Related Compounds by Capillary Electrophoresis, Sep. Purif. Rev. 46 (2017) 108–151. https://doi.org/10.1080/15422119.2016.1212378.

[10] Y. Song, C. Xu, H. Kuroki, Y. Liao, M. Tsunoda, Recent trends in analytical methods for the determination of amino acids in biological samples, J. Pharm. Biomed. Anal. 147 (2018) 35–49. https://doi.org/10.1016/j.jpba.2017.08.050.

[11] G. Lunn, L.C. Hellwig, Handbook of Derivatization Reactions for HPLC, Wiley-Interscience, 1998.

[12] T. Toyo'oka, Modern derivatization methods for separation sciences, Wiley and sons, 1999. http://centlib.ajums.ac.ir/multiMediaFile/58841790-4-1.pdf.

[13] M.T. Kelly, H. Fabre, D. Perrett, Determination of taurine in plasma by capillary zone electrophoresis following derivatisation with fluorescamine, Electrophoresis. 21 (2000) 699–705. https://doi.org/10.1002/(SICI)1522-2683(20000301)21:4<699::AID-ELPS699>3.0.CO;2-Z.

[14] N. V. Komarova, J.S. Kamentsev, A.P. Solomonova, R.M. Anufrieva, Determination of amino acids in fodders and raw materials using capillary zone electrophoresis, J. Chromatogr. B Anal. Technol. Biomed. Life Sci. 800 (2004) 135–143. https://doi.org/10.1016/j.jchromb.2003.08.052.

[15] J.W. Jorgenson, K.D.A. Lukacs, Zone Electrophoresis in Open-Tubular Glass Capillaries, Anal. Chem. 53 (1981) 1298–1302. https://doi.org/10.1021/ac00231a037.

[16] Z. Chen, K. Uchiyama, T. Hobo, Chiral resolution of dansyl amino acids by ligand exchange-capillary electrophoresis using Cu(II)-L-prolinamides as chiral selector, Anal. Chim. Acta. 523 (2004) 1–7. https://doi.org/10.1016/j.aca.2004.07.024.

[17] Z. Chen, M. Niitsuma, T. Nakagama, K. Uchiyama, T. Hobo, Enantioseparations of dansyl amino acids by capillary electrophoresis using Cu(II) complexes with L-amino acylamides as chiral selectors in electrolytes, J. Sep. Sci. 25 (2002) 1197–1201. https://doi.org/10.1002/1615-9314(20021101)25:15/17<1197::AID-JSSC1197>3.0.CO;2-2.

[18] L. Qi, G. Yang, Enantioseparation of dansyl amino acids by ligandexchange capillary electrophoresis with zinc(II)-L-phenylalaninamide complex, J. Sep. Sci. 32 (2009) 3209–3214. https://doi.org/10.1002/jssc.200900328.

[19] X. Mu, L. Qi, J. Qiao, X. Yang, H. Ma, Enantioseparation of dansyl amino acids and dipeptides by chiral ligand exchange capillary electrophoresis based on Zn(II)-l-hydroxyproline complexes coordinating with γ-cyclodextrins, Anal. Chim. Acta. 846 (2014) 68–74. https://doi.org/10.1016/j.aca.2014.07.022.

[20] Y. Su, X. Mu, L. Qi, Development of a capillary electrophoresis system with Mn(II) complexes and β-cyclodextrin as the dual chiral selectors for enantioseparation of dansyl amino acids and its application in screening enzyme inhibitors, RSC Adv. 5 (2015) 28762–28768. https://doi.org/10.1039/C5RA02744F.

[21] G. Nouadje, F. Couderc, P. Puig, L. Hernandez, Combination of micellar electrokinetic chromatography and laser-induced fluorescence detection for the determination of presser amines and some principal amine acids in wine. J. Cap Electrophoresis, 1995, 2, 117, J Cap Elec. 2 (1995) 117–123.

[22] J. Ols, L. Cvak, Enantioseparation of dansyl amino acids on Part I : Capillary electrophoretic separation, J. Sep. Sci. (2003) 851–856. https://doi.org/10.1002/jssc.200301440.

[23] S. Ren, S. Xue, X. Sun, M. Rui, L. Wang, Q. Zhang, Investigation of the synergistic effect of chiral ionic liquids as additives in non-aqueous capillary electrophoresis for enantioseparation, J. Chromatogr. A. 1609 (2020) 460519. https://doi.org/10.1016/j.chroma.2019.460519.

[24] D.H. Rosenblatt, P. Hlinka, J. Epstein, Use of 1 , 2-Naphthoquinone-4-sulfonate for the estimation of ethylenimine and primary Amines, Anal. Chem. 27 (1955) 1290–1293. https://doi.org/10.1021/ac60104a024.

[25] R.M. Latorre, J. Saurina, S. Hernández-Cassou, Determination of amino acids in overlapped capillary electrophoresis peaks by means of partial least-squares regression, J. Chromatogr. A. 871 (2000) 331–340. https://doi.org/10.1016/S0021-9673(99)00853-5.

[26] R.M. Latorre, J. Saurina, S. Hernández-Cassou, Resolution of overlapped peaks of amino acid derivatives in capillary electrophoresis using multivariate curve resolution based on alternating least squares, Electrophoresis. 21 (2000) 563–572. https://doi.org/10.1002/(SICI)1522-2683(20000201)21:3<563::AID-ELPS563>3.0.CO;2-5.

[27] R.M. Latorre, J. Saurina, S. Hernández-Cassou, Sensitivity enhancement by on-line preconcentration and in-capillary derivatization for the electrophoretic determination of amino acids, Electrophoresis. 22 (2001) 4355–4361. https://doi.org/10.1002/1522-2683(200112)22:20<4355::AID-ELPS4355>3.0.CO;2-T.

[28] Y. Zhang, F.A. Gomez, On-column derivatization and analysis of amino acids, peptides, and alkylamines by anhydrides using capillary electrophoresis, Electrophoresis. 21 (2000) 3305–3310. https://doi.org/10.1002/1522-2683(20000901)21:15<3305::AID-ELPS3305>3.0.CO;2-1.

[29] Z. Glatz, On-capillary derivatisation as an approach to enhancing sensitivity in capillary electrophoresis, Electrophoresis. 36 (2015) 744–763. https://doi.org/10.1002/elps.201400449.

[30] A.S. Ptolemy, P. Britz-McKibbin, Sample preconcentration with chemical derivatization in capillary electrophoresis: Capillary as preconcentrator, microreactor and chiral selector for high-throughput metabolite screening, J. Chromatogr. A. 1106 (2006) 7–18. https://doi.org/10.1016/j.chroma.2005.11.012.

[31] A.S. Ptolemy, P. Britz-McKibbin, Single-step analysis of low abundance phosphoamino acids via on-line sample preconcentration with chemical derivatization by capillary electrophoresis, Analyst. 130 (2005) 1263. https://doi.org/10.1039/b504480d.

[32] S. Oguri, Y. Yoneya, M. Mizunuma, Y. Fujiki, K. Otsuka, S. Terabe, Selective detection of biogenic amines using capillary electrochromatography with an on-column derivatization technique, Anal. Chem. 74 (2002) 3463–3469. https://doi.org/10.1021/ac025592d.

[33] D. Koval, J. Jirásková, K. Střížovský, J. Konvalinka, V. Kašička, Capillary electrophoresis method for determination of D-serine and its application for monitoring of serine racemase activity, Electrophoresis. 27 (2006) 2558–2566. https://doi.org/10.1002/elps.200500946.

[34] F.M. Lin, H.S. Kou, S.M. Wu, S.H. Chen, A.L. Kwan, H.L. Wu, An ionizable chromophoric reagent for the analysis of primary amine-containing drugs by capillary electrophoresis, Electrophoresis. 26 (2005) 621–626. https://doi.org/10.1002/elps.200410282.

[35] J.H. Lee, O.-K. Choi, H.S. Jung, K.-R. Kim, D.S. Chung, Capillary electrophoresis of nonprotein and protein amino acids without derivatization, Electrophoresis. 21 (2000) 930–934. https://doi.org/10.1002/(SICI)1522-2683(20000301)21:5<930::AID-ELPS930>3.0.CO;2-8.

[36] M.W. Crowder, A. Numan F., Haddadian, M. Weitzel, N.D. Danielson Capillary electrophoresis of phosphoamino acids with indirect photometric detection, Anal. Chim. Acta. 384 (1999) 127–133. https://doi.org/10.1016/S0003-2670(98)00810-1.

[37] G. Žunić, Z. Jelić-Ivanović, M. Čolić, S. Spasić, Optimization of a free separation of 30 free amino acids and peptides by capillary zone electrophoresis with indirect absorbance detection: A potential for quantification in physiological fluids, J. Chromatogr. B Anal. Technol. Biomed. Life Sci. 772 (2002) 19–33. https://doi.org/10.1016/S1570-0232(02)00014-4.

[38] R. Sekar, S. Azhaguvel, Indirect photometric assay determination of gabapentin in bulk drug and capsules by capillary electrophoresis, J. Pharm. Biomed. Anal. 36 (2004) 663–667. https://doi.org/10.1016/j.jpba.2004.07.033.

[39] G.D. Žunić, S. Spasić, Z. Jelić-Ivanović, Capillary Electrophoresis of Free Amino Acids in Physiological Fluids Without Derivatization Employing Direct or Indirect Absorbance Detection, in: M.A. Altermann (Ed.), Amin. Acid Anal. Methods Protoc., Second Ed., Humana Press, New York, 2019: pp. 315–327. https://doi.org/10.1007/978-1-61779-445-2_19.

[40] X. Xu, Z. Jia, Y. Shu, L. Liu, Dynamic pH junction-sweeping technique for on-line concentration of acidic amino acids in human serum by capillary electrophoresis with indirect UV detection, J. Chromatogr. B Anal. Technol. Biomed. Life Sci. 980 (2015) 20–27. https://doi.org/10.1016/j.jchromb.2014.12.009.

[41] H. Ren, X. Liu, S. Jiang, Preconcentration of 3-nitrotyrosine in urine by transient isotachophoresis in MEKC, J. Pharm. Biomed. Anal. 78–79 (2013) 100–104. https://doi.org/10.1016/j.jpba.2013.02.002.

[42] L. Zhang, Y. Liu, G. Chen, Simultaneous determination of allantoin, choline and L-arginine in Rhizoma Dioscoreae by capillary electrophoresis, J. Chromatogr. A. 1043 (2004) 317–321. https://doi.org/10.1016/j.chroma.2004.06.003.

[43] X. Jiang, Z. Xia, W. Wei, Q. Gou, Direct UV detection of underivatized amino acids using capillary electrophoresis with online sweeping enrichment, J. Sep. Sci. 32 (2009) 1927–1933. https://doi.org/10.1002/jssc.200900013.

[44] Y.H. Tak, G.W. Somsen, G.J. De Jong, Optimization of dynamic pH junction for the sensitive determination of amino acids in urine by capillary electrophoresis, Anal. Bioanal. Chem. 401 (2011) 3275–3281. https://doi.org/10.1007/s00216-011-5445-x.

[45] J. Hlaváček, M. Vítovcová, P. Sázelová, J. Pícha, V. Vaněk, M. Buděšínský, J. Jiráček, D.M. Gillner, R.C. Holz, I. Mikšík, V. Kašička, Mono-N-acyl-2,6-diaminopimelic acid derivatives: Analysis by electromigration and spectroscopic methods and examination of enzyme inhibitory activity, Anal. Biochem. 467 (2014) 4–13. https://doi.org/10.1016/j.ab.2014.08.032.

[46] Y. Henchoz, J. Schappler, L. Geiser, J. Prat, P.A. Carrupt, J.L. Veuthey, Rapid determination of pK a values of 20 amino acids by CZE with UV and capacitively coupled contactless conductivity detections, Anal. Bioanal. Chem. 389 (2007) 1869–1878. https://doi.org/10.1007/s00216-007-1568-5.

[47] L. Yang, Z. Yuan, Determination of dissociation constants of amino acids by capillary zone electrophoresis, Electrophoresis. 20 (1999) 2877–2883. https://doi.org/10.1002/(SICI)1522-2683(19991001)20:14<2877::AID-ELPS2877>3.0.CO;2-Q.

[48] A.J. Zemann, E. Schnell, D. Volgger, G.K. Bonn, Contactless Conductivity Detection for Capillary Electrophoresis, Anal. Chem. 70 (1998) 563–567. https://doi.org/10.1021/ac9707592.

[49] J.A. Fracassi da Silva, C.L. do Lago, An Oscillometric Detector for Capillary Electrophoresis, Anal. Chem. 70 (1998) 4339–4343. https://doi.org/10.1021/ac980185g.

[50] P. Kubáň, P.C. Hauser, 20th anniversary of axial capacitively coupled contactless conductivity detection in capillary electrophoresis, TrAC Trends Anal. Chem. 102 (2018) 311–321. https://doi.org/10.1016/j.trac.2018.03.007.

[51] P. Coufal, J. Zuska, T. van de Goor, V. Smith, B. Gaš, Separation of twenty underivatized essential amino acids by capillary zone electrophoresis with contactless conductivity detection, Electrophoresis. 24 (2003) 671–677. https://doi.org/10.1002/elps.200390079.

[52] J. Tanyanyiwa, K. Schweizer, P.C. Hauser, High-voltage contactless conductivity detection of underivatized amino

acids in capillary electrophoresis, Electrophoresis. 24 (2003) 2119–2124. https://doi.org/10.1002/elps.200305422.
[53] A. Rainelli, P.C. Hauser, Fast electrophoresis in conventional capillaries by employing a rapid injection device and contactless conductivity detection, Anal. Bioanal. Chem. 382 (2005) 789–794. https://doi.org/10.1007/s00216-005-3063-1.
[54] E. Samcová, P. Tůma, Determination of Proteinogenic Amino Acids in Human Plasma by Capillary Electrophoresis with Contactless Conductivity Detection, Electroanalysis. 18 (2006) 152–157. https://doi.org/10.1002/elan.200503380.
[55] P. Tůma, E. Samcová, F. Opekar, V. Jurka, K. Štulík, Determination of 1-methylhistidine and 3-methylhistidine by capillary and chip electrophoresis with contactless conductivity detection, Electrophoresis. 28 (2007) 2174–2180. https://doi.org/10.1002/elps.200600697.
[56] P. Tůma, K. Málková, E. Samcová, K. Štulík, Rapid monitoring of arrays of amino acids in clinical samples using capillary electrophoresis with contactless conductivity detection, J. Sep. Sci. 33 (2010) 2394–2401. https://doi.org/10.1002/jssc.201000137.
[57] W. Pormsila, R. Morand, S. Krähenbühl, P.C. Hauser, Capillary electrophoresis with contactless conductivity detection for the determination of carnitine and acylcarnitines in clinical samples, J. Chromatogr. B Anal. Technol. Biomed. Life Sci. 879 (2011) 921–926. https://doi.org/10.1016/j.jchromb.2011.02.046.
[58] M. Dvořák, L. Ryšavá, P. Kubáň, Capillary Electrophoresis with Capacitively Coupled Contactless Conductivity Detection for Quantitative Analysis of Dried Blood Spots with Unknown Blood Volume, Anal. Chem. 92 (2020) 1557–1564. https://doi.org/10.1021/acs.analchem.9b04845.
[59] M.S. Ferreira Santos, T.G. Cordeiro, A.C. Noell, C.D. Garcia, M.F. Mora, Analysis of inorganic cations and amino acids in high salinity samples by capillary electrophoresis and conductivity detection: Implications for in-situ exploration of ocean worlds, Electrophoresis. 39 (2018) 2890–2897. https://doi.org/10.1002/elps.201800266.
[60] Y.G. Xiao, P. Kubáň, J. Tanyanyiwa, P.C. Hauser, Separation of enantiomers in capillary electrophoresis with contactless conductivity detection, J. Chromatogr. A. 1082 (2005) 230–234. https://doi.org/10.1016/j.chroma.2005.05.076.
[61] X.Y. Gong, P.C. Hauser, Determination of different classes of amines with capillary zone electrophoresis and contactless conductivity detection, Electrophoresis. 27 (2006) 468–473. https://doi.org/10.1002/elps.200500423.
[62] W. Pormsila, X.Y. Gong, P.C. Hauser, Determination of the enantiomers of α-hydroxy- and α-amino acids in capillary electrophoresis with contactless conductivity detection, Electrophoresis. 31 (2010) 2044–2048. https://doi.org/10.1002/elps.201000127.
[63] P. Tůma, M. Soukupová, E. Samcová, K. Štulík, A determination of submicromolar concentrations of glycine in periaqueductal gray matter microdialyzates using capillary zone electrophoresis with contactless conductivity detection, Electrophoresis. 30 (2009) 3436–3441. https://doi.org/10.1002/elps.200900187.
[64] P. Tůma, M. Šustková-Fišerová, F. Opekar, V. Pavlíček, K. Málková, Large-volume sample stacking for in vivo monitoring of trace levels of γ-aminobutyric acid, glycine and glutamate in microdialysates of periaqueductal gray matter by capillary electrophoresis with contactless conductivity detection, J. Chromatogr. A. 1303 (2013) 94–99. https://doi.org/10.1016/j.chroma.2013.06.019.
[65] P. Tůma, B. Sommerová, M. Šiklová, Monitoring of adipose tissue metabolism using microdialysis and capillary electrophoresis with contactless conductivity detection, Talanta. 192 (2019) 380–386. https://doi.org/10.1016/j.talanta.2018.09.076.
[66] P. Tůma, J. Gojda, B. Sommerová, D. Koval, Measuring venous-arterial differences of valine, isoleucine, leucine, alanine and glutamine in skeletal muscles using counter-current electrophoresis with contactless conductivity detection, J. Electroanal. Chem. 857 (2020). https://doi.org/10.1016/j.jelechem.2019.113772.
[67] H.A. Duong, M.T. Vu, T.D. Nguyen, M.H. Nguyen, T.D. Mai, Determination of 10-hydroxy-2-decenoic acid and free amino acids in royal jelly supplements with purpose-made capillary electrophoresis coupled with contactless

conductivity detection, J. Food Compos. Anal. 87 (2020). https://doi.org/10.1016/j.jfca.2020.103422.
[68] T.D. Nguyen, M.H. Nguyen, M.T. Vu, H.A. Duong, H.V. Pham, T.D. Mai, Dual-channeled capillary electrophoresis coupled with contactless conductivity detection for rapid determination of choline and taurine in energy drinks and dietary supplements, Talanta. 193 (2019) 168–175. https://doi.org/10.1016/j.talanta.2018.10.002.
[69] K. Včeláková, I. Zusková, E. Kenndler, B. Gaš, Determination of cationic mobilities and pKa values of 22 amino acids by capillary zone electrophoresis, Electrophoresis. 25 (2004) 309–317. https://doi.org/10.1002/elps.200305751.
[70] I. Zusková, A. Novotná, K. Včeláková, B. Gaš, Determination of limiting mobilities and dissociation constants of 21 amino acids by capillary zone electrophoresis at very low pH, J. Chromatogr. B Anal. Technol. Biomed. Life Sci. 841 (2006) 129–134. https://doi.org/10.1016/j.jchromb.2006.03.015.
[71] J. Jorgenson, K. Lukacs, Capillary zone electrophoresis, Science. 222 (1983) 266–272. https://doi.org/10.1126/science.6623076.
[72] J. Bergquist, R. Ekman, S.D. Gilman, A.G. Ewing, Analysis of Human Cerebrospinal Fluid by Capillary Electrophoresis with Laser-Induced Fluorescence Detection, Anal. Chem. 66 (1994) 3512–3518. https://doi.org/10.1021/ac00092a034.
[73] M.L. Marina, M. Castro-Puyana, Derivatization in Capillary Electrophoresis, in: P. Schmitt-Kopplin (Ed.), Capill. Electrophor. Methods Mol. Biol. Vol 1483., Humana Press, New York, NY, 2016: pp. 37–52. https://doi.org/10.1007/978-1-4939-6403-1_3.
[74] A. Wuethrich, J.P. Quirino, Derivatisation for separation and detection in capillary electrophoresis (2015–2017), Electrophoresis. 39 (2018) 82–96. https://doi.org/10.1002/elps.201700252.
[75] B.J. de Kort, G.J. de Jong, G.W. Somsen, Native fluorescence detection of biomolecular and pharmaceutical compounds in capillary electrophoresis: Detector designs, performance and applications: A review, Anal. Chim. Acta. 766 (2013) 13–33. https://doi.org/10.1016/j.aca.2012.12.006.
[76] F. Couderc, V. Ong-Meang, V. Poinsot, Capillary electrophoresis hyphenated with UV-native-laser induced fluorescence detection (CE/UV-native-LIF), Electrophoresis. 38 (2017) 135–149. https://doi.org/10.1002/elps.201600248.
[77] K.C. Chan, G.M. Muschik, H.J. Issaq, Solid-state UV laser-induced fluorescence detection in capillary electrophoresis, Electrophoresis. 21 (2000) 2062–2066. https://doi.org/10.1002/1522-2683(20000601)21:10<2062::AID-ELPS2062>3.0.CO;2-Z.
[78] C. Bayle, N. Siri, V. Poinsot, M. Treilhou, E. Caussé, F. Couderc, Analysis of tryptophan and tyrosine in cerebrospinal fluid by capillary electrophoresis and “ball lens” UV-pulsed laser-induced fluorescence detection, J. Chromatogr. A. 1013 (2003) 123–130. https://doi.org/10.1016/S0021-9673(03)00939-7.
[79] X. Zhang, J. V. Sweedler, Ultraviolet native fluorescence detection in capillary electrophoresis using a metal vapor NeCu laser, Anal. Chem. 73 (2001) 5620–5624. https://doi.org/10.1021/ac010458z.
[80] G.K. Belin, V. Gärtner, S. Seeger, Rapid analysis and sensitive detection of dl-tryptophan by using shorter capillary column coupled with deep-UV fluorescence detector, J. Chromatogr. B Anal. Technol. Biomed. Life Sci. 877 (2009) 3753–3756. https://doi.org/10.1016/j.jchromb.2009.09.010.
[81] R. Beyreiss, S. Ohla, S. Nagl, D. Belder, Label-free analysis in chip electrophoresis applying deep UV fluorescence lifetime detection, Electrophoresis. 32 (2011) 3108–3114. https://doi.org/10.1002/elps.201100204.
[82] Y.H. Park, X. Zhang, S.S. Rubakhin, J. V. Sweedler, Independent optimization of capillary electrophoresis separation and native fluorescence detection conditions for indolamine and catecholamine measurements, Anal. Chem. 71 (1999) 4997–5002. https://doi.org/10.1021/ac990659r.
[83] A. Rodat, P. Gavard, F. Couderc, Improving detection in capillary electrophoresis with laser induced fluorescence via a bubble cell capillary and laser power adjustment, Biomed. Chromatogr. 23 (2009) 42–47. https://doi.org/10.1002/bmc.1080.

[84] D.Č. Radenović, B.J. de Kort, G.W. Somsen, Lamp-based native fluorescence detection of proteins in capillary electrophoresis, J. Chromatogr. A. 1216 (2009) 4629–4632. https://doi.org/10.1016/j.chroma.2009.03.080.
[85] C.A. Dailey, N. Garnier, S.S. Rubakhin, J. V. Sweedler, Automated method for analysis of tryptophan and tyrosine metabolites using capillary electrophoresis with native fluorescence detection, Anal. Bioanal. Chem. 405 (2013) 2451–2459. https://doi.org/10.1007/s00216-012-6685-0.
[86] E. Okerberg, J.B. Shear, Attomole-level protein fingerprinting based on intrinsic peptide fluorescence, Anal. Chem. 73 (2001) 1610–1613. https://doi.org/10.1021/ac0012703.
[87] E.S. Gallagher, T.J. Comi, K.L. Braun, C.A. Aspinwall, Online photolytic optical gating of caged fluorophores in capillary zone electrophoresis utilizing an ultraviolet light-emitting diode, Electrophoresis. 33 (2012) 2903–2910. https://doi.org/10.1002/elps.201200279.
[88] M.M. Hsieh, H.T. Chang, Discontinuous electrolyte systems for improved detection of biologically active amines and acids by capillary electrophoresis with laser-induced native fluorescence detection, Electrophoresis. 26 (2005) 187–195. https://doi.org/10.1002/elps.200406123.
[89] M.S. Heywood, P.B. Farnsworth, Optimization of Native Fluorescence Detection of Proteins Using a Pulsed Nanolaser Excitation Source, Appl. Spectrosc. 64 (2010) 1283–1288. https://doi.org/10.1366/000370210793335016.
[90] A. Boutonnet, A. Morin, P. Petit, P. Vicendo, V. Poinsot, F. Couderc, Pulsed lasers versus continuous light sources in capillary electrophoresis and fluorescence detection studies: Photodegradation pathways and models, Anal. Chim. Acta. 912 (2016) 146–155. https://doi.org/10.1016/j.aca.2016.01.036.
[91] G. Rammouz, M. Lacroix, J.C. Garrigues, V. Poinsot, F. Couderc, The use of naphthalene-2,3-dicarboxaldehyde for the analysis of primary amines using high-performance liquid chromatography and capillary electrophoresis, Biomed. Chromatogr. 21 (2007) 1223–1239. https://doi.org/10.1002/bmc.893.
[92] Y. Liu, S. Zhao, Microanalysis of D / L -Amino Acid Residues in Peptides and Proteins., LCGC North Am. 19 (2001) 7–10.
[93] F. Robert, B. Renaud, L. Bert, L. Denoroy, Capillary Zone Electrophoresis with Laser-Induced Fluorescence Detection for the Determination of Nanomolar Concentrations of Noradrenaline and Dopamine: Application to Brain Microdialysate Analysis, Anal. Chem. 67 (1995) 1838–1844. https://doi.org/10.1021/ac00107a013.
[94] F. Robert, L. Bert, S. Parrot, L. Denoroy, L. Stoppini, B. Renaud, Coupling on-line brain microdialysis, precolumn derivatization and capillary electrophoresis for routine minute sampling of O-phosphoethanolamine and excitatory amino acids, J. Chromatogr. A. 817 (1998) 195–203. https://doi.org/10.1016/S0021-9673(98)00321-5.
[95] N. Siri, M. Lacroix, J.C. Garrigues, V. Poinsot, F. Couderc, HPLC-fluorescence detection and MEKC-LIF detection for the study of amino acids and catecholamines labelled with naphthalene-2,3-dicarboxyaldehyde, Electrophoresis. 27 (2006) 4446–4455. https://doi.org/10.1002/elps.200600165.
[96] J.E. Melanson, C.A. Lucy, Violet (405 nm) diode laser for laser induced fluorescence detection in capillary electrophoresis, Analyst. 125 (2000) 1049–1052. https://doi.org/10.1039/b002510k.
[97] C.K. Chen, K.T. Liu, T.C. Chiu, H.T. Chang, Separation of amino acids and amines by capillary electrophoresis using poly(ethylene oxide) solution containing cetyltrimethylammonium bromide, J. Chromatogr. A. 1216 (2009) 7576–7581. https://doi.org/10.1016/j.chroma.2009.02.054.
[98] F. Tan, B. Yang, Y. Guan, Simultaneous light emitting diode-induced fluorescence and contactless conductivity detection for capillary electrophoresis, Anal. Sci. 21 (2005) 583–585. https://doi.org/10.2116/analsci.21.583.
[99] M.-M. Hsieh, P.-L. Chang, Separation of Amino Acids by Capillary Electrophoresis with Light-Emitting Diode-Induced Fluorescence in the Presence of Electroosmotic Flow, in: N. Volpi, F. Maccari (Eds.), Capill. Electrophor. Biomol. Methods Protoc. Methods Mol. Biol. Vol. 984, Springer Science and Business Media, 2013: pp. 121–129. https://doi.org/10.1007/978-1-62703-296-4_9.
[100] Y.H. Rezenom, J.M. Lancaster, J.L. Pittman, S.D. Gilman, Laser ablation construction of on-column reagent addition devices for capillary electrophoresis, Anal. Chem. 74 (2002) 1572–1577.

https://doi.org/10.1021/ac015693w.
[101] L.Y. Zhang, M.X. Sun, Capillary electrophoresis of phosphorylated amino acids with fluorescence detection, J. Chromatogr. B Anal. Technol. Biomed. Life Sci. 859 (2007) 30–36. https://doi.org/10.1016/j.jchromb.2007.09.022.
[102] A. Celá, A. Mádr, Z. Glatz, Electrophoretically mediated microanalysis for simultaneous on-capillary derivatization of standard amino acids followed by micellar electrokinetic capillary chromatography with laser-induced fluorescence detection, J. Chromatogr. A. 1499 (2017) 203–210. https://doi.org/10.1016/j.chroma.2017.03.080.
[103] A. Celá, A. Mádr, T. Dědová, M. Pelcová, M. Ješeta, J. Žáková, I. Crha, Z. Glatz, MEKC-LIF method for analysis of amino acids after on-capillary derivatization by transverse diffusion of laminar flow profiles mixing of reactants for assessing developmental capacity of human embryos after in vitro fertilization, Electrophoresis. 37 (2016) 2305–2312. https://doi.org/10.1002/elps.201500587.
[104] C.Z. Yu, Y.Z. He, F. Han, G.N. Fu, Post-column reactor of coaxial-gap mode for laser-induced fluorescence detection in capillary electrophoresis, J. Chromatogr. A. 1171 (2007) 133–139. https://doi.org/10.1016/j.chroma.2007.09.046.
[105] M. Lacroix, J.C. Garrigues, F. Couderc, Reaction of Naphthalene-2,3-Dicarboxaldehyde with Enkephalins for LC-Fluorescence and LC-MS Analysis: Conformational Studies by Molecular Modeling and H/D Exchange Mass Spectrometry, J. Am. Soc. Mass Spectrom. 18 (2007) 1706–1713. https://doi.org/10.1016/j.jasms.2007.07.007.
[106] X. Yang, H. Yuan, C. Wang, S. Zhao, D. Xiao, M.M.F. Choi, In-column fiber-optic laser-induced flourescene detection for CE, Electrophoresis. 28 (2007) 3105–3114. https://doi.org/10.1002/elps.200600815.
[107] S. Zhao, H. Yuan, D. Xiao, Optical fiber light-emitting diode-induced fluorescence for capillary electrophoresis, Electrophoresis. 27 (2006) 461–467. https://doi.org/10.1002/elps.200500300.
[108] C.A. Vyas, S.M. Rawls, R.B. Raffa, J.G. Shackman, Glutamate and aspartate measurements in individual planaria by rapid capillary electrophoresis, J. Pharmacol. Toxicol. Methods. 63 (2011) 119–122. https://doi.org/10.1016/j.vascn.2010.08.002.
[109] J. Liu, Y.Z. Hsieh, D. Wiesler, M. Novotny, Design of 3-(4-Carboxybenzoyl)-2-quinolinecarboxaldehyde as a Reagent for Ultrasensitive Determination of Primary Amines by Capillary Electrophoresis Using Laser Fluorescence Detection, Anal. Chem. 63 (1991) 408–412. https://doi.org/10.1021/ac00005a004.
[110] H.Y. Ta, L. Perquis, C. Sarazin, V. Ong-Meang, F. Collin, F. Couderc, Tryptophan, valine and isoleucine analysis by CE and LED induced fluorescence or conductivity detections: a comparison., Electrophoresis. submitted (2020).
[111] O. Boulat, D.G. McLaren, E.A. Arriaga, D.D.Y. Chen, Separation of free amino acids in human plasma by capillary electrophoresis with laser induced fluorescence: Potential for emergency diagnosis of inborn errors of metabolism, J. Chromatogr. B Biomed. Sci. Appl. 754 (2001) 217–228. https://doi.org/10.1016/S0378-4347(00)00611-3.
[112] E.A. Arriaga, Y. Zhang, N.J. Dovichi, Use of 3-(p-carboxybenzoyl)quinoline-2-carboxaldehyde to label amino acids for high-sensitivity fluorescence detection in capillary electrophoresis, Anal. Chim. Acta. 299 (1995) 319–326. https://doi.org/10.1016/0003-2670(94)00315-D.
[113] M. Ummadi, B.C. Weimer, Use of capillary electrophoresis and laser-induced fluorescence for attomole detection of amino acids, J. Chromatogr. A. 964 (2002) 243–253. https://doi.org/10.1016/S0021-9673(02)00692-1.
[114] A. Barmada, S.A. Shippy, Thread-based assay for quantitative small molecule analysis of mice tear fluid by capillary electrophoresis, Anal. Bioanal. Chem. 411 (2019) 329–338. https://doi.org/10.1007/s00216-018-1488-6.
[115] J.C. Ehlen, H.E. Albers, E.D. Breyer, MEKC-LIF of γ-amino butyric acid in microdialysate: Systematic optimization of the separation conditions by factorial analysis, J. Neurosci. Methods. 147 (2005) 36–47. https://doi.org/10.1016/j.jneumeth.2005.03.012.
[116] N. Zhang, H.S. Zhang, H. Wang, Separation of free amino acids and catecholamines in human plasma and rabbit vitreous samples using a new fluorogenic reagent 3-(4-bromobenzoyl)-2- quinolinecarboxaldehyde with CE-LIF detection, Electrophoresis. 30 (2009) 2258–2265. https://doi.org/10.1002/elps.200800667.
[117] N. Zhang, X.F. Guo, H. Wang, H.S. Zhang, Determination of amino acids and catecholamines derivatized with 3-(4-

chlorobenzoyl)-2-quinolinecarboxaldehyde in PC12 and HEK293 cells by capillary electrophoresis with laser-induced fluorescence detection, Anal. Bioanal. Chem. 401 (2011) 297–304. https://doi.org/10.1007/s00216-011-5056-6.

[118] D. Kutlán, I. Molnár-Perl, New aspects of the simultaneous analysis of amino acids and amines as their o-phthaldialdehyde derivatives by high-performance liquid chromatography: Analysis of wine, beer and vinegar, J. Chromatogr. A. 987 (2003) 311–322. https://doi.org/10.1016/S0021-9673(02)01538-8.

[119] S. Hapuarachchi, G.A. Janaway, C.A. Aspinwall, Capillary electrophoresis with a UV light-emitting diode source for chemical monitoring of native and derivatized fluorescent compounds, Electrophoresis. 27 (2006) 4052–4059. https://doi.org/10.1002/elps.200600232.

[120] D. Yamamoto, T. Kaneta, T. Imasaka, Postcolumn reactor using a laser-drilled capillary for light-emitting diode-induced fluorescence detection in CE, Electrophoresis. 28 (2007) 4143–4149. https://doi.org/10.1002/elps.200700274.

[121] R. Kühnreich, U. Holzgrabe, Indirect Enantioseparation of Amino Acids by CE Using Automated In-Capillary Derivatization with ortho-Phthalaldehyde and N-Acetyl-l-Cysteine, Chromatographia. 79 (2016) 1013–1022. https://doi.org/10.1007/s10337-016-3122-0.

[122] C.C. Shen, W.L. Tseng, M.M. Hsieh, Selective enrichment of aminothiols using polysorbate 20-capped gold nanoparticles followed by capillary electrophoresis with laser-induced fluorescence, J. Chromatogr. A. 1216 (2009) 288–293. https://doi.org/10.1016/j.chroma.2008.11.044.

[123] N. Maddukuri, Q. Zhang, N. Zhang, M. Gong, Rapid labeling of amino acid neurotransmitters with a fluorescent thiol in the presence of o-phthalaldehyde, Electrophoresis. 38 (2017) 507–512. https://doi.org/10.1002/elps.201600374.

[124] H. Kawauchi, K. Tuzimura, H. Maeda, N. Ishida, Reaction of fluorescein-isothiocynate with proteins and amino acids: II. preparation of fluorescein-thiohydantoin amino acids and their thin-layer chromatography, J. Biochem. 66 (1969) 783–789. https://doi.org/10.1093/oxfordjournals.jbchem.a129208.

[125] Y. Cheng, N. Dovichi, Subattomole amino acid analysis by capillary zone electrophoresis and laser-induced fluorescence, Science (80-.). 242 (1988) 562–564. https://doi.org/10.1126/science.3140381.

[126] E.P. De Jong, C.A. Lucy, Low-picomolar limits of detection using high-power light-emitting diodes for fluorescence, Analyst. 131 (2006) 664–669. https://doi.org/10.1039/b602193j.

[127] F.B. Yang, J.Z. Pan, T. Zhang, Q. Fang, A low-cost light-emitting diode induced fluorescence detector for capillary electrophoresis based on an orthogonal optical arrangement, Talanta. 78 (2009) 1155–1158. https://doi.org/10.1016/j.talanta.2009.01.033.

[128] J. Xu, S. Chen, Y. Xiong, B. Yang, Y. Guan, A glycerol assisted light-emitting diode-induced fluorescence detector for capillary flow systems, Talanta. 75 (2008) 885–889. https://doi.org/10.1016/j.talanta.2007.11.064.

[129] S.L. Wang, X.J. Huang, Z.L. Fang, P.K. Dasgupta, A miniaturized liquid core waveguide-capillary electrophoresis system with flow injection sample introduction and fluorometric detection using light-emitting diodes, Anal. Chem. 73 (2001) 4545–4549. https://doi.org/10.1021/ac010341a.

[130] V. Kostal, M. Zeisbergerova, Z. Hrotekova, K. Slais, V. Kahle, Miniaturized liquid core waveguide-based fluorimetric detection cell for capillary separation methods : Application in CE of amino acids, (2006) 4658–4665. https://doi.org/10.1002/elps.200600222.

[131] Y. Zhu, N. Chen, Q. Li, Q. Fang, Improving the sensitivity of confocal laser induced fluorescence detection to the sub-picomolar scale for round capillaries by laterally shifting the laser focus point, Analyst. 138 (2013) 4642. https://doi.org/10.1039/c3an00345k.

[132] X.X. Fang, H.Y. Li, P. Fang, J.Z. Pan, Q. Fang, A handheld laser-induced fluorescence detector for multiple applications, Talanta. 150 (2016) 135–141. https://doi.org/10.1016/j.talanta.2015.12.018.

[133] M.M. Martin, L. Lindqvist, The pH dependence of fluorescein fluorescence, J. Lumin. 10 (1975) 381–390.

https://doi.org/10.1016/0022-2313(75)90003-4.
[134] R. Sjöback, J. Nygren, M. Kubista, Absorption and fluorescence properties of fluorescein, Spectrochim. Acta Part A Mol. Spectrosc. 51 (1995). https://doi.org/10.1016/0584-8539(95)01421-P.
[135] S.P.D. Lalljie, P. Sandra, Practical and quantitative aspects in the analysis of FITC and DTAF amino acid derivatives by capillary electrophoresis and LIF detection, Chromatographia. 40 (1995) 519–526. https://doi.org/10.1007/BF02290262.
[136] G. Nouadje, H. Rubie, E. Chatelut, P. Canal, M. Nertz, P. Puig, F. Couderc, Child cerebrospinal fluid analysis by capillary electrophoresis and laser-induced fluorescence detection, J. Chromatogr. A. 717 (1995) 293–298. https://doi.org/10.1016/0021-9673(95)00747-3.
[137] G. Nouadje, N. Siméon, F. Dedieu, M. Nertz, P. Puig, F. Couderc, Determination of twenty eight biogenic amines and amino acids during wine aging by micellar electrokinetic chromatography and laser-induced fluorescence detection, J. Chromatogr. A. 765 (1997) 337–343. https://doi.org/10.1016/S0021-9673(96)00925-9.
[138] J. Mattusch, K. Dittrich, Improvement of laser-induced fluorescence detection of amino acids in capillary zone electrophoresis, J. Chromatogr. A. 680 (1994) 279–285. https://doi.org/10.1016/0021-9673(94)80078-2.
[139] A. Zinellu, S. Sotgia, E. Pisanu, B. Scanu, M. Sanna, M. Franca Usai, R. Chessa, L. Deiana, C. Carru, Quantification of neurotransmitter amino acids by capillary electrophoresis laser-induced fluorescence detection in biological fluids, Anal. Bioanal. Chem. 398 (2010) 1973–1978. https://doi.org/10.1007/s00216-010-4134-5.
[140] X. Li, H. Ren, X. Le, M. Qi, I.D. Ireland, N.J. Dovichi, Migration time correction for the analysis of derivatized amino acids and oligosaccharides by micellar capillary electrochromatography, 869 (2000) 375–384.
[141] J. Wang, G. Sun, J. Bai, L. Wang, Capillary array electrophoresis with confocal fluorescence rotary scanner, Analyst. 128 (2003) 1434–1438. https://doi.org/10.1039/b310833c.
[142] F. Huo, H. Yuan, M.C. Breadmore, D. Xiao, Multi-wavelength light emitting diode array as an excitation source for light emitting diode-induced fluorescence detection in capillary electrophoresis, Electrophoresis. 31 (2010) 2589–2595. https://doi.org/10.1002/elps.201000071.
[143] S. Casado-Terrones, S. Cortacero-Ramírez, A. Carrasco-Pancorbo, A. Segura-Carretero, A. Fernández-Gutiérrez, Comparative study between a commercial and a homemade capillary electrophoresis instrument for the simultaneous determination of aminated compounds by induced fluorescence detection, Anal. Bioanal. Chem. 386 (2006) 1835–1847. https://doi.org/10.1007/s00216-006-0731-8.
[144] S. Chen, B.F. Liu, L. Fu, T. Xiong, T. Liu, Z. Zhang, Z.L. Huang, Q. Lu, Y. Di Zhao, Q. Luo, Continuous wave-based multiphoton excitation fluorescence for capillary electrophoresis, J. Chromatogr. A. 1109 (2006) 160–166. https://doi.org/10.1016/j.chroma.2005.11.033.
[145] X. Feng, S. Chen, Y. Xu, W. Du, Q. Luo, B.F. Liu, Separation and determination of biogenic amines in fish using MEKC with novel multiphoton excitation fluorescence detection, J. Sep. Sci. 31 (2008) 824–828. https://doi.org/10.1002/jssc.200700514.
[146] X. Liu, Y.Q. Hu, L. Ma, Y.T. Lu, Determination of phosphoamino acids derivatized with 5-(4,6-dichloro-s- triazin-2-ylamino)fluorescein by micellar electrokinetic chromatography, J. Chromatogr. A. 1049 (2004) 237–242. https://doi.org/10.1016/j.chroma.2004.08.005.
[147] M. Molina, M. Silva, In-capillary derivatization and analysis of amino acids, amino phosphonic acid-herbicides and biogenic amines by capillary electrophoresis with laser-induced fluorescence detection, Electrophoresis. 23 (2002) 2333–2340. https://doi.org/10.1002/1522-2683(200207)23:14<2333::AID-ELPS2333>3.0.CO;2-5.
[148] Y.H. Deng, R.J. Li, H.S. Zhang, X.L. Du, H. Wang, Liquid chromatographic analysis of phosphoamino acids at femtomole level using chemical derivatization with N-hydroxysuccinimidyl fluorescein-O-acetate, Anal. Chim. Acta. 601 (2007) 118–124. https://doi.org/10.1016/j.aca.2007.08.023.
[149] V. Kostal, M. Zeisbergerova, Z. Hrotekova, K. Slais, V. Kahle, Miniaturized liquid core waveguide-based fluorimetric detection cell for capillary separation methods: Application in CE of amino acids, Electrophoresis. 27

(2006) 4658–4665. https://doi.org/10.1002/elps.200600222.
[150] S.Y. Chang, F.Y. Wang, Determination of gabapentin in human plasma by capillary electrophoresis with laser-induced fluorescence detection and acetonitrile stacking technique, J. Chromatogr. B Anal. Technol. Biomed. Life Sci. 799 (2004) 265–270. https://doi.org/10.1016/j.jchromb.2003.10.052.
[151] L. Cao, H. Wang, H. Zhang, Analytical potential of 6-oxy-(N-succinimidyl acetate)-9-(2′-methoxycarbonyl) fluorescein for the determination of amino compounds by capillary electrophoresis with laser-induced fluorescence detection, Electrophoresis. 26 (2005) 1954–1962. https://doi.org/10.1002/elps.200410227.
[152] E. Caussé, N. Siri, H. Bellet, S. Champagne, C. Bayle, P. Valdiguié, R. Salvayre, F. Couderc, Plasma Homocysteine Determined by Capillary Electrophoresis with Laser-induced Fluorescence Detection, Clin. Chem. 45 (1999) 412–414. https://doi.org/10.1093/clinchem/45.3.412.
[153] C. Chassaing, J. Gonin, C.S. Wilcox, I.W. Wainer, Determination of reduced and oxidized homocysteine and related thiols in plasma by thiol-specific pre-column derivatization and capillary electrophoresis with laser-induced fluorescence detection, J. Chromatogr. B Biomed. Sci. Appl. 735 (1999) 219–227. https://doi.org/10.1016/S0378-4347(99)00425-9.
[154] P. Lochman, T. Adam, D. Friedecký, E. Hlídková, Z. Škopková, High-throughput capillary electrophoretic method for determination of total aminothiols in plasma and urine, Electrophoresis. 24 (2003) 1200–1207. https://doi.org/10.1002/elps.200390154.
[155] S. Udenfriend, S. Stein, P. Bohlen, W. Dairman, W. Leimgruber, M. Weigele, Fluorescamine: A Reagent for Assay of Amino Acids, Peptides, Proteins, and Primary Amines in the Picomole Range, Science. 178 (1972) 871–872. https://doi.org/10.1126/science.178.4063.871.
[156] A.M. Skelley, R.A. Mathies, Chiral separation of fluorescamine-labeled amino acids using microfabricated capillary electrophoresis devices for extraterrestrial exploration, J. Chromatogr. A. 1021 (2003) 191–199. https://doi.org/10.1016/j.chroma.2003.08.096.
[157] A.M. Skelley, J.R. Scherer, A.D. Aubrey, W.H. Grover, R.H.C. Ivester, P. Ehrenfreund, F.J. Grunthaner, J.L. Bada, R.A. Mathies, Development and evaluation of a microdevice for amino acid biomarker detection and analysis on Mars, Proc. Natl. Acad. Sci. U. S. A. 102 (2005) 1041–1046. https://doi.org/10.1073/pnas.0406798102.
[158] S.H. Kang, W. Wei, E.S. Yeung, On-column derivatization for the analysis of homocysteine and other thiols by capillary electrophoresis with laser-induced fluorescence detection, J. Chromatogr. B Biomed. Sci. Appl. 744 (2000) 149–156. https://doi.org/10.1016/S0378-4347(00)00241-3.
[159] H. Ruyters, S. V. der Wal, Fully Automated Analysis of Amino Acid Enantiomers by Derivatization and Chiral Separation on a Capillary Electrophoresis Instrument, J. Liq. Chromatogr. 17 (1994) 1883–1897. https://doi.org/10.1080/10826079408013466.
[160] L.A.M. Preston, M.L. Weber, G.M. Murray, Micellar electrokinetic capillary chromatography with laser-induced fluorimetric detection of amines in beer, J. Chromatogr. B Biomed. Appl. 695 (1997) 175–180. https://doi.org/10.1016/S0378-4347(97)00176-X.
[161] K. Imai, Y. Watanabe, Fluorimetric determination of secondary amino acids by 7-fluoro-4-nitrobenzo-2-oxa-1,3-diazole, Anal. Chim. Acta. 130 (1981) 377–383. https://doi.org/10.1016/S0003-2670(01)93016-8.
[162] H. Zhang, I. Le Potier, C. Smadja, J. Zhang, M. Taverna, Fluorescent detection of peptides and amino acids for capillary electrophoresis via on-line derivatization with 4-fluoro-7-nitro-2,1,3- benzoxadiazole, Anal. Bioanal. Chem. 386 (2006) 1387–1394. https://doi.org/10.1007/s00216-006-0709-6.
[163] S. Zhao, H. Yuan, D. Xiao, Detection of D-Serine in rat brain by capillary electrophoresis with laser induced fluorescence detection, J. Chromatogr. B Anal. Technol. Biomed. Life Sci. 822 (2005) 334–338. https://doi.org/10.1016/j.jchromb.2005.06.027.
[164] P.B. Ghosh, M.W. Whitehouse, 7-chloro-4-nitrobenzo-2-oxa-1,3-diazole: a new fluorigenic reagent for amino acids and other amines, Biochem. J. 108 (1968) 155–156. https://doi.org/10.1042/bj1080155.

[165] F. Chen, Y. Rang, Y. Weng, L. Lin, H. Zeng, H. Nakajim, J.-M. Lin, K. Uchiyama, Drop-by-drop chemical reaction and sample introduction for capillary electrophoresis, Analyst. 140 (2015) 3953–3959. https://doi.org/10.1039/C5AN00040H.

[166] W. Bi, S. Lei, X. Yang, Z. Xu, H. Yuan, D. Xiao, M.M.F. Choi, Talanta Separation of tyrosine enantiomer derivatives by capillary electrophoresis with light-emitting diode-induced fluorescence detection, 78 (2009) 1167–1172. https://doi.org/10.1016/j.talanta.2009.01.042.

[167] J. Hodáková, J. Preisler, F. Foret, P. Kubáň, Sensitive determination of glutathione in biological samples by capillary electrophoresis with green (515nm) laser-induced fluorescence detection, J. Chromatogr. A. 1391 (2015) 102–108. https://doi.org/10.1016/j.chroma.2015.02.062.

[168] C. Fanali, G. D'Orazio, S. Fanali, Capillary electrophoresis-mass spectrometry, in: Hyphenations Capill. Chromatogr. with Mass Spectrom., Elsevier, 2020: pp. 413–447. https://doi.org/10.1016/B978-0-12-809638-3.00011-9.

[169] S. Ferré, V. González-Ruiz, D. Guillarme, S. Rudaz, Analytical strategies for the determination of amino acids: Past, present and future trends, J. Chromatogr. B Anal. Technol. Biomed. Life Sci. 1132 (2019) 121819. https://doi.org/10.1016/j.jchromb.2019.121819.

[170] T. Soga, D.N. Neiger, Amino acid analysis by capillary electrophoresis electrospray ionization mass spectrometry, Anal. Chem. 72 (2000) 1236–1241. https://doi.org/10.1021/ac990976y.

[171] M. Moini, Capillary electrophoresis mass spectrometry and its application to the analysis of biological mixtures, Anal. Bioanal. Chem. 373 (2002) 466–480. https://doi.org/10.1007/s00216-002-1283-1.

[172] C. Desiderio, F. Iavarone, D.V. Rossetti, I. Messana, M. Castagnola, Capillary electrophoresis-mass spectrometry for the analysis of amino acids, J. Sep. Sci. 33 (2010) 2385–2393. https://doi.org/10.1002/jssc.201000171.

[173] C.W. Klampfl, W. Ahrer, Determination of free amino acids in infant food by capillary zone electrophoresis with mass spectrometric detection, Electrophoresis. 22 (2001) 1579–1584. https://doi.org/10.1002/1522-2683(200105)22:8<1579::AID-ELPS1579>3.0.CO;2-C.

[174] S.H. Hung, W.S. Cheng, J.L. Huang, C.W. Wang, G.R. Her, Chiral electrokinetic chromatography-electrospray ionization-mass spectrometry using a double junction interface, Electrophoresis. 33 (2012) 546–551. https://doi.org/10.1002/elps.201100384.

[175] M. Moini, Design and performance of a universal sheathless capillary electrophoresis to mass spectrometry interface using a split-flow technique, Anal. Chem. 73 (2001) 3497–3501. https://doi.org/10.1021/ac010189c.

[176] C.L. Schultz, M. Moini, Analysis of underivatized amino acids and their D/L-enantiomers by sheathless capillary electrophoresis/electrospray ionization-mass spectrometry, Anal. Chem. 75 (2003) 1508–1513. https://doi.org/10.1021/ac0263925.

[177] R. Wojcik, O.O. Dada, M. Sadilek, N.J. Dovichi, Simplified capillary electrophoresis nanospray sheath- flow interface for high efficiency and sensitive peptide analysis, Rapid Commun. Mass Spectrom. 24 (2010) 1457–1466. https://doi.org/10.1002/rcm.

[178] S.A. Sarver, N.M. Schiavone, J. Arceo, E.H. Peuchen, Z. Zhang, L. Sun, N.J. Dovichi, Capillary Electrophoresis Coupled to Negative Mode Electrospray Ionization-Mass Spectrometry Using an Electrokinetically-Pumped Nanospray Interface with Primary Amines Grafted to the Interior of a Glass Emitter, Talanta. 165 (2017) 522–525. https://doi.org/10.1016/j.talanta.2017.01.002.Capillary.

[179] M. Mamani-Huanca, A. Gradillas, A. Gil de la Fuente, Á. López-Gonzálvez, C. Barbas, Unveiling the Fragmentation Mechanisms of Modified Amino Acids as the Key for Their Targeted Identification, Anal. Chem. (2020) 2–11. https://doi.org/10.1021/acs.analchem.9b04313.

[180] T. Soga, Y. Kakazu, M. Robert, M. Tomita, T. Nishioka, Qualitative and quantitative analysis of amino acids by capillary electrophoresis-electrospray ionization-tandem mass spectrometry, Electrophoresis. 25 (2004) 1964–1972. https://doi.org/10.1002/elps.200305791.

[181] A. Meulemans, Capillary electrophoresis of the electrochemical oxidation products of Ng-hydroxy-L-arginine at physiological pH, J. Chromatogr. B Anal. Technol. Biomed. Life Sci. 824 (2005) 308–311. https://doi.org/10.1016/j.jchromb.2005.07.002.
[182] A. Hirayama, T. Soga, Chapter 8, Amino Acid Analysis by Capillary Electrophoresis-Mass Spectrometry, Methods Mol. Biol. 828 (2012) 77–82. https://doi.org/10.1007/978-1-61779-445-2.
[183] V. Hruška, M. Jaroš, B. Gaš, Simul 5 - Free dynamic simulator of electrophoresis, Electrophoresis. 27 (2006) 984–991. https://doi.org/10.1002/elps.200500756.
[184] R. Lee, A.S. Ptolemy, L. Niewczas, P. Britz-McKibbin, Integrative metabolomics for characterizing unknown low-abundance metabolites by capillary electrophoresis-mass spectrometry with computer simulations, Anal. Chem. 79 (2007) 403–415. https://doi.org/10.1021/ac061780i.
[185] M.G.M. Kok, G.J. de Jong, G.W. Somsen, Sensitivity enhancement in capillary electrophoresis-mass spectrometry of anionic metabolites using a triethylamine-containing background electrolyte and sheath liquid, Electrophoresis. 32 (2011) 3016–3024. https://doi.org/10.1002/elps.201100271.
[186] S. Acket, A. Degournay, M. Gosset, F. Merlier, M.A. Troncoso-Ponce, B. Thomasset, Analysis of 13 C labeling amino acids by capillary electrophoresis – High resolution mass spectrometry for fluxomic studies, Anal. Biochem. 547 (2018) 14–18. https://doi.org/10.1016/j.ab.2018.02.009.
[187] K. Sasaki, H. Sagawa, M. Suzuki, H. Yamamoto, M. Tomita, T. Soga, Y. Ohashi, Metabolomics Platform with Capillary Electrophoresis Coupled with High-Resolution Mass Spectrometry for Plasma Analysis, Anal. Chem. 91 (2019) 1295–1301. https://doi.org/10.1021/acs.analchem.8b02994.
[188] K.R. Chalcraft, P. Britz-McKibbin, Newborn screening of inborn errors of metabolism by capillary electrophoresis-electrospray ionization-mass spectrometry: A second-tier method with improved specificity and sensitivity, Anal. Chem. 81 (2009) 307–314. https://doi.org/10.1021/ac8020455.
[189] K.R. Chalcraft, R. Lee, C. Mills, P. Britz-McKibbin, Virtual quantification of metabolites by capillary electrophoresis- electrospray ionization-mass spectrometry: Predicting ionization efficiency without chemical standards, Anal. Chem. 81 (2009) 2506–2515. https://doi.org/10.1021/ac802272u.
[190] M. Wakayama, N. Aoki, H. Sasaki, R. Ohsugi, Simultaneous analysis of amino acids and carboxylic acids by capillary electrophoresis-mass spectrometry using an acidic electrolyte and uncoated fused-silica capillary, Anal. Chem. 82 (2010) 9967–9976. https://doi.org/10.1021/ac1019039.
[191] L. Sánchez-Hernández, M.L. Marina, A.L. Crego, A capillary electrophoresis-tandem mass spectrometry methodology for the determination of non-protein amino acids in vegetable oils as novel markers for the detection of adulterations in olive oils, J. Chromatogr. A. 1218 (2011) 4944–4951. https://doi.org/10.1016/j.chroma.2011.01.045.
[192] T. Atherton, R. Croxton, M. Baron, J. Gonzalez-Rodriguez, L. Gámiz-Gracia, A.M. García-Campaña, Analysis of amino acids in latent fingerprint residue by capillary electrophoresis-mass spectrometry, J. Sep. Sci. 35 (2012) 2994–2999. https://doi.org/10.1002/jssc.201200398.
[193] X. Wang, I. Davis, A. Liu, S.A. Shamsi, Development of a CZE-ESI-MS assay with a sulfonated capillary for profiling picolinic acid and quinolinic acid formation in multienzyme system, Electrophoresis. 34 (2013) 1828–1835. https://doi.org/10.1002/elps.201200679.
[194] S. Lee, S.J. Kim, E. Bang, Y.C. Na, Chiral separation of intact amino acids by capillary electrophoresis-mass spectrometry employing a partial filling technique with a crown ether carboxylic acid, J. Chromatogr. A. 1586 (2019) 128–138. https://doi.org/10.1016/j.chroma.2018.12.001.
[195] R.C. Moldovan, E. Bodoki, A.C. Servais, B. Chankvetadze, J. Crommen, R. Oprean, M. Fillet, Capillary electrophoresis-mass spectrometry of derivatized amino acids for targeted neurometabolomics – pH mediated reversal of diastereomer migration order, J. Chromatogr. A. 1564 (2018) 199–206. https://doi.org/10.1016/j.chroma.2018.06.030.
[196] E. Domínguez-Vega, L. Sánchez-Hernández, C. García-Ruiz, A.L. Crego, M.L. Marina, Development of a CE-ESI-

ITMS method for the enantiomeric determination of the non-protein amino acid ornithine, Electrophoresis. 30 (2009) 1724–1733. https://doi.org/10.1002/elps.200800679.

[197] A. Giuffrida, C. León, V. García-Cañas, V. Cucinotta, A. Cifuentes, Modified cyclodextrins for fast and sensitive chiral-capillary electrophoresis-mass spectrometry, Electrophoresis. 30 (2009) 1734–1742. https://doi.org/10.1002/elps.200800333.

[198] V. Vacchina, S. Oguey, C. Ionescu, D. Bravo, R. Lobinski, Characterization of metal glycinate complexes by electrospray Q-TOF-MS/MS and their determination by capillary electrophoresis-ICP-MS: Application to premix samples, Anal. Bioanal. Chem. 398 (2010) 435–449. https://doi.org/10.1007/s00216-010-3907-1.

[199] L. Ruzik, P. Kwiatkowski, Application of CE-ICP-MS and CE-ESI-MS/MS for identification of Zn-binding ligands in Goji berries extracts, Talanta. 183 (2018) 102–107. https://doi.org/10.1016/j.talanta.2018.02.040.

[200] M. Moini, Simplifying CE-MS operation. 2. Interfacing low-flow separation techniques to mass spectrometry using a porous tip, Anal. Chem. 79 (2007) 4241–4246. https://doi.org/10.1021/ac0704560.

[201] M. Moini, K. Klauenberg, M. Ballard, Dating silk by capillary electrophoresis mass spectrometry., Anal. Chem. 83 (2011) 7577–7581. https://doi.org/10.1021/ac201746u.

[202] M. Moini, High-Throughput Capillary Electrophoresis–Mass Spectrometry: From Analysis of Amino Acids to Analysis of Protein Complexes, in: Methods Mol. Biol., 2013: pp. 79–119. https://doi.org/10.1007/978-1-62703-296-4_8.

[203] W. Zhang, F. Guled, T. Hankemeier, R. Ramautar, Utility of sheathless capillary electrophoresis-mass spectrometry for metabolic profiling of limited sample amounts, J. Chromatogr. B Anal. Technol. Biomed. Life Sci. 1105 (2019) 10–14. https://doi.org/10.1016/j.jchromb.2018.12.004.

[204] R. Ramautar, Sheathless Capillary Electrophoresis-Mass Spectrometry for the Profiling of Charged Metabolites in Biological Samples, Methods Mol. Biol. 1738 (2007) 46–48.

[205] T. Huang, M. Armbruster, R. Lee, D.S. Hui, J.L. Edwards, Metabolomic analysis of mammalian cells and human tissue through one-pot two stage derivatizations using sheathless capillary electrophoresis-electrospray ionization-mass spectrometry, J. Chromatogr. A. 1567 (2018) 219–225. https://doi.org/10.1016/j.chroma.2018.07.007.

[206] J.S. Jeong, S.K. Kim, S.R. Park, Capillary electrophoresis mass spectrometry with sheathless electrospray ionization for high sensitivity analysis of underivatized amino acids, Electrophoresis. 33 (2012) 2112–2121. https://doi.org/10.1002/elps.201200005.

[207] G. Bonvin, Fundamental Aspects in the Coupling of Capillary Electrophoresis with Mass Spectrometry, Université de Genève, 2014.

[208] A. Hirayama, S. Ikeda, A. Sato, T. Soga, Amino Acid Analysis by Capillary Electrophoresis-Mass Spectrometry, in: Curr. Protoc. Protein Sci., 2019: pp. 307–313. https://doi.org/10.1007/978-1-4939-9639-1_23.

[209] K.T. Rodrigues, D. Mekahli, M.F.M. Tavares, A. van Schepdael, Development and validation of a CE-MS method for the targeted assessment of amino acids in urine, Electrophoresis. 37 (2016) 1039–1047. https://doi.org/10.1002/elps.201500534.

[210] K.T. Rodrigues, M.F.M. Tavares, A. Van Schepdael, CE-MS for the analysis of amino acids, Methods Mol. Biol. 1730 (2018) 305–313. https://doi.org/10.1007/978-1-4939-7592-1_23.

[211] H. Yamamoto, K. Sasaki, Metabolomics-based approach for ranking the candidate structures of unidentified peaks in capillary electrophoresis time-of-flight mass spectrometry, Electrophoresis. 38 (2017) 1053–1059. https://doi.org/10.1002/elps.201600328.

[212] H. Mischak, J.J. Coon, J. Novak, E.M. Weissinger, J.P. Schanstra, A.F. Dominiczak, Capillary electrophoresis-mass spectrometry as a powerful tool in biomarker discovery and clinical diagnosis: An update of recent developments, Mass Spectrom. Rev. 28 (2009) 703–724. https://doi.org/10.1002/mas.20205.

[213] K. Kami, T. Fujimori, H. Sato, M. Sato, H. Yamamoto, Y. Ohashi, N. Sugiyama, Y. Ishihama, H. Onozuka, A. Ochiai, H. Esumi, T. Soga, M. Tomita, Metabolomic profiling of lung and prostate tumor tissues by capillary

electrophoresis time-of-flight mass spectrometry, Metabolomics. 9 (2013) 444–453. https://doi.org/10.1007/s11306-012-0452-2.

[214] T. Ogawa, J. Washio, T. Takahashi, S. Echigo, N. Takahashi, Glucose and glutamine metabolism in oral squamous cell carcinoma: Insight from a quantitative metabolomic approach, Oral Surg. Oral Med. Oral Pathol. Oral Radiol. 118 (2014) 218–225. https://doi.org/10.1016/j.oooo.2014.04.003.

[215] F. Ohka, M. Ito, M. Ranjit, T. Senga, A. Motomura, K. Motomura, K. Saito, K. Kato, Y. Kato, T. Wakabayashi, T. Soga, A. Natsume, Quantitative metabolome analysis profiles activation of glutaminolysis in glioma with IDH1 mutation, Tumor Biol. 35 (2014) 5911–5920. https://doi.org/10.1007/s13277-014-1784-5.

[216] T. Saito, M. Sugimoto, K. Igarashi, K. Saito, L. Shao, T. Katsumi, K. Tomita, C. Sato, K. Okumoto, Y. Nishise, H. Watanabe, M. Tomita, Y. Ueno, T. Soga, Dynamics of serum metabolites in patients with chronic hepatitis C receiving pegylated interferon plus ribavirin: A metabolomics analysis, Metabolism. 62 (2013) 1577–1586. https://doi.org/10.1016/j.metabol.2013.07.002.

[217] M. Sugimoto, D.T. Wong, A. Hirayama, T. Soga, M. Tomita, Capillary electrophoresis mass spectrometry-based saliva metabolomics identified oral, breast and pancreatic cancer-specific profiles, Metabolomics. 6 (2010) 78–95. https://doi.org/10.1007/s11306-009-0178-y.

[218] M. Ohshima, K. Sugahara, K. Kasahara, A. Katakura, Metabolomic analysis of the saliva of Japanese patients with oral squamous cell carcinoma, Oncol. Rep. 37 (2017) 2727–2734. https://doi.org/10.3892/or.2017.5561.

[219] M. Tokunaga, K. Kami, S. Ozawa, J. Oguma, A. Kazuno, H. Miyachi, Y. Ohashi, M. Kusuhara, M. Terashima, Metabolome analysis of esophageal cancer tissues using capillary electrophoresis-time-of-flight mass spectrometry, Int. J. Oncol. 52 (2018) 1947–1958. https://doi.org/10.3892/ijo.2018.4340.

[220] M.S. MacLennan, M.G.M. Kok, L. Soliman, A. So, A. Hurtado-Coll, D.D.Y. Chen, Capillary electrophoresis-mass spectrometry for targeted and untargeted analysis of the sub-5 kDa urine metabolome of patients with prostate or bladder cancer: A feasibility study, J. Chromatogr. B Anal. Technol. Biomed. Life Sci. 1074–1075 (2018) 79–85. https://doi.org/10.1016/j.jchromb.2018.01.007.

[221] L.C. Soliman, Y. Hui, A.K. Hewavitharana, D.D.Y. Chen, Monitoring potential prostate cancer biomarkers in urine by capillary electrophoresis-tandem mass spectrometry, J. Chromatogr. A. 1267 (2012) 162–169. https://doi.org/10.1016/j.chroma.2012.07.021.

[222] F. Badoud, K.P. Lam, A. Dibattista, M. Perreault, M.A. Zulyniak, B. Cattrysse, S. Stephenson, P. Britz-Mckibbin, D.M. Mutch, Serum and adipose tissue amino acid homeostasis in the metabolically healthy obese, J. Proteome Res. 13 (2014) 3455–3466. https://doi.org/10.1021/pr500416v.

[223] N.L. Kuehnbaum, J.B. Gillen, M.J. Gibala, P. Britz-McKibbin, Personalized metabolomics for predicting glucose tolerance changes in sedentary women after high-intensity interval training, Sci. Rep. 4 (2014) 1–12. https://doi.org/10.1038/srep06166.

[224] S.G. Ra, S. Maeda, R. Higashino, T. Imai, S. Miyakawa, Metabolomics of salivary fatigue markers in soccer players after consecutive games, Appl. Physiol. Nutr. Metab. 39 (2014) 1120–1126. https://doi.org/10.1139/apnm-2013-0546.

[225] D. Shimura, G. Nakai, Q. Jiao, K. Osanai, K. Kashikura, K. Endo, T. Soga, N. Goda, S. Minamisawa, Metabolomic profiling analysis reveals chamber-dependent metabolite patterns in the mouse heart, Am. J. Physiol. Circ. Physiol. 305 (2013) H494–H505. https://doi.org/10.1152/ajpheart.00867.2012.

[226] T. Uehara, A. Horinouchi, Y. Morikawa, Y. Tonomura, K. Minami, A. Ono, J. Yamate, H. Yamada, Y. Ohno, T. Urushidani, Identification of metabolomic biomarkers for drug-induced acute kidney injury in rats, J. Appl. Toxicol. 34 (2014) 1087–1095. https://doi.org/10.1002/jat.2933.

[227] J. Zeng, H. Kuang, C. Hu, X. Shi, M. Yan, L. Xu, L. Wang, C. Xu, G. Xu, Effect of bisphenol A on rat metabolic profiling studied by using capillary electrophoresis time-of-flight mass spectrometry, Environ. Sci. Technol. 47 (2013) 7457–7465. https://doi.org/10.1021/es400490f.

[228] G.A.B. Canuto, E.A. Castilho-Martins, M.F.M. Tavares, L. Rivas, C. Barbas, Á. López-Gonzálvez, Multi-analytical platform metabolomic approach to study miltefosine mechanism of action and resistance in Leishmania, Anal. Bioanal. Chem. 406 (2014) 3459–3476. https://doi.org/10.1007/s00216-014-7772-1.

[229] J. Piestansky, D. Olesova, J. Galba, K. Marakova, V. Parrak, P. Secnik, P. Secnik, B. Kovacech, A. Kovac, Z. Zelinkova, P. Mikus, Profiling of amino acids in urine samples of patients suffering from inflammatory bowel disease by capillary electrophoresis-mass spectrometry, Molecules. 24 (2019). https://doi.org/10.3390/molecules24183345.

[230] C. Balderas, F.J. Rupérez, E. Ibañez, J. Señorans, J. Guerrero-Fernández, I.G. Casado, R. Gracia-Bouthelier, A. García, C. Barbas, Plasma and urine metabolic fingerprinting of type 1 diabetic children, Electrophoresis. 34 (2013) 2882–2890. https://doi.org/10.1002/elps.201300062.

[231] S. Bernardo-Bermejo, E. Sánchez-López, M. Castro-Puyana, S. Benito-Martínez, F.J. Lucio-Cazaña, M.L. Marina, A Non-Targeted Capillary Electrophoresis-Mass Spectrometry Strategy to Study Metabolic Differences in an In Vitro Model of High-Glucose Induced Changes in Human Proximal Tubular HK-2 Cells, Molecules. 25 (2020) 512. https://doi.org/10.3390/molecules25030512.

[232] T. Mitsui, S. Kira, T. Ihara, N. Sawada, H. Nakagomi, T. Miyamoto, H. Shimura, H. Yokomichi, M. Takeda, Metabolomics Approach to Male Lower Urinary Tract Symptoms: Identification of Possible Biomarkers and Potential Targets for New Treatments, J. Urol. 199 (2018) 1312–1318. https://doi.org/10.1016/j.juro.2017.11.070.

[233] H. Umehara, S. Numata, S.Y. Watanabe, Y. Hatakeyama, M. Kinoshita, Y. Tomioka, K. Nakahara, T. Nikawa, T. Ohmori, Altered KYN/TRP, Gln/Glu, and Met/methionine sulfoxide ratios in the blood plasma of medication-free patients with major depressive disorder, Sci. Rep. 7 (2017) 1–8. https://doi.org/10.1038/s41598-017-05121-6.

[234] A. Yoshikawa, F. Nishimura, A. Inai, Y. Eriguchi, M. Nishioka, A. Takaya, M. Tochigi, Y. Kawamura, T. Umekage, K. Kato, T. Sasaki, Y. Ohashi, K. Iwamoto, K. Kasai, C. Kakiuchi, Mutations of the glycine cleavage system genes possibly affect the negative symptoms of schizophrenia through metabolomic profile changes, Psychiatry Clin. Neurosci. 72 (2018) 168–179. https://doi.org/10.1111/pcn.12628.

[235] S. Koike, M. Bundo, K. Iwamoto, M. Suga, H. Kuwabara, Y. Ohashi, K. Shinoda, Y. Takano, N. Iwashiro, Y. Satomura, T. Nagai, T. Natsubori, M. Tada, H. Yamasue, K. Kasai, A snapshot of plasma metabolites in first-episode schizophrenia: A capillary electrophoresis time-of-flight mass spectrometry study, Transl. Psychiatry. 4 (2014) 1–8. https://doi.org/10.1038/tp.2014.19.

[236] Z. Cieslarova, F.S. Lopes, C.L. do Lago, M.C. França, A.V. Colnaghi Simionato, Capillary electrophoresis tandem mass spectrometry determination of glutamic acid and homocysteine's metabolites: Potential biomarkers of amyotrophic lateral sclerosis, Talanta. 170 (2017) 63–68. https://doi.org/10.1016/j.talanta.2017.03.103.

[237] A.N. MacEdo, S. Mathiaparanam, L. Brick, K. Keenan, T. Gonska, L. Pedder, S. Hill, P. Britz-McKibbin, The Sweat Metabolome of Screen-Positive Cystic Fibrosis Infants: Revealing Mechanisms beyond Impaired Chloride Transport, ACS Cent. Sci. 3 (2017) 904–913. https://doi.org/10.1021/acscentsci.7b00299.

[238] P. Dubot, J. Liang, J. Dubs, Y. Missiak, C. Sarazin, F. Couderc, E. Caussé, Sweat chloride quantification using capillary electrophoresis, Pract. Lab. Med. 13 (2019) 1–6. https://doi.org/10.1016/j.plabm.2018.e00114.

[239] N.L. Kuehnbaum, A. Kormendi, P. Britz-Mckibbin, Multisegment injection-capillary electrophoresis-mass spectrometry: A high-throughput platform for metabolomics with high data fidelity, Anal. Chem. 85 (2013) 10664–10669. https://doi.org/10.1021/ac403171u.

[240] E. Mishima, S. Fukuda, C. Mukawa, A. Yuri, Y. Kanemitsu, Y. Matsumoto, Y. Akiyama, N.N. Fukuda, H. Tsukamoto, K. Asaji, H. Shima, K. Kikuchi, C. Suzuki, T. Suzuki, Y. Tomioka, T. Soga, S. Ito, T. Abe, Evaluation of the impact of gut microbiota on uremic solute accumulation by a CE-TOFMS–based metabolomics approach, Kidney Int. 92 (2017) 634–645. https://doi.org/10.1016/j.kint.2017.02.011.

[241] T. Ooga, H. Sato, A. Nagashima, K. Sasaki, M. Tomita, T. Soga, Y. Ohashi, Metabolomic anatomy of an animal model revealing homeostatic imbalances in dyslipidaemia, Mol. Biosyst. 7 (2011) 1217.

https://doi.org/10.1039/c0mb00141d.
[242] M. Castro-Puyana, R. Pérez-Míguez, L. Montero, M. Herrero, Reprint of: Application of mass spectrometry-based metabolomics approaches for food safety, quality and traceability, TrAC Trends Anal. Chem. 96 (2017) 62–78. https://doi.org/10.1016/j.trac.2017.08.007.
[243] M. Kusano, Z. Yang, Y. Okazaki, R. Nakabayashi, A. Fukushima, K. Saito, Using metabolomic approaches to explore chemical diversity in rice, Mol. Plant. 8 (2015) 58–67. https://doi.org/10.1016/j.molp.2014.11.010.
[244] Y. Onda, A. Miyagi, K. Takahara, H. Uchimiya, M. Kawai-Yamada, Effects of NAD kinase 2 overexpression on primary metabolite profiles in rice leaves under elevated carbon dioxide, Plant Biol. 16 (2014) 819–824. https://doi.org/10.1111/plb.12131.
[245] D. Sato, M. Sugimoto, H. Akashi, M. Tomita, T. Soga, Comparative metabolite profiling of foxglove aphids (Aulacorthum solani Kaltenbach) on leaves of resistant and susceptible soybean strains, Mol. Biosyst. 10 (2014) 909–915. https://doi.org/10.1039/c3mb70595a.
[246] K. Tawaraya, R. Horie, S. Saito, T. Wagatsuma, K. Saito, A. Oikawa, Metabolite Profiling of Root Exudates of Common Bean under Phosphorus Deficiency, Metabolites. 4 (2014) 599–611. https://doi.org/10.3390/metabo4030599.
[247] M. Sato, A. Miyagi, S. Yoneyama, S. Gisusi, Y. Tokuji, M. Kawai-Yamada, CE–MS-based metabolomics reveals the metabolic profile of maitake mushroom (Grifola frondosa) strains with different cultivation characteristics, Biosci. Biotechnol. Biochem. 81 (2017) 2314–2322. https://doi.org/10.1080/09168451.2017.1387049.
[248] S. Muroya, M. Oe, I. Nakajima, K. Ojima, K. Chikuni, CE-TOF MS-based metabolomic profiling revealed characteristic metabolic pathways in postmortem porcine fast and slow type muscles, Meat Sci. 98 (2014) 726–735. https://doi.org/10.1016/j.meatsci.2014.07.018.
[249] H. Koyama, S. Okamoto, N. Watanabe, N. Hoshino, M. Jimbo, K. Yasumoto, S. Watabe, Dynamic changes in the accumulation of metabolites in brackish water clam Corbicula japonica associated with alternation of salinity, Comp. Biochem. Physiol. Part - B Biochem. Mol. Biol. 181 (2015) 59–70. https://doi.org/10.1016/j.cbpb.2014.11.007.
[250] Y. Ohashi, A. Hirayama, T. Ishikawa, S. Nakamura, K. Shimizu, Y. Ueno, M. Tomita, T. Soga, Depiction of metabolome changes in histidine-starved Escherichia coli by CE-TOFMS, Mol. Biosyst. 4 (2008) 135–147. https://doi.org/10.1039/b714176a.
[251] T. Osanai, A. Oikawa, T. Shirai, A. Kuwahara, H. Iijima, K. Tanaka, M. Ikeuchi, A. Kondo, K. Saito, M.Y. Hirai, Capillary electrophoresis-mass spectrometry reveals the distribution of carbon metabolites during nitrogen starvation in Synechocystis sp. PCC 6803, Environ. Microbiol. 16 (2014) 512–524. https://doi.org/10.1111/1462-2920.12170.
[252] G. Das, J.K. Patra, S.Y. Lee, C. Kim, J.G. Park, K.H. Baek, Analysis of metabolomic profile of fermented Orostachys japonicus A. Berger by capillary electrophoresis time of flight mass spectrometry, PLoS One. 12 (2017) 1–13. https://doi.org/10.1371/journal.pone.0181280.
[253] T.J. Comi, M.A. Makurath, M.C. Philip, S.S. Rubakhin, J. V. Sweedler, MALDI MS Guided Liquid Microjunction Extraction for Capillary Electrophoresis-Electrospray Ionization MS Analysis of Single Pancreatic Islet Cells, Anal. Chem. 89 (2017) 7765–7772. https://doi.org/10.1021/acs.analchem.7b01782.
[254] C. Bayle, E. Caussé, F. Couderc, Determination of aminothiols in body fluids, cells, and tissues by capillary electrophoresis, Electrophoresis. 25 (2004) 1457–1472. https://doi.org/10.1002/elps.200305874.
[255] E. Caussé, R. Terrier, S. Champagne, M. Nertz, P. Valdiguié, R. Salvayre, F. Couderc, Quantitation of homocysteine in human plasma by capillary electrophoresis and laser-induced fluorescence detection, J. Chromatogr. A. 817 (1998) 181–185. https://doi.org/10.1016/S0021-9673(98)00363-X.
[256] C. Bayle, E. Causse, M. Arellano, N. Simeon, F. Couderc, Quelques applications cliniques de l'electrophorese capillaire, Analusis. 27 (1999) 138–143. https://doi.org/10.1051/analusis:1999270138.
[257] E. Caussé, N. Siri, H. Bellet, S. Champagne, C. Bayle, P. Valdiguié, R. Salvayre, F. Couderc, Plasma homocysteine determined by capillary electrophoresis with laser-induced fluorescence detection., Clin. Chem. 45 (1999) 412–4.

http://www.ncbi.nlm.nih.gov/pubmed/10053046.

[258] E. Caussé, C. Issac, P. Malatray, C. Bayle, P. Valdiguié, R. Salvayre, F. Couderc, Assays for total homocysteine and other thiols by capillary electrophoresis-laser-induced fluorescence detection - I. Preanalytical condition studies, J. Chromatogr. A. 895 (2000) 173–178. https://doi.org/10.1016/S0021-9673(00)00672-5.

[259] E. Caussé, P. Malatray, R. Calaf, P. Charpiot, M. Candito, C. Bayle, P. Valdiguié, R. Salvayre, F. Couderc, Plasma total homocysteine and other thiols analyzed by capillary electrophoresis/laser-induced fluorescence detection: Comparison with two other methods, Electrophoresis. 21 (2000) 2074–2079. https://doi.org/10.1002/1522-2683(20000601)21:10<2074::AID-ELPS2074>3.0.CO;2-L.

[260] A. Tripodi, V. Chantarangkul, R. Lombardi, A. Lecchi, P.M. Mannucci, M. Cattaneo, Multicenter study of homocysteine measurement - Performance characteristics of different methods, influence of standards on interlaboratory agreement of results, Thromb. Haemost. 85 (2001) 291–295.

[261] A. Zinellu, S. Sotgia, L. Deiana, C. Carru, Quantification of Thiol-Containing Amino Acids Linked by Disulfides to LDL, Clin. Chem. 51 (2005) 658–660. https://doi.org/10.1373/clinchem.2004.043943.

[262] A. Zinellu, S. Sotgia, M.F. Usai, R. Chessa, L. Deiana, C. Carru, Thiol redox status evaluation in red blood cells by capillary electrophoresis-laser induced fluorescence detection, Electrophoresis. 26 (2005) 1963–1968. https://doi.org/10.1002/elps.200400042.

[263] A. Zinellu, S. Sotgia, L. Deiana, C. Carru, Quantification of Thiol-Containing Amino Acids Linked by Disulfides to LDL, Clin. Chem. 51 (2005) 658–660. https://doi.org/10.1373/clinchem.2004.043943.

[264] A. Zinellu, S. Sotgia, B. Scanu, L. Deiana, G. Talanas, P.F. Terrosu, C. Carru, Low density lipoprotein S-homocysteinylation is increased in acute myocardial infarction patients, Clin. Biochem. 45 (2012) 359–362. https://doi.org/10.1016/j.clinbiochem.2011.12.017.

[265] A. Zinellu, E. Zinellu, S. Sotgia, M. Formato, G.M. Cherchi, L. Deiana, C. Carru, Factors affecting S-homocysteinylation of LDL apoprotein B, Clin. Chem. 52 (2006) 2054–2059. https://doi.org/10.1373/clinchem.2006.071142.

[266] C. Carru, L. Deiana, S. Sotgia, M.F. Usai, A. Zinellu, Relationships between white blood cell count and levels of serum homocysteine and cysteine in healthy subjects., Haematologica. 90 (2005) 136–7. http://www.ncbi.nlm.nih.gov/pubmed/15710562.

[267] A. Pinna, C. Carru, A. Zinellu, S. Dore, L. Deiana, F. Carta, Plasma homocysteine and cysteine levels in retinal vein occlusion, Investig. Ophthalmol. Vis. Sci. 47 (2006) 4067–4071. https://doi.org/10.1167/iovs.06-0290.

[268] A. Zinellu, S. Sotgia, A.M. Posadino, V. Pasciu, M.G. Perino, B. Tadolini, L. Deiana, C. Carru, Highly sensitive simultaneous detection of cultured cellular thiols by laser induced fluorescence-capillary electrophoresis, Electrophoresis. 26 (2005) 1063–1070. https://doi.org/10.1002/elps.200406191.

[269] C. Carru, L. Deiana, S. Sotgia, G.M. Pes, A. Zinellu, Plasma thiols redox status by laser-induced fluorescence capillary electrophoresis, Electrophoresis. 25 (2004) 882–889. https://doi.org/10.1002/elps.200305768.

[270] A. Zinellu, S. Sotgia, B. Scanu, M.F. Usai, A.G. Fois, V. Spada, A. Deledda, L. Deiana, P. Pirina, C. Carru, Simultaneous detection of N-acetyl-l-cysteine and physiological low molecular mass thiols in plasma by capillary electrophoresis, Amino Acids. 37 (2009) 395–400. https://doi.org/10.1007/s00726-008-0167-x.

[271] A. Zinellu, S. Sotgia, B. Scanu, E. Pisanu, M. Sanna, S. Sati, L. Deiana, S. Sengupta, C. Carru, Determination of homocysteine thiolactone, reduced homocysteine, homocystine, homocysteine-cysteine mixed disulfide, cysteine and cystine in a reaction mixture by overimposed pressure/voltage capillary electrophoresis, Talanta. 82 (2010) 1281–1285. https://doi.org/10.1016/j.talanta.2010.06.054.

[272] P. Furmaniak, P. Kubalczyk, R. Głowacki, Determination of homocysteine thiolactone in urine by field amplified sample injection and sweeping MEKC method with UV detection, J. Chromatogr. B Anal. Technol. Biomed. Life Sci. 961 (2014) 36–41. https://doi.org/10.1016/j.jchromb.2014.04.051.

[273] A. Zinellu, S. Sotgia, M.F. Usai, E. Zinellu, A.M. Posadino, L. Gaspa, R. Chessa, A. Pinna, F. Carta, L. Deiana, C.

Carru, Plasma methionine determination by capillary electrophoresis-UV assay: Application on patients affected by retinal venous occlusive disease, Anal. Biochem. 363 (2007) 91–96. https://doi.org/10.1016/j.ab.2007.01.009.

[274] P. Ševčíková, Z. Glatz, J. Tomandl, Determination of homocysteine in human plasma by micellar electrokinetic chromatography and in-capillary detection reaction with 2,2′-dipyridyl disulfide, J. Chromatogr. A. 990 (2003) 197–204. https://doi.org/10.1016/S0021-9673(03)00048-7.

[275] P. Kubalczyk, E. Bald, Transient pseudo-isotachophoretic stacking in analysis of plasma for homocysteine by capillary zone electrophoresis, Anal. Bioanal. Chem. 384 (2006) 1181–1185. https://doi.org/10.1007/s00216-005-0271-7.

[276] Y. Zhang, X. Ke, W. Shen, Y. Liu, Relationship of homocysteine and gene polymorphisms of its related metabolic enzymes with Alzheimer's disease., Chinese Med. Sci. J. = Chung-Kuo i Hsueh k'o Hsueh Tsa Chih. 20 (2005) 247–51. http://www.ncbi.nlm.nih.gov/pubmed/16422253.

[277] E. Caussé, N. Siri, J.. Arnal, C. Bayle, P. Malatray, P. Valdiguié, R. Salvayre, F. Couderc, Determination of asymmetrical dimethylarginine by capillary electrophoresis–laser-induced fluorescence, J. Chromatogr. B Biomed. Sci. Appl. 741 (2000) 77–83. https://doi.org/10.1016/S0378-4347(00)00034-7.

[278] G. Trapp, K. Sydow, M.T. Dulay, T. Chou, J.P. Cooke, R.N. Zare, Capillary electrophoretic and micellar electrokinetic separations of asymmetric dimethyl-L-arginine and structurally related amino acids: Quantitation in human plasma, J. Sep. Sci. 27 (2004) 1483–1490. https://doi.org/10.1002/jssc.200401918.

[279] A. Zinellu, S. Sotgia, E. Zinellu, A. Pinna, F. Carta, L. Gaspa, L. Deiana, C. Carru, High-throughput CZE-UV determination of arginine and dimethylated arginines in human plasma, Electrophoresis. 28 (2007) 1942–1948. https://doi.org/10.1002/elps.200600534.

[280] T.H. Linz, S.M. Lunte, Heat-assisted extraction for the determination of methylarginines in serum by CE, Electrophoresis. 34 (2013) 1693–1700. https://doi.org/10.1002/elps.201200567.

[281] Z. Lohinai, B. Keremi, E. Szoko, T. Tabi, C. Szabo, Z. Tulassay, M. Levine, Bacterial Lysine Decarboxylase Influences Human Dental Biofilm Lysine Content, Biofilm Accumulation, and Subclinical Gingival Inflammation, J. Periodontol. 83 (2012) 1048–1056. https://doi.org/10.1902/jop.2011.110474.

[282] T. Tábi, Z. Lohinai, M. Pálfi, M. Levine, É. Szökő, CE-LIF determination of salivary cadaverine and lysine concentration ratio as an indicator of lysine decarboxylase enzyme activity, Anal. Bioanal. Chem. 391 (2008) 647–651. https://doi.org/10.1007/s00216-008-2026-8.

[283] M. Casado, M. Molero, C. Sierra, A. García-Cazorla, A. Ormazabal, R. Artuch, Analysis of cerebrospinal fluid γ-aminobutyric acid by capillary electrophoresis with laser-induced fluorescence detection, Electrophoresis. 35 (2014) 1181–1187. https://doi.org/10.1002/elps.201300261.

[284] E. Sbrana, E. Bramanti, M.C. Spinetti, G. Raspi, S-Adenosyl methionine/S-adenosyl-L-homocysteine ratio determination by capillary electrophoresis employed as a monitoring tool for the antiviral effectiveness of adenosine analogs, Electrophoresis. 25 (2004) 1518–1521. https://doi.org/10.1002/elps.200305851.

[285] E. Sbrana, A. Paladini, E. Bramanti, M.C. Spinetti, G. Raspi, Quantitation of reduced glutathione and cysteine in human immunodeficiency virus-infected patients, Electrophoresis. 25 (2004) 1522–1529. https://doi.org/10.1002/elps.200305848.

[286] S. Sotgia, E. Pisanu, G. Pintus, G.L. Erre, G.A. Pinna, L. Deiana, C. Carru, A. Zinellu, Plasma L-Ergothioneine Measurement by High-Performance Liquid Chromatography and Capillary Electrophoresis after a Pre-Column Derivatization with 5-Iodoacetamidofluorescein (5-IAF) and Fluorescence Detection, PLoS One. 8 (2013) e70374. https://doi.org/10.1371/journal.pone.0070374.

[287] S. Sotgia, A. Zinellu, A.A. Mangoni, G. Pintus, J. Attia, C. Carru, M. McEvoy, Clinical and biochemical correlates of serum L-ergothioneine concentrations in community-dwelling middle-aged and older adults, PLoS One. 9 (2014) 1–5. https://doi.org/10.1371/journal.pone.0084918.

[288] M.P. Lorenzo, A. Villaseñor, A. Ramamoorthy, A. Garcia, Optimization and validation of a capillary electrophoresis

laser-induced fluorescence method for amino acids determination in human plasma: Application to bipolar disorder study, Electrophoresis. 34 (2013) 1701–1709. https://doi.org/10.1002/elps.201200632.

[289] L. Perquis, H.Y. Ta, V. Ong-Meang, A. Poinso, F. Collin, V. Poinsot, F. Couderc, Capillary electrophoresis/visible-LED induced fluorescence of tryptophan: What's new?, Electrophoresis. 40 (2019) 2342–2348. https://doi.org/10.1002/elps.201900058.

[290] Y.C. Chen, P.L. Chang, Baseline separation of amino acid biomarkers of hepatocellular carcinoma by polyvinylpyrrolidone-filled capillary electrophoresis with light-emitting diode-induced fluorescence in the presence of mixed micelles, Analyst. 140 (2015) 847–853. https://doi.org/10.1039/c4an01550a.

[291] C. Massip, P. Riollet, E. Quemener, C. Bayle, R. Salvayre, F. Couderc, E. Caussé, Choice of different dyes to label tyrosine and nitrotyrosine, J. Chromatogr. A. 979 (2002) 209–215. https://doi.org/10.1016/S0021-9673(02)01502-9.

[292] J.B. Zhang, M.J. Li, Z. Li, X.J. Yan, J.Q. Yuan, W.X. Dong, Y. Zhang, Q.C. Chu, J.N. Ye, Study on urinary profile of inborn errors of metabolism by 18-crown-6 modified capillary electrophoresis with laser-induced fluorescence detection, J. Chromatogr. B Anal. Technol. Biomed. Life Sci. 929 (2013) 102–106. https://doi.org/10.1016/j.jchromb.2013.04.016.

[293] N. Ota, S.S. Rubakhin, J. V. Sweedler, D-Alanine in the islets of Langerhans of rat pancreas, Biochem. Biophys. Res. Commun. 447 (2014) 328–333. https://doi.org/10.1016/j.bbrc.2014.03.153.

[294] I. Campesi, A. Galistu, C. Carru, F. Franconi, M. Fois, A. Zinellu, Glutamyl cycle in the rat liver appears to be sex-gender specific, Exp. Toxicol. Pathol. 65 (2013) 585–589. https://doi.org/10.1016/j.etp.2012.05.004.

[295] Z. Shen, Z. Sun, L. Wu, K. Wu, S. Sun, Z. Huang, Rapid method for the determination of amino acids in serum by capillary electrophoresis, J. Chromatogr. A. 979 (2002) 227–232. https://doi.org/10.1016/S0021-9673(02)01251-7.

[296] M. Zhu, D.E. Nix, R.D. Adam, J.M. Childs, C.A. Peloquin, Pharmacokinetics of Cycloserine under Fasting Conditions and with High-Fat Meal, Orange Juice, and Antacids, Pharmacotherapy. 21 (2001) 891–897. https://doi.org/10.1592/phco.21.11.891.34524.

[297] E.A. Clark, J.C. Fanguy, C.S. Henry, High-throughput multi-analyte screening for renal disease using capillary electrophoresis, J. Pharm. Biomed. Anal. 25 (2001) 795–801. https://doi.org/10.1016/S0731-7085(01)00340-5.

[298] J.N. Kim, J.S. Yun, H.W. Ryu, Simultaneous determination of δ-aminolevulinic acid, porphobilinogen, levulinic acid and glycine in culture broth by capillary electrophoresis, J. Chromatogr. A. 938 (2001) 137–143. https://doi.org/10.1016/S0021-9673(01)01149-9.

[299] Y. Takagai, S. Igarashi, Determination of ppb Levels of Tryptophan Derivatives by Capillary Electrophoresis with Homogeneous Liquid–Liquid Extraction and Sweeping Method, Chem. Pharm. Bull. (Tokyo). 51 (2003) 373–377. https://doi.org/10.1248/cpb.51.373.

[300] M. Forteschi, S. Sotgia, S. Assaretti, D. Arru, D. Cambedda, E. Sotgiu, A. Zinellu, C. Carru, Simultaneous determination of aromatic amino acids in human blood plasma by capillary electrophoresis with UV-absorption detection, J. Sep. Sci. 38 (2015) 1794–1799. https://doi.org/10.1002/jssc.201500038.

[301] A. Zinellu, M.A. Caria, C. Tavera, S. Sotgia, R. Chessa, L. Deiana, C. Carru, Plasma creatinine and creatine quantification by capillary electrophoresis diode array detector, Anal. Biochem. 342 (2005) 186–193. https://doi.org/10.1016/j.ab.2005.01.045.

[302] A. Zinellu, S. Sotgia, E. Zinellu, R. Chessa, L. Deiana, C. Carru, Assay for the simultaneous determination of guanidinoacetic acid, creatinine and creatine in plasma and urine by capillary electrophoresis UV-detection, J. Sep. Sci. 29 (2006) 704–708. https://doi.org/10.1002/jssc.200500428.

[303] S. Sotgia, C. Carru, M.A. Caria, B. Tadolini, L. Deiana, A. Zinellu, Acute variations in homocysteine levels are related to creatine changes induced by physical activity, Clin. Nutr. 26 (2007) 444–449. https://doi.org/10.1016/j.clnu.2007.05.003.

[304] H. Ren, X. Liu, S. Jiang, Preconcentration of 3-nitrotyrosine in urine by transient isotachophoresis in MEKC, J. Pharm. Biomed. Anal. 78–79 (2013) 100–104. https://doi.org/10.1016/j.jpba.2013.02.002.

[305] P. Tůma, Rapid and Sensitive Determination of Branched-Chain Amino Acids in Human Plasma by Capillary Electrophoresis with Contactless Conductivity Detection for Physiological Studies, in: Clin. Appl. Capill. Electrophor. Methods Protoc. Methods Mol. Biol., 2019: pp. 15–24. https://doi.org/10.1007/978-1-4939-9213-3_2.

[306] P. Tůma, J. Gojda, Rapid determination of branched chain amino acids in human blood plasma by pressure-assisted capillary electrophoresis with contactless conductivity detection, Electrophoresis. 36 (2015) 1969–1975. https://doi.org/10.1002/elps.201400585.

[307] P. Kubacák, I. Valásková, E. Havránek, [Optimal conditions for determination of L-cystine using capillary isotachophoresis]., Ceska Slov. Farm. 51 (2002) 257–60. http://www.ncbi.nlm.nih.gov/pubmed/12407926.

[308] L. Hernandez, J. Escalona, P. Verdeguer, N.A. Guzman, In Vivo Monitoring of Brain Glutamate by Microdialysis Coupled to Capillary Electrophoresis and Laser Induced Fluorescence Detection, J. Liq. Chromatogr. 16 (1993) 2149–2160. https://doi.org/10.1080/10826079308019921.

[309] F. Robert, L. Bert, L. Denoroy, B. Renaud, Capillary zone electrophoresis with laser-induced fluorescence detection for the determination of nanomolar concentrations of noradrenaline and dopamine: application to brain microdialyzate analysis, Anal. Chem. 67 (1995) 1838–1844. https://doi.org/10.1021/ac00107a013.

[310] F. Robert, L. Bert, L. Lambás-Señas, L. Denoroy, B. Renaud, In vivo monitoring of extracellular noradrenaline and glutamate from rat brain cortex with 2-min microdialysis sampling using capillary electrophoresis with laser-induced fluorescence detection, J. Neurosci. Methods. 70 (1996) 153–162. https://doi.org/10.1016/S0165-0270(96)00113-6.

[311] M.W. Lada, T.W. Vickroy, R.T. Kennedy, High Temporal Resolution Monitoring of Glutamate and Aspartate in Vivo Using Microdialysis On-Line with Capillary Electrophoresis with Laser-Induced Fluorescence Detection, Anal. Chem. 69 (1997) 4560–4565. https://doi.org/10.1021/ac970518u.

[312] M.W. Lada, R.T. Kennedy, Quantitative in Vivo Monitoring of Primary Amines in Rat Caudate Nucleus Using Microdialysis Coupled by a Flow-Gated Interface to Capillary Electrophoresis with Laser-Induced Fluorescence Detection, Anal. Chem. 68 (1996) 2790–2797. https://doi.org/10.1021/ac960178x.

[313] F. Robert, L. Bert, S. Parrot, L. Denoroy, L. Stoppini, B. Renaud, Coupling on-line brain microdialysis, precolumn derivatization and capillary electrophoresis for routine minute sampling of O-phosphoethanolamine and excitatory amino acids, J. Chromatogr. A. 817 (1998) 195–203. https://doi.org/10.1016/S0021-9673(98)00321-5.

[314] M.W. Lada, T.W. Vickroy, R.T. Kennedy, Evidence for Neuronal Origin and Metabotropic Receptor-Mediated Regulation of Extracellular Glutamate and Aspartate in Rat Striatum In Vivo Following Electrical Stimulation of the Prefrontal Cortex, J. Neurochem. 70 (2002) 617–625. https://doi.org/10.1046/j.1471-4159.1998.70020617.x.

[315] L.A. Dawson, Capillary electrophoresis and microdialysis: current technology and applications, J. Chromatogr. B Biomed. Sci. Appl. 697 (1997) 89–99. https://doi.org/10.1016/S0378-4347(96)00533-6.

[316] T. Lapainis, J. V Sweedler, Contributions of capillary electrophoresis to neuroscience, J. Chromatogr. A. 1184 (2008) 144–158. https://doi.org/10.1016/j.chroma.2007.10.098.

[317] S. Parrot, L. Bert, L. Mouly-Badina, V. Sauvinet, J. Colussi-Mas, L. Lambás-Señas, F. Robert, J.P. Bouilloux, M.F. Suaud-Chagny, L. Denoroy, B. Renaud, Microdialysis monitoring of catecholamines and excitatory amino acids in the rat and mouse brain: Recent developments based on capillary electrophoresis with laser-induced fluorescence detection - A mini-review, Cell. Mol. Neurobiol. 23 (2003) 793–804. https://doi.org/10.1023/A:1025009221285.

[318] P. Nandi, S.M. Lunte, Recent trends in microdialysis sampling integrated with conventional and microanalytical systems for monitoring biological events: A review, Anal. Chim. Acta. 651 (2009) 1–14. https://doi.org/10.1016/j.aca.2009.07.064.

[319] V. Sauvinet, S. Parrot, N. Benturquia, E. Bravo-Moratón, B. Renaud, L. Denoroy, In vivo simultaneous monitoring of γ-aminobutyric acid, glutamate, and L-aspartate using brain microdialysis and capillary electrophoresis with laser-induced fluorescence detection: Analytical developments and in vitro/in vivo validations, Electrophoresis. 24 (2003) 3187–3196. https://doi.org/10.1002/elps.200305565.

[320] N. Benturquia, S. Parrot, V. Sauvinet, B. Renaud, L. Denoroy, Simultaneous determination of vigabatrin and amino

acid neurotransmitters in brain microdialysates by capillary electrophoresis with laser-induced fluorescence detection, J. Chromatogr. B Anal. Technol. Biomed. Life Sci. 806 (2004) 237–244. https://doi.org/10.1016/j.jchromb.2004.03.061.

[321] S. Parrot, V. Sauvinet, V. Riban, A. Depaulis, B. Renaud, L. Denoroy, High temporal resolution for in vivo monitoring of neurotransmitters in awake epileptic rats using brain microdialysis and capillary electrophoresis with laser-induced fluorescence detection, J. Neurosci. Methods. 140 (2004) 29–38. https://doi.org/10.1016/j.jneumeth.2004.03.025.

[322] L. Denoroy, S. Parrot, L. Renaud, B. Renaud, L. Zimmer, In-capillary derivatization and capillary electrophoresis separation of amino acid neurotransmitters from brain microdialysis samples, J. Chromatogr. A. 1205 (2008) 144–149. https://doi.org/10.1016/j.chroma.2008.07.043.

[323] S. Kaul, M.D. Faiman, C.E. Lunte, Determination of GABA, glutamate and carbamathione in brain microdialysis samples by capillary electrophoresis with fluorescence detection, Electrophoresis. 32 (2011) 284–291. https://doi.org/10.1002/elps.201000463.

[324] K.B. O'Brien, A.Z. Sharrief, E.J. Nordstrom, A.J. Travanty, M. Huynh, M.P. Romero, K.C. Bittner, M.T. Bowser, F.H. Burton, Biochemical markers of striatal desensitization in cortical-limbic hyperglutamatergic TS- & OCD-like transgenic mice, J. Chem. Neuroanat. 89 (2018) 11–20. https://doi.org/10.1016/j.jchemneu.2018.02.007.

[325] C.M. Ciriacks, M.T. Bowser, Measuring the effect of glutamate receptor agonists on extracellular d-serine concentrations in the rat striatum using online microdialysis-capillary electrophoresis, Neurosci. Lett. 393 (2006) 200–205. https://doi.org/10.1016/j.neulet.2005.09.080.

[326] K.B. O'Brien, M. Esguerra, C.T. Klug, R.F. Miller, M.T. Bowser, A high-throughput on-line microdialysis-capillary assay for D-serine, Electrophoresis. 24 (2003) 1227–1235. https://doi.org/10.1002/elps.200390158.

[327] Z. Li, A. Zharikova, J. Bastian, L. Esperon, N. Hebert, C. Mathes, N.E. Rowland, J. Peris, High temporal resolution of amino acid levels in rat nucleus accumbens during operant ethanol self-administration: Involvement of elevated glycine in anticipation, J. Neurochem. 106 (2008) 170–181. https://doi.org/10.1111/j.1471-4159.2008.05346.x.

[328] J.M. Kasper, R.G. Booth, J. Peris, Serotonin-2C receptor agonists decrease potassium-stimulated GABA release in the nucleus accumbens, Synapse. 69 (2015) 78–85. https://doi.org/10.1002/syn.21790.

[329] B.J. Venton, T.E. Robinson, R.T. Kennedy, Transient changes in nucleus accumbens amino acid concentrations correlate with individual responsivity to the predator fox odor 2,5-dihydro-2,4,5- trimethylthiazoline, J. Neurochem. 96 (2006) 236–246. https://doi.org/10.1111/j.1471-4159.2005.03549.x.

[330] R.K. Harstad, M.T. Bowser, High-Speed Microdialysis–Capillary Electrophoresis Assays for Measuring Branched Chain Amino Acid Uptake in 3T3-L1 cells, Anal. Chem. 88 (2016) 8115–8122. https://doi.org/10.1021/acs.analchem.6b01846.

[331] M.M. Weisenberger, M.T. Bowser, In Vivo Monitoring of Amino Acid Biomarkers from Inguinal Adipose Tissue Using Online Microdialysis-Capillary Electrophoresis, Anal. Chem. 89 (2017) 1009–1014. https://doi.org/10.1021/acs.analchem.6b04516.

[332] A.L. Hogerton, M.T. Bowser, Monitoring neurochemical release from astrocytes using in vitro microdialysis coupled with high-speed capillary electrophoresis, Anal. Chem. 85 (2013) 9070–9077. https://doi.org/10.1021/ac401631k.

[333] G. Zachar, Z. Wagner, E. Ba, Differential Changes of Extracellular Aspartate and Glutamate in the Striatum of Domestic Chicken Evoked by High Potassium or Distress : An In Vivo Microdialysis Study, (2012) 1730–1737. https://doi.org/10.1007/s11064-012-0783-4.

[334] L. Betancourt, P. Rada, D. Paredes, L. Hernández, In vivo monitoring of cerebral agmatine by microdialysis and capillary electrophoresis, J. Chromatogr. B. 880 (2012) 58–65. https://doi.org/10.1016/j.jchromb.2011.11.016.

[335] M. Skirzewski, W. López, E. Mosquera, L. Betancourt, B. Catlow, M. Chiurillo, N. Loureiro, L. Hernández, P. Rada, Enhanced GABAergic tone in the ventral pallidum: memory of unpleasant experiences?, Neuroscience. 196

(2011) 131–146. https://doi.org/10.1016/j.neuroscience.2011.08.058.
[336] N. Calderón, L. Betancourt, L. Hernández, P. Rada, A ketogenic diet modifies glutamate, gamma-aminobutyric acid and agmatine levels in the hippocampus of rats: A microdialysis study, Neurosci. Lett. 642 (2017) 158–162. https://doi.org/10.1016/j.neulet.2017.02.014.
[337] L. Betancourt, P. Rada, L. Hernandez, H. Araujo, G.A. Ceballos, L.E. Hernandez, P. Tucci, Z. Mari, M. De Pasquale, D.A. Paredes, Micellar electrokinetic chromatography with laser induced fluorescence detection shows increase of putrescine in erythrocytes of Parkinson's disease patients, J. Chromatogr. B. 1081–1082 (2018) 51–57. https://doi.org/10.1016/j.jchromb.2018.02.015.
[338] N. Téllez, N. Aguilera, B. Quiñónez, E. Silva, L.E. González, L. Hernández, Arginine and glutamate levels in the gingival crevicular fluid from patients with chronic periodontitis, Braz. Dent. J. 19 (2008) 318–322. https://doi.org/10.1590/s0103-64402008000400006.
[339] G. Zachar, T. Jakó, I. Vincze, Z. Wagner, T. Tábi, E. Bálint, S. Mezey, É. Szökö, A. Csillag, Age-related and function-dependent regional alterations of free L- and D-Aspartate in postembryonic chick brain, Acta Biol. Hung. 69 (2018) 1–15. https://doi.org/10.1556/018.68.2018.1.1.
[340] H. Li, Z. ying Yan, Analysis of amino acid neurotransmitters in hypothalamus of rats during cerebral ischemia-reperfusion by microdialysis and capillary electrophoresis, Biomed. Chromatogr. 24 (2010) 1185–1192. https://doi.org/10.1002/bmc.1425.
[341] H. Li, C. Li, Z. Yan, J. Yang, H. Chen, Simultaneous monitoring multiple neurotransmitters and neuromodulators during cerebral ischemia/reperfusion in rats by microdialysis and capillary electrophoresis, J. Neurosci. Methods. 189 (2010) 162–168. https://doi.org/10.1016/j.jneumeth.2010.03.022.
[342] H.-L. Chen, X.-J. Zhang, S.-D. Qi, H.-X. Xu, J.J.Y. Sung, Z.-X. Bian, Simultaneous determination of glutamate and aspartate in rat periaqueductal gray matter microdialysates by capillary electrophoresis with laser-induced fluorescence, J. Chromatogr. B. 877 (2009) 3248–3252. https://doi.org/10.1016/j.jchromb.2009.08.006.
[343] J. Wu, Z. Chen, N.J. Dovichi, Reaction rate, activation energy, and detection limit for the reaction of 5-furoylquinoline-3-carboxaldehyde with neurotransmitters in artificial cerebrospinal fluid, J. Chromatogr. B Biomed. Sci. Appl. 741 (2000) 85–88. https://doi.org/10.1016/S0378-4347(99)00540-X.
[344] Z. Chen, J. Wu, G.B. Baker, M. Parent, N.J. Dovichi, Application of capillary electrophoresis with laser-induced fluorescence detection to the determination of biogenic amines and amino acids in brain microdialysate and homogenate samples, J. Chromatogr. A. 914 (2001) 293–298. https://doi.org/10.1016/S0021-9673(01)00539-8.
[345] N. Benturquia, F. Couderc, V. Sauvinet, C. Orset, S. Parrot, C. Bayle, B. Renaud, L. Denoroy, Analysis of serotonin in brain microdialysates using capillary electrophoresis and native laser-induced fluorescence detection, Electrophoresis. 26 (2005) 1071–1079. https://doi.org/10.1002/elps.200410150.
[346] Y. Takada, M. Yoshida, M. Sakairi, H. Koizumi, Detection of γ-aminobutyric acid in a rat brain usingin vivo microdialysis-capillary electrophoresis/mass spectrometry, Rapid Commun. Mass Spectrom. 9 (1995) 895–896. https://doi.org/10.1002/rcm.1290091006.
[347] Z. Zhang, H. Ye, J. Wang, L. Hui, L. Li, Pressure-assisted capillary electrophoresis coupling with matrix-assisted laser desorption/ionization-mass spectrometric imaging for quantitative analysis of complex peptide mixtures, Anal. Chem. 84 (2012) 7684–7691. https://doi.org/10.1021/ac300628s.
[348] J. Wang, M. Ma, R. Chen, L. Li, Enhanced neuropeptide profiling via capillary electrophoresis off-line coupled with MALDI FTMS, Anal. Chem. 80 (2008) 6168–6177. https://doi.org/10.1021/ac800382t.
[349] J. Wang, H. Ye, Z. Zhang, F. Xiang, G. Girdaukas, L. Li, Advancing matrix-assisted laser desorption/ionization-mass spectrometric imaging for capillary electrophoresis analysis of peptides, Anal. Chem. 83 (2011) 3462–3469. https://doi.org/10.1021/ac200708f.
[350] S. Jiang, Z. Liang, L. Hao, L. Li, Investigation of signaling molecules and metabolites found in crustacean hemolymph via in vivo microdialysis using a multi-faceted mass spectrometric platform, Electrophoresis. 37 (2016)

1031–1038. https://doi.org/10.1002/elps.201500497.
[351] C. Simó, C. Barbas, A. Cifuentes, Capillary electrophoresis-mass spectrometry in food analysis, Electrophoresis. 26 (2005) 1306–1318. https://doi.org/10.1002/elps.200410108.
[352] R.H.F. Cheung, P.J. Marriott, D.M. Small, CE methods applied to the analysis of micronutrients in foods, Electrophoresis. 28 (2007) 3390–3413. https://doi.org/10.1002/elps.200700100.
[353] R.M. Callejón, A.M. Troncoso, M.L. Morales, Determination of amino acids in grape-derived products: A review, Talanta. 81 (2010) 1143–1152. https://doi.org/10.1016/j.talanta.2010.02.040.
[354] F.J. V. Gomez, R.P. Monasterio, V.C.S. Vargas, M.F. Silva, Analytical characterization of wine and its precursors by capillary electrophoresis, Electrophoresis. 33 (2012) 2240–2252. https://doi.org/10.1002/elps.201100595.
[355] M. Herrero, C. Simó, V. García-Cañas, S. Fanali, A. Cifuentes, Chiral capillary electrophoresis in food analysis, Electrophoresis. 31 (2010) 2106–2114. https://doi.org/10.1002/elps.200900770.
[356] M. Herrero, V. Garci-a-Canas, C. Simo, A. Cifuentes, Recent advances in the application of capillary electromigration methods for food analysis and Foodomics, Electrophoresis. 31 (2010) 205–228. https://doi.org/10.1002/elps.200900365.
[357] V. García-Cañas, C. Simó, M. Castro-Puyana, A. Cifuentes, Recent advances in the application of capillary electromigration methods for food analysis and Foodomics, Electrophoresis. 35 (2014) 147–169. https://doi.org/10.1002/elps.201300315.
[358] M.A.L. de Oliveira, B.L.S. Porto, C. de A. Bastos, C.M. Sabarense, F.A.S. Vaz, L.N.O. Neves, L.M. Duarte, N. da S. Campos, P.R. Chellini, P.H.F. da Silva, R.A. de Sousa, R. Marques, R.T. Sato, R.M. Grazul, T.P. Lisboa, T. de O. Mendes, V.C. Rios, Analysis of amino acids, proteins, carbohydrates and lipids in food by capillary electromigration methods: a review, Anal. Methods. 8 (2016) 3649–3680. https://doi.org/10.1039/C5AY02736E.
[359] R. Pérez-Míguez, M.L. Marina, M. Castro-Puyana, Capillary electrophoresis determination of non-protein amino acids as quality markers in foods, J. Chromatogr. A. 1428 (2016) 97–114. https://doi.org/10.1016/j.chroma.2015.07.078.
[360] A. Papetti, R. Colombo, High-performance capillary electrophoresis for food quality evaluation, in: Eval. Technol. Food Qual., Elsevier, 2019: pp. 301–377. https://doi.org/10.1016/B978-0-12-814217-2.00014-7.
[361] R. Pérez-Míguez, S. Salido-Fortuna, M. Castro-Puyana, M.L. Marina, Advances in the Determination of Nonprotein Amino Acids in Foods and Biological Samples by Capillary Electrophoresis, Crit. Rev. Anal. Chem. 49 (2019) 459–475. https://doi.org/10.1080/10408347.2018.1546113.
[362] M. Castro-Puyana, M.L. Marina, Chiral Analysis of Non-Protein Amino Acids by Capillary Electrophoresis, in: M. Alterman (Ed.), Amino Acid Analysis. Methods Mol. Biol. Vol 2030, Humana Press, New York, NY, 2019: pp. 277–291. https://doi.org/10.1007/978-1-4939-9639-1_21.
[363] C. Simó, P.J. Martín-Alvarez, C. Barbas, A. Cifuentes, Application of stepwise discriminant analysis to classify commercial orange juices using chiral micellar electrokinetic chromatography-laser induced fluorescence data of amino acids, Electrophoresis. 25 (2004) 2885–2891. https://doi.org/10.1002/elps.200305838.
[364] C. Simó, A. Rizzi, C. Barbas, A. Cifuentes, Chiral capillary electrophoresis-mass spectrometry of amino acids in foods, Electrophoresis. 26 (2005) 1432–1441. https://doi.org/10.1002/elps.200406199.
[365] H.M. Passos, Z. Cieslarova, A.V.C. Simionato, CE-UV for the characterization of passion fruit juices provenance by amino acids profile with the aid of chemometric tools, Electrophoresis. 37 (2016) 1923–1929. https://doi.org/10.1002/elps.201500483.
[366] B. Van de Poel, I. Bulens, P. Lagrain, J. Pollet, M.L.A.T.M. Hertog, J. Lammertyn, M.P. De Proft, B.M. Nicolaï, A.H. Geeraerd, Determination of S-Adenosyl-l-methionine in Fruits by Capillary Electrophoresis, Phytochem. Anal. 21 (2010) 602–608. https://doi.org/10.1002/pca.1241.
[367] P. Kubalczyk, E. Bald, Analysis of orange juice for total cysteine and glutathione content by CZE with UV-absorption detection, Electrophoresis. 30 (2009) 2280–2283. https://doi.org/10.1002/elps.200800741.

[368] A. Santalad, P. Teerapornchaisit, R. Burakham, S. Srijaranai, Pre-Capillary Derivatisation and Capillary Zone Electrophoresis for Amino Acids Analysis in Beverages, Ann. Chim. 97 (2007) 935–945. https://doi.org/10.1002/adic.200790078.
[369] H. Ueno, J. Wang, N. Kaji, M. Tokeshi, Y. Baba, Quantitative determination of amino acids in functional foods by microchip electrophoresis, J. Sep. Sci. 31 (2008) 898–903. https://doi.org/10.1002/jssc.200700517.
[370] M.-M. Hsieh, S.-M. Chen, Determination of amino acids in tea leaves and beverages using capillary electrophoresis with light-emitting diode-induced fluorescence detection, Talanta. 73 (2007) 326–331. https://doi.org/10.1016/j.talanta.2007.03.049.
[371] Y.-S. Su, Y.-P. Lin, F.-C. Cheng, J.-F. Jen, In-Capillary Derivatization and Stacking Electrophoretic Analysis of γ-Aminobutyric Acid and Alanine in Tea Samples To Redeem the Detection after Dilution To Decrease Matrix Interference, J. Agric. Food Chem. 58 (2010) 120–126. https://doi.org/10.1021/jf902958u.
[372] Z. Yang, E. Kobayashi, T. Katsuno, T. Asanuma, T. Fujimori, T. Ishikawa, M. Tomomura, K. Mochizuki, T. Watase, Y. Nakamura, N. Watanabe, Characterisation of volatile and non-volatile metabolites in etiolated leaves of tea (Camellia sinensis) plants in the dark, Food Chem. 135 (2012) 2268–2276. https://doi.org/10.1016/j.foodchem.2012.07.066.
[373] M. Bouri, R. Salghi, M. Zougagh, A. Ríos, Capillary electrophoresis coupled to evaporative light scattering detection for direct determination of underivatized amino acids: Application to tea samples using carboxyled single-walled carbon nanotubes for sample preparation, Electrophoresis. 34 (2013) 2623–2631. https://doi.org/10.1002/elps.201300145.
[374] R. Mandrioli, E. Morganti, L. Mercolini, E. Kenndler, M.A. Raggi, Fast analysis of amino acids in wine by capillary electrophoresis with laser-induced fluorescence detection, Electrophoresis. 32 (2011) 2809–2815. https://doi.org/10.1002/elps.201100112.
[375] M. Tian, J. Zhang, A.C. Mohamed, Y. Han, L. Guo, L. Yang, Efficient capillary electrophoresis separation and determination of free amino acids in beer samples, Electrophoresis. 35 (2014) 577–584. https://doi.org/10.1002/elps.201300416.
[376] R.H. Nugroho, K. Yoshikawa, H. Shimizu, Metabolomic analysis of acid stress response in Saccharomyces cerevisiae, J. Biosci. Bioeng. 120 (2015) 396–404. https://doi.org/10.1016/j.jbiosc.2015.02.011.
[377] H. Turkia, H. Sirén, M. Penttilä, J.-P. Pitkänen, Capillary electrophoresis with laser-induced fluorescence detection for studying amino acid uptake by yeast during beer fermentation, Talanta. 131 (2015) 366–371. https://doi.org/10.1016/j.talanta.2014.07.101.
[378] A. Jastrzębska, S. Kowalska, E. Szłyk, Determination of Free Tryptophan in Beer Samples by Capillary Isotachophoretic Method, Food Anal. Methods. (2020) 850–862. https://doi.org/10.1007/s12161-020-01699-2.
[379] L. Qi, M. Liu, Z. Guo, M. Xie, C. Qiu, Y. Chen, Assay of aromatic amino acid enantiomers in rice-brewed suspensions by chiral ligand-exchange CE, Electrophoresis. 28 (2007) 4150–4155. https://doi.org/10.1002/elps.200700281.
[380] C.N. Jayarajah, A.M. Skelley, A.D. Fortner, R.A. Mathies, Analysis of Neuroactive Amines in Fermented Beverages Using a Portable Microchip Capillary Electrophoresis System, Anal. Chem. 79 (2007) 8162–8169. https://doi.org/10.1021/ac071306s.
[381] M. Lechtenberg, K. Henschel, U. Liefländer-Wulf, B. Quandt, A. Hensel, Fast determination of N-phenylpropenoyl-l-amino acids (NPA) in cocoa samples from different origins by ultra-performance liquid chromatography and capillary electrophoresis, Food Chem. 135 (2012) 1676–1684. https://doi.org/10.1016/j.foodchem.2012.06.006.
[382] D. Zhao, M. Lu, Z. Cai, Separation and determination of B vitamins and essential amino acids in health drinks by CE-LIF with simultaneous derivatization, Electrophoresis. 33 (2012) 2424–2432. https://doi.org/10.1002/elps.201200040.
[383] C.D.M. Campos, F.G.R. Reyes, A. Manz, J.A.F. da Silva, On-line electroextraction in capillary electrophoresis:

Application on the determination of glutamic acid in soy sauces, Electrophoresis. 40 (2019) 322–329. https://doi.org/10.1002/elps.201800203.
[384] T.D. Nguyen, M.H. Nguyen, M.T. Vu, H.A. Duong, H.V. Pham, T.D. Mai, Dual-channeled capillary electrophoresis coupled with contactless conductivity detection for rapid determination of choline and taurine in energy drinks and dietary supplements, Talanta. 193 (2019) 168–175. https://doi.org/10.1016/j.talanta.2018.10.002.
[385] M.D. Le, H.A. Duong, M.H. Nguyen, J. Sáiz, H.V. Pham, T.D. Mai, Screening determination of pharmaceutical pollutants in different water matrices using dual-channel capillary electrophoresis coupled with contactless conductivity detection, Talanta. 160 (2016) 512–520. https://doi.org/10.1016/j.talanta.2016.07.032.
[386] S. Lee, S.J. Kim, E. Bang, Y.C. Na, Chiral separation of intact amino acids by capillary electrophoresis-mass spectrometry employing a partial filling technique with a crown ether carboxylic acid, J. Chromatogr. A. 1586 (2019) 128–138. https://doi.org/10.1016/j.chroma.2018.12.001.
[387] K. Takahashi, H. Kohno, Different Polar Metabolites and Protein Profiles between High- and Low-Quality Japanese Ginjo Sake, PLoS One. 11 (2016) e0150524. https://doi.org/10.1371/journal.pone.0150524.
[388] A. Tirelli, Improved Method for the Determination of Furosine in Food by Capillary Electrophoresis, J. Food Prot. 61 (1998) 1400–1404. https://doi.org/10.4315/0362-028X-61.10.1400.
[389] J.M. Izco, M. Tormo, R. Jiménez-Flores, Rapid Simultaneous Determination of Organic Acids, Free Amino Acids, and Lactose in Cheese by Capillary Electrophoresis, J. Dairy Sci. 85 (2002) 2122–2129. https://doi.org/10.3168/jds.S0022-0302(02)74290-2.
[390] T. Hagi, M. Kobayashi, M. Nomura, Metabolome analysis of milk fermented by γ-aminobutyric acid-producing Lactococcus lactis, J. Dairy Sci. 99 (2016) 994–1001. https://doi.org/10.3168/jds.2015-9945.
[391] J. Enzonga, V. Ong-Meang, F. Couderc, A. Boutonnet, V. Poinsot, M.M. Tsieri, T. Silou, J. Bouajila, Determination of free amino acids in african gourd seed milks by capillary electrophoresis with light-emitting diode induced fluorescence and laser-induced fluorescence detection, Electrophoresis. 34 (2013) 2632–2638. https://doi.org/10.1002/elps.201300136.
[392] M. Sacristán, A. Varela, M.M. Pedrosa, C. Burbano, C. Cuadrado, M.E. Legaz, M. Muzquiz, Determination of β-N-oxalyl-l-α,β-diaminopropionic acid and homoarginine in Lathyrus sativus and Lathyrus cicera by capillary zone electrophoresis, J. Sci. Food Agric. 95 (2015) 1414–1420. https://doi.org/10.1002/jsfa.6792.
[393] X. Liu, D.F. Li, Y. Wang, Y.T. Lu, Determination of 1-aminocyclopropane-1-carboxylic acid in apple extracts by capillary electrophoresis with laser-induced fluorescence detection, J. Chromatogr. A. 1061 (2004) 99–104. https://doi.org/10.1016/j.chroma.2004.10.067.
[394] R. Kubec, E. Dadáková, Quantitative determination of S-alk(en)ylcysteine-S-oxides by micellar electrokinetic capillary chromatography, J. Chromatogr. A. 1212 (2008) 154–157. https://doi.org/10.1016/j.chroma.2008.10.024.
[395] A.C. Valese, L. Vitali, R. Fett, G.A. Micke, M.A.L. de Oliveira, A.C. Oliveira Costa, A Rapid Method for Analysis of Phenylalanine in Cereal Products by MEKC-UV Using LC/MS/MS as a Comparative Method, J. AOAC Int. 98 (2015) 1632–1639. https://doi.org/10.5740/jaoacint.15-052.
[396] O. Hodek, T. Křížek, P. Coufal, H. Ryšlavá, Design of experiments for amino acid extraction from tobacco leaves and their subsequent determination by capillary zone electrophoresis, Anal. Bioanal. Chem. 409 (2017) 2383–2391. https://doi.org/10.1007/s00216-017-0184-2.
[397] L. Li, J. Zhao, Y. Zhao, X. Lu, Z. Zhou, C. Zhao, G. Xu, Comprehensive investigation of tobacco leaves during natural early senescence via multi-platform metabolomics analyses, Sci. Rep. 6 (2016) 2–11. https://doi.org/10.1038/srep37976.
[398] J. Zhao, Y. Zhao, C. Hu, C. Zhao, J. Zhang, L. Li, J. Zeng, X. Peng, X. Lu, G. Xu, Metabolic Profiling with Gas Chromatography-Mass Spectrometry and Capillary Electrophoresis-Mass Spectrometry Reveals the Carbon-Nitrogen Status of Tobacco Leaves Across Different Planting Areas, J. Proteome Res. 15 (2016) 468–476. https://doi.org/10.1021/acs.jproteome.5b00807.

[399] L. Bell, H.N. Yahya, O.O. Oloyede, L. Methven, C. Wagstaff, Changes in rocket salad phytochemicals within the commercial supply chain: Glucosinolates, isothiocyanates, amino acids and bacterial load increase significantly after processing, Food Chem. 221 (2017) 521–534. https://doi.org/10.1016/j.foodchem.2016.11.154.
[400] A. Miyagi, H. Uchimiya, M. Kawai-Yamada, Synergistic effects of light quality, carbon dioxide and nutrients on metabolite compositions of head lettuce under artificial growth conditions mimicking a plant factory, Food Chem. 218 (2017) 561–568. https://doi.org/10.1016/j.foodchem.2016.09.102.
[401] C. Bignardi, A. Cavazza, C. Corradini, Determination of furosine in food products by capillary zone electrophoresis-tandem mass spectrometry, Electrophoresis. 33 (2012) 2382–2389. https://doi.org/10.1002/elps.201100582.
[402] Y.S. Gao, B.C. Hsieh, T.J. Cheng, R.L.C. Chen, Judgment of pure fermented soy sauce by fluorescence resonance energy transfer of OPA-tryptophan adduct, Food Chem. 178 (2015) 122–127. https://doi.org/10.1016/j.foodchem.2015.01.028.

Figure 1: Normalized number of publications related to CE and AA in reports published since 2000 (source Web of science). The obtained curves are polynomes of the third degree. The data for each curve are normalized to obtain a clear presentation. The maximum number of yearly publications related to the different curves are indicated in parentheses: CE (994), CE and AA (227), CE/MS and AA (57), CE/fluorescence and AA (65), CE/C^4D and AA (16).

Figure 2: Electropherograms of five-fold diluted deproteinized plasma samples without A) and spiked with B) 100 mM standard-free AA/peptide mixture. Electropherograms of 30 AAs. BGE: 8 mM *p*-aminosalicylic acid –2 mM $NaCO_3$ at pH 10.15, 87 cm long 75 µm ID capillary (effective length: 80 cm), 15 kV. Detection: UV absorption at 254 nm. (1) Arg, (2) Lys, (3) Orn, (4) Pro, (5) GABA, (6) hydroxy-Lys, (7) Ala, (8) carnosine, (9) Leu/ Ile, (10) Trp, (11) Citruline, (12) Val, (13) Phe, (14) Ala, (15) His, (16) Met, (17) Gln, (18) Thr, (19) Asn, (20) Gly, (21) Ser, (22) Tyr, (23) homocystine, (24) Hcy, (25) cystine (26) oxydated gluthathione (GSSG), (27) Glu, (28), reduced glutathione (GSH), (29) Asp. Ref [37], with permission.

Figure 3: AA determination using CE-C^4D in DBS eluate of five individuals (20 µL of DBS eluted with methanol/water (50/50, v/v)). The separation was realized using 1.6 M acetic acid, 1 mM 18-crown-6, 0.1% (v/v), Tween 20, pH 2.1. 30 kV. (1) Choline, (2) Creatinine, (3) Orn,

(4) Lys, (5) Arg, (6) His, (7) Gly, (8) Ala, (9) Val, (10) Ile, (11) Leu, (12) Ser, (13) Thr, (14) Gln, (15) Glu, (16) Phe, (17) Tyr, (18) Pro; *, unknown. Ref [58], with permission.

Figure 4: Electropherogram of diluted cerebrospinal fluid (20× in water) (1) Trp, (2) Tyr, (3) hydroxyindole acetic acid; (u) represent unidentified compounds. The separation was realized using 10 mM CAPS, 15 mM sodium tetraborate, pH 9.2, 15 kV with a 75 µm ID capillary of length 60 cm (effective length 53 cm). Detection was performed using a UV-LIF detector equipped with a 266-nm pulsed laser. Ref [78], with permission

Figure 5: I) Schematic illustration of processes occurring in EMMA. Step A) Injection of "sweeping plug" and reactants. The depicted plug length ratios are equal to the real plug length ratios. Step B) Mixing of reactants using EMMA. The injected plug of NaCN is pushed out from the capillary by the EOF, whereas the merged plugs of reactants (derivatization plug) are retained within the capillary. Step C) Reaction incubation at zero potential allowing a high reaction yield. Step D) SDS from the "sweeping plug" sweeps NDA-labeled AAs and results in improved peak shapes. Step E) Separation of NDA-labeled AAs. Steps D and E occur simultaneously. The inlet capillary end was immersed either in NaCN solution or in the BGE, and in all cases, the outlet capillary end was immersed in the BGE. [NaCN] = 250 mM [NDA] = 8 mM in MeOH/isopropanol (4/1, v/v), BGE: 73 mM SDS, 6.7% (v/v) 1-propanol, 0.5 mM HP-β-CD, 135 mM H_3BO_3/NaOH, pH 9. **II)** A) Electropherograms of model samples of AAs recorded after on-capillary derivatization with NDA/NaCN using EMMA mixing strategy. Peak order differences and migration time shifts between the electropherograms originate from the sweeping performed in EMMA, which provides additional selectivity. Capillary 50 µM ID 66.0/45.0 cm total/effective length, 30 kV; (1) Asn, (2) Ser, (3),Gln, (4) Thr, (5) His, (6) cystine-mono-labelled, (7) Glu, (8) Gly, (9) Tyr, (10) Ala, (11) Asp, (12) Tau, (13) Ala-Gln, (14) Val, (15) Met, (16) norVal, (17) Trp, (18) Ile, (19) Leu, (20) Phe, (21) Arg, (22) cysteine di-labelled NDA, and (23) Lys. Imp.: Impurity from the Tau standard. Cond. benzoin-type condensation products of NDA catalyzed by the cyanide anion. B) Same electropherogram as that depicted in A without peak identification. C) 100× diluted pooled human plasma, D) 100× diluted culture medium. The peak corresponding to NDA-labeled-Ile was the only peak identified by the standard addition method in all samples (and the only one selected for the matrix effect study). Ref [102], with permission

Figure 6: (A) Plot of 22 consecutive electropherograms collected on-line during step change in Glu and Asp concentrations. These AAs were labelled using a low-gated injection interface and BME. UV-LEDIF detection (100 mW, λ_{max} = 365 nm) was performed. Analyte concentration changed from 0.5 to 2 µM and back to 0.5 µM. Reaction conditions: injection, 1 s; crossflow, 1 mL/min (10 mM phosphate, pH 7.4); capillary ID, 25 µm; EL, 8 cm. Ref [119], with permission

Figure 7: A) Extracted-ion electropherograms for evaluating the separation efficiency achieved for human-plasma extract. (1) Orn, (2) Lys, (3) Arg, (4) His, (5) β-Ala, (6) Ala, (7) sarcosine, (8) GABA, (9) N,N-dimethyl-Gly, (10) Gly, (11) creatine, (12) Val, (13) betaine, (14) Ser, (15) homo-Ser, (16) Thr, (17) iso-Leu, (18) Leu, (19) Asn, (20) Met, (21) Gln, (22) Pro, (23) Glu, (24) Trp, (25) citrulline, (26) Phe, (27) Tyr, and (28) Asp were detected during cation analysis. The electropherograms of (29) 3-hydroxybutyric acid, (30) 2-hydroxybutyric acid, (31) lactic acid, (32) fumaric acid, (33) citric acid, and (34) isocitric acid were detected during anion analysis. B) Overview of the 270 metabolites identified during metabolome analysis of human plasma extract using CE-high resolution MS. Ref [187] with permission.

Figure 8: CE/LIF (488 nm) of plasma samples derivatized using 5-IAF. The analysis presents the electropherograms of A) total; B) free; C) reduced thiols of healthy (thick black line) and hyperhomocysteinemic subjects (dotted line). Reagents used: 5 mmol/L sodium phosphate, 5 mM boric acid as electrolyte solution with 75 mM N-methyl-D-glucamine, pH 11. 45 °C, 30 kV. Ref [269], with permission.

Figure 9: CE/UV of Phe, Trp, methyl-Trp (IS, 200 µM), and Tyr in human plasma using 80 mM Tris phosphate solution titrated at pH 1.4 with 85% m/m phosphoric acid. UV absorbance: 200 nm. The samples were prepared using 50 µL of plasma, to which 50 µL of water was added, along with 20 µL of 200 µM of methyl-Trp and 25 µL of sulfosalicylic acid (15% m/v). After centrifugation, 50 µL of the supernatant was use for CE. Unk= unknown compounds. Ref [300], with permission.

Figure 10: Schematic of the A) microdialysis-capillary electrophoresis instrument; B) flow gate (with 43 mM OPA (9/1 methanol/75 mM borate, pH 10.5, 10 µL/h)/114 mM BME (in artificial

CSF (aCSF), (10 µL/h) capillary and CE/UV-LIF (351 nm) separation capillary); C) microdialysis probe (0.33 µL/min) with aCSF. The mix exited the cross into a 9 cm long, 150 µm ID capillary. The derivatized dialysate was injected into the CE capillary using a flow-gated interface, comprising an acrylic block that held the reaction capillary and the separation capillary (8 cm long, 5 µm ID end-to-end with a 50-µm gap between them; the BGE was pumped through this gap at a rate of 40 mL/h). D) Electropherograms of dialysate sampled from the rat striatum under normal conditions. The labeled peaks represent (1) L-2-aminoadipic acid (internal standard), (2) glutamate, (3) GABA, (4) taurine, (5) D-Ser, and (6) L-Ser. BGE: 100 mM borate/20 mM HP-β-CD, pH 10.5; 20 kV. (E) Maximum percent change in Glu, GABA, D-Ser, and L-Ser concentrations observed during a 3-min application of 100 µM N-methyl-D-aspartate (NMDA) and 100 µM NMDA+ 200 µM MK-801 (a NMDA receptor antagonist). *p < 0.05 compared to 100 µM NMDA. **p = 0.08 compared to 100 µM NMDA. p-values were determined using the *t*-test. Ref [325], with permission

Figure 11: Extracted ion electropherogram of CE-ESI^{+}-MS of: A) standard D/L-Asp, -Glu, -Ser, -Ala, -Asn, -Pro, -Arg, and GABA derivatized with FITC at 125 µM of each AA, B) orange juice sample adulterated with 0.8% D/L Asp. CE conditions: polymer-coated capillary (87 cm ID, 50 µm ID); BGE, 100 mM ammonium acetate, pH 6, 5 mM β-CD; 15 kV. Sheath liquid: MeOH/water (1/1 v/v) with 25% BGE without β-CD, flow rate 3.5 µL/min. Ref [364], with permission.

3483 Fig1

3484

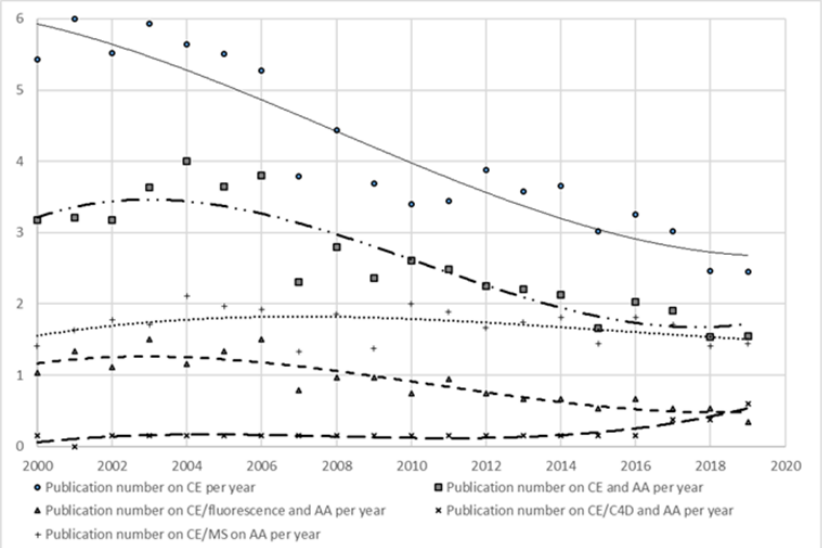

3485

3486 Fig 1

3487

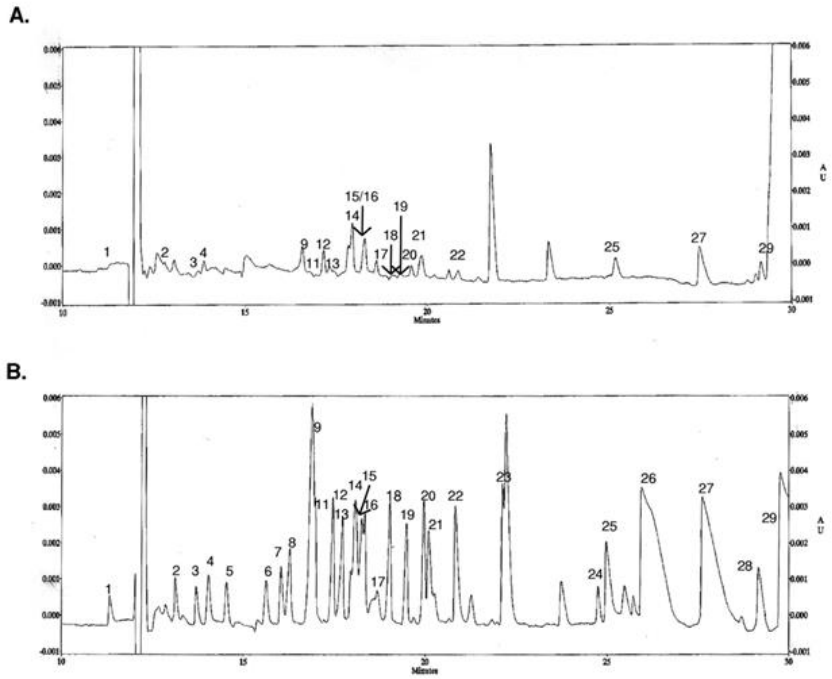

3488

3489 Fig 2

3490

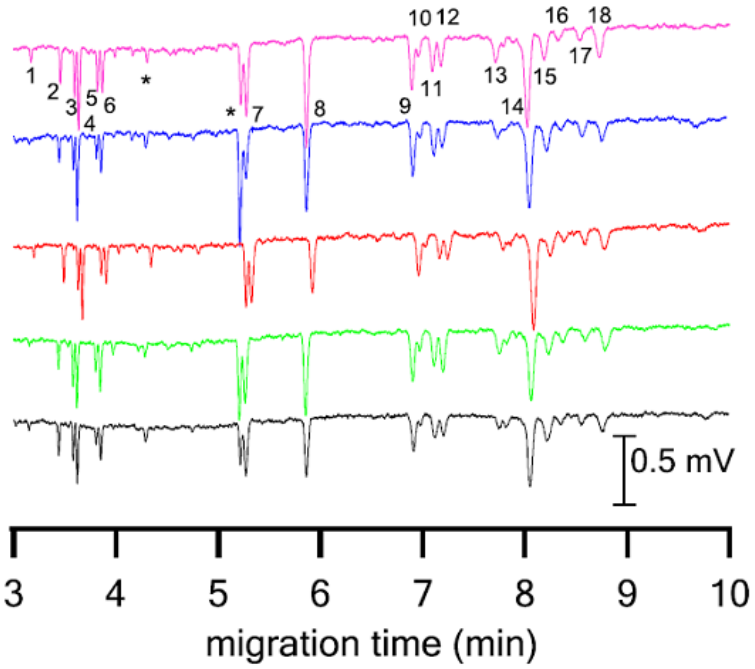

3491

3492 Fig 3

3493

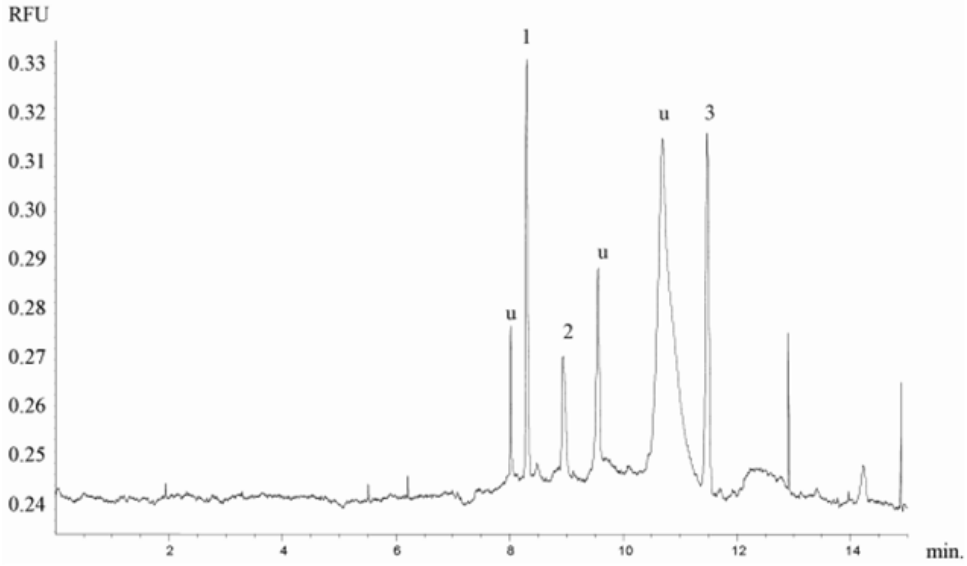
RFU
0.33
0.32
0.31
0.30
0.29
0.28
0.27
0.26
0.25
0.24
1
u
2
u
u
3
2
4
6
8
10
12
14
min.

Fig 4

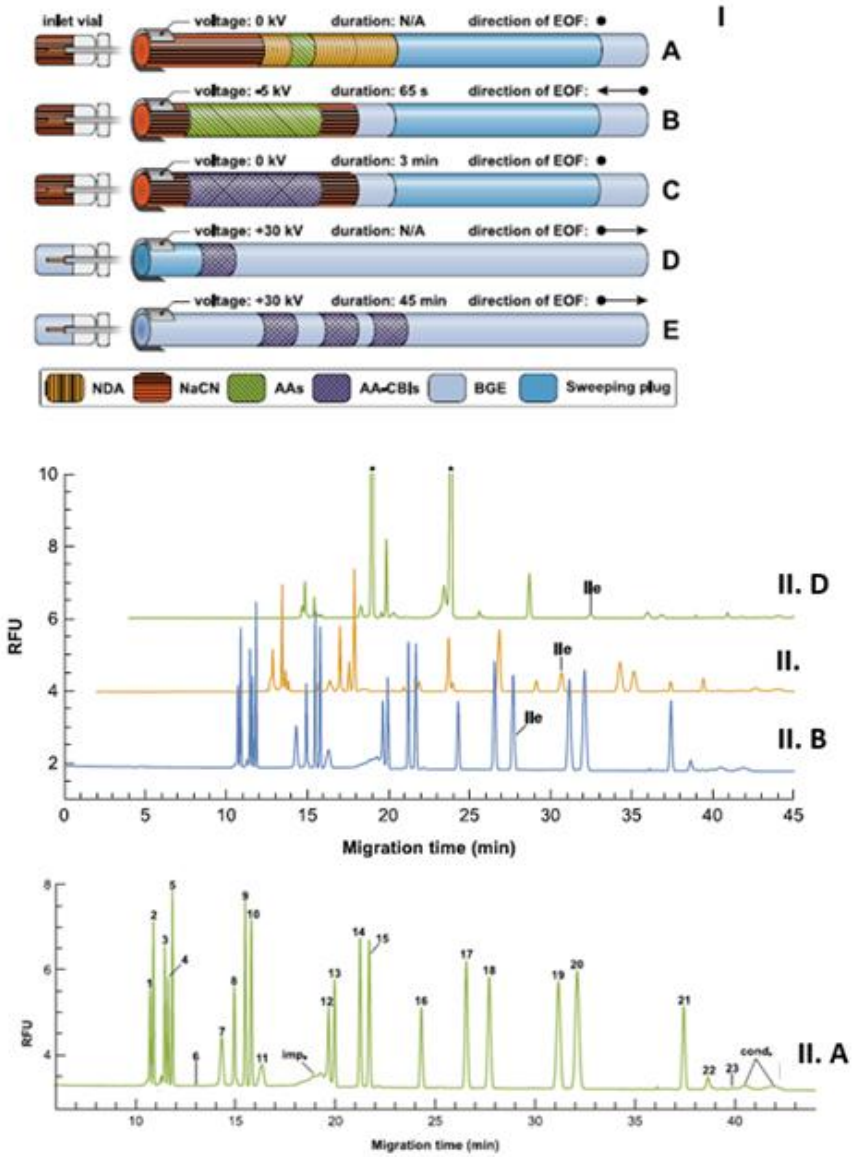

3497

3498 Fig 5

3499

3500 Fig 6

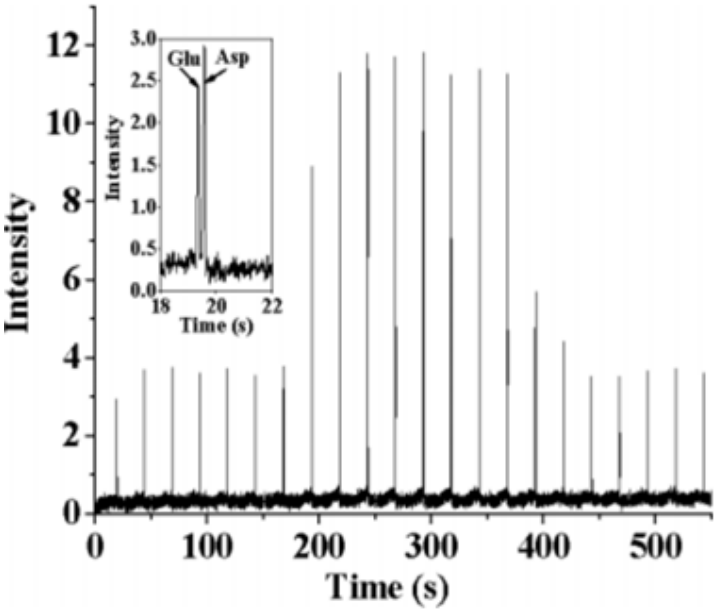

3501

3502

3503

3504 Fig 7

3505

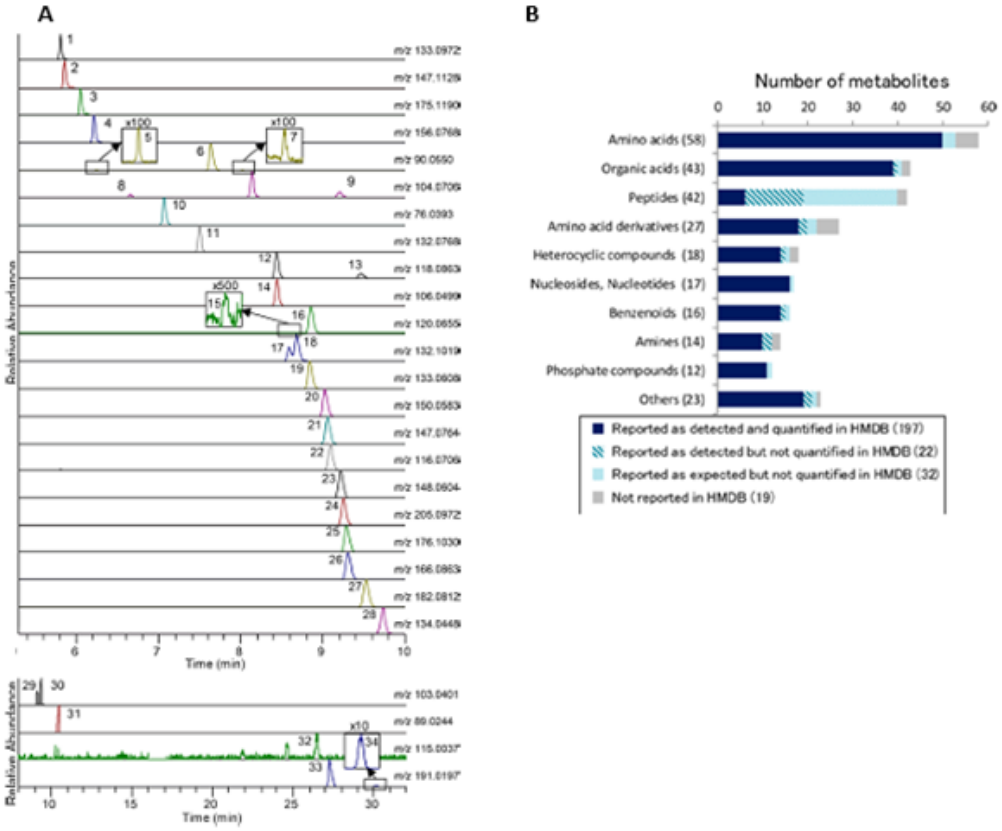

3506

3507

3508 Fig 8

3509

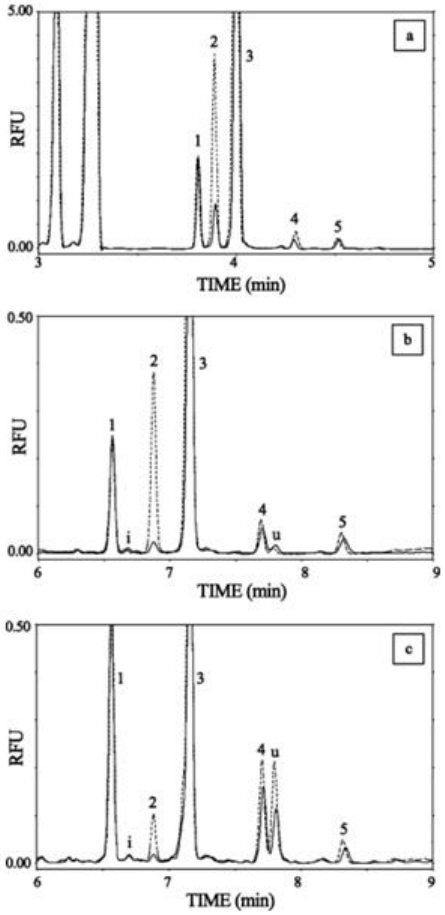

3510

3511

3512

3513

3514 Fig 9

3515

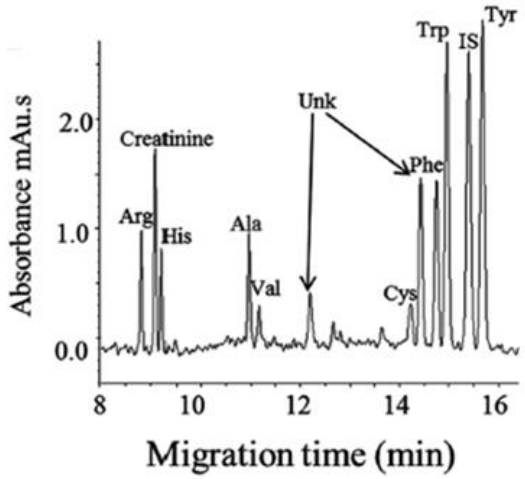

3516

3517

3518 Fig 10

3519

3520

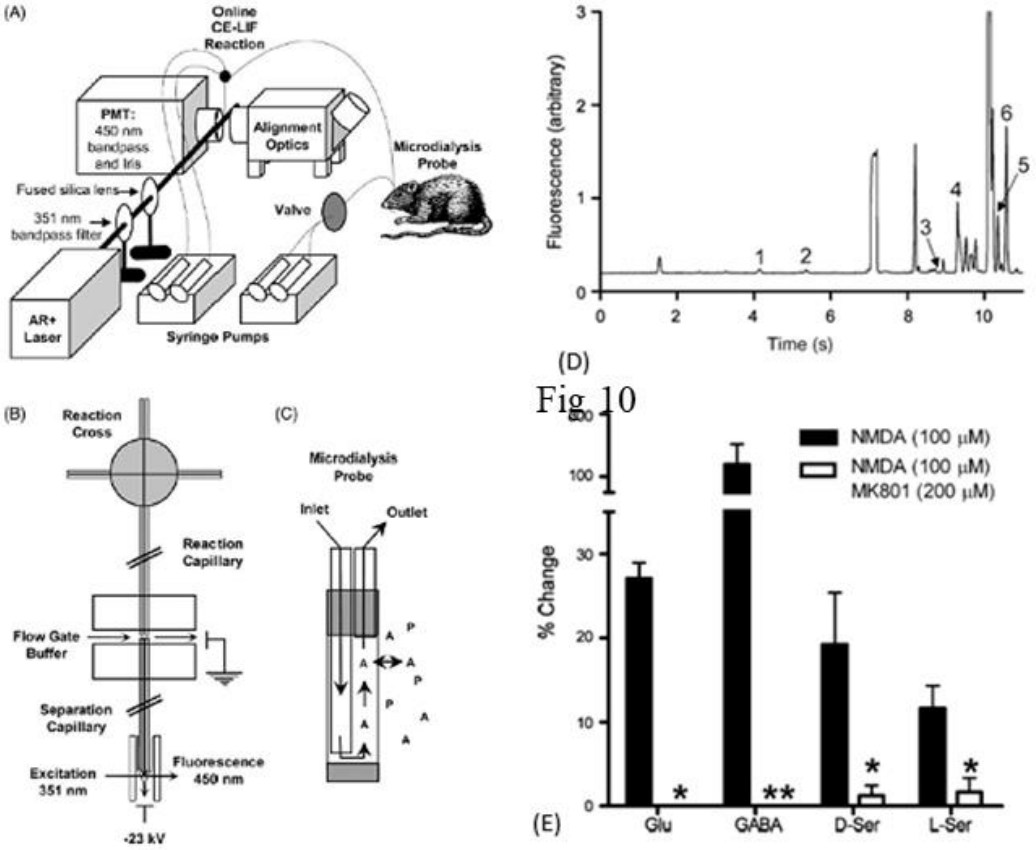

Fig 10

3521

3522

3523

Fig 11

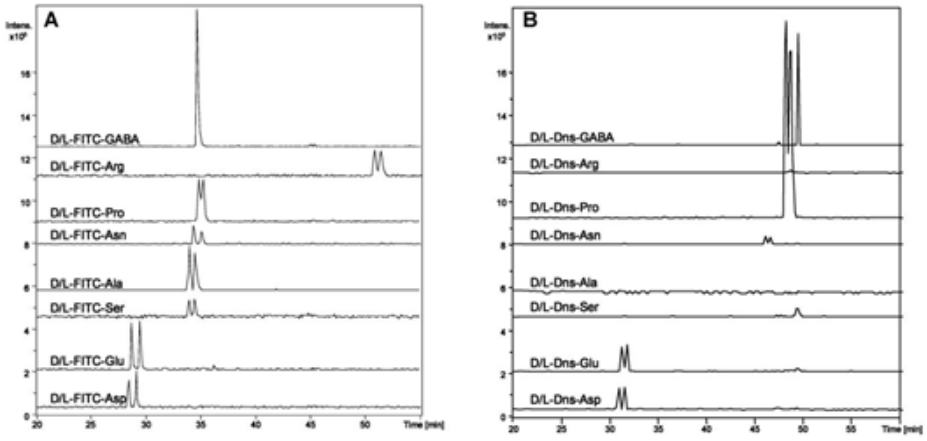
A
D/L-FITC-GABA
D/L-FITC-Arg
D/L-FITC-Pro
D/L-FITC-Asn
D/L-FITC-Ala
D/L-FITC-Ser
D/L-FITC-Glu
D/L-FITC-Asp
Time [min]
B
D/L-Dns-GABA
D/L-Dns-Arg
D/L-Dns-Pro
D/L-Dns-Asn
D/L-Dns-Ala
D/L-Dns-Ser
D/L-Dns-Glu
D/L-Dns-Asp
Time [min]

Table 1: Separation and detection parameters adopted in the major publications reviewed in the chapter CE/UV

(AA, amino acid; nd, not determined; ID, inner diameter of the capillary; EL, effective length of the capillary; TL, total length of capillary; IS, internal standard)

AA	Sample and sample treatment	Separation conditions	Detection λ (nm)	LOD	Ref
Taurine, homotaurine (IS)	100 µL human, (or feline, or bovine) plasma + 150 µL ACN votexed, then centrifuged. 200 µL supernatant react with 20 µL **fluorescamine** (5 mg/L) in ACN.	75 µm ID, 50 cm TL, 40 cm EL capillary. Citric acid pH=3. -27.5 kV	266	nd	[13]
All proteinogenic AA (except Trp)	16 hours, 6 M HCl hydrolysis (110 °C) of 100 mg fish flour, filtered, evaporated. 500 µL water diluted. 100 µL were reacted with 100 µL Na_2CO_3 (0.1 M).300 µL isopropanol, 5 µL **PITC**, 35 min. Excess PITC removed with hexane.	50 µm ID, 65 cm TL, 55 cm EL capillary, phosphate (30 mM, pH 7.4), 4 mM β-CD, +25 kV. Leu/ Ile not separated	254	1 µM	[14]
D/L-Glu, D/L-Ser, D/L-Met, D/L α-amino-n-butyric acid, D/L Trp, D/L norLeu, D/L Asp, D/L Ser	Standard **dansylated** AAs diluted in BGE.	50 µm ID, 55 cm TL, 40 cm EL capillary. 10 mM $Cu(CH_3COO)_2$, 20 mM L-phenylalaninamide, 20 mM CH_3COONH_4, pH 5. 15 kV.	254	nd	[16]
D/L-Glu, D/L-Leu, D/L-Val, D/L-Met, D/L-Thr, D/L-Ser, D/L-norVal, D/L-Asp, D/L α-amino-n-butyric acid, D/L-Trp, D/L-Phe, D/L-norLeu	Standard **dansylated** AAs diluted in BGE.	50 µm ID, 50 cm TL, 36.5 cm EL capillary. 10 mM $Cu(CH_3COO)_2$, 20 mM L-prolinamide, 20 mM CH_3COONH_4, at pH 6 or 5. +13.6 kV.	254	nd	[17]
D/L-Asn, D/L-Met, D/L-Thr, D/L-Ser, D/L-Asp, D/L-Trp, D/L-Phe, D/L-Ile, D/L-Tyr	100 µL standards AA + 200 µL 40.0 mM Li_2CO_3 +100 µL **dansyl chloride**, 35.0 min, then 5 µL 2.0% ethylamine.	50 µm ID, 65 cm TL, 50 cm EL capillary. 5 mM CH_3COONH_4, 100 mM boric acid, 4 mM Zn(II), 8 mM L-phenylalaninamide, pH 8.2. -23 kV.	254	nd	[18]
D/L proteinogenic AA, D/L Orn	20 µL AA (+ 20 µL 40.0 mM Li_2CO_3 + 20 µL **dansyl chloride (**5.6 mM in acetone), 35.0 min, then 5 µL 2.0% ethylamine. Test applied for screening tyrosinase inhibitors	75 µm ID, 60 cm TL, 45 cm EL capillary. 100 mM boric acid, 5 mM CH_3COONH_4, 2.5 mM Mn(II), 5 mM [1-butyl-3-methyl imidazolium][L-Ala] and 5.0 mM β-CD at pH 8.3. -23 kV.	254	3 µM	[20]

D-Ser	Standard **dansylated** AAs diluted in BGE.	75 µm ID, 35 cm TL, 28 cm EL capillary coated with a linear polyacrylamide. 200 mM β-alanine/acetate (pH 4.20) – MeOH (1/1, v/v); 20 mM (+)-1-allyl-(5R,8S,10R)-terguride. 20 kV.	254	Below 0.01% D-Ser	[22]
D/L-Trp, D/L-Phe, D/L-Tyr, D/L-His, D/L Cys, D/L-Ala	200 µL standards AA (1 mg/L) in 40.0 mM Li_2CO_3 + 300 µL **dansyl chloride (**5.6 mM in ACN), 35.0 min, then 50 µL 2.0% ethylamine.	50 µm ID, 40 cm TL, 32 cm EL capillary. 100 mM β-CD, 10 mM tetramethylammonium-L-Arg in N -methylformamide containing 50 mM Tris and 35 mM citric acid (pH 7.85). 30 kV;	254	nd	[23]
Phe, Ile, Tyr, His, Leu	0.03 M **1,2-naphthoquinone-4-sulfonate** in HCl 0.1 M, reacted with AAs in 50 mM sodium borate/ 90 mM NaCl pH=10.	75 µm ID, 70 cm TL, 58 cm EL capillary. 40 mM sodium tetraborate–isopropanol (3:1, v/v)	DAD 225-550	nd	[24]
Pro, Gly, Trp, Val, Thr, Ser, Phe, Asn, Ala, Ile, Leu, Glu, Asp, Cys	0. 1 g of commercial pharmaceuticals or 10 g of feed dissolved in 0.1 L 10 mM HCl. Diluted in water, filtered. In-capillary derivatization using **1,2-naphthoquinone-4-sulfonate**.	75 µm ID, 50 cm TL, 43 cm EL capillary. Sandwiched in-capillary derivatization: 0.03 M 1,2-naphthoquinone-4-sulfonate in HCl 0.1 M/sample/0.03 M 1,2-naphthoquinone-4-sulfonate in HCl 0.1 M. (Pressure.time: Pa.s: 166/103/166) BGE: 40 mM sodium tetraborate (pH=9,2)/isopropanol (4:1 v/v). Stacking process 3 min, -20 kV. Separation +20 kV	230	0.7 µM (Pro) to 2.1 µM (Cys)	[27]
His, Trp, Leu, Met, Thr, Ser, Gly, and nine aliphatic amines.	Standard AAs, on-column derivatization using **phtalic anhydride**.	50 µm ID, 47 cm TL, 40.5 cm EL capillary. 1 s pressure injection of 10 mM phallic acid in ACN, 1 s injection AA in ACN/water 9:1. Separation: 20 mM phosphate pH=10. 24 kV	200	nd	[28]
Arg, histamine, serotonin, tyramine, putrescine, and cadaverine among 16 AAs	5 g pieces of mackeral or tuna (fish) in 20 mL HCl (0.5 M) homogenized, 1 M NaOH neutralized diluted in 50 mL water. Injection: 5 kV for 3 s, specific injection of neutral biogenic amines for in-capillary **OPA/BM** labeling.	On column derivatization with OPA/BME and separation in a capillary filled with Capcell Pak C18 (5 µm) type UG 120 (Shiseido, Tokyo, Japan). Capillary filled with 5 mM OPA/2ME and 70% acetonitrile/10 mM borate (pH 10). Cathode vial 70% acetonitrile/10 mM borate (pH 10).	340	50-100 µM	[32]
D/L Ser, Gly (IS)	100 µL of serine racemase reaction media, containing 20 µM pyridoxal-5'-phosphate, 1 mM $MgCl_2$, 1 mM ATP, 5 mM DTT, 0.5 mM enzyme+20 µL 30 mM EDTA, 6 mM	75 µm ID, 40 cm TL, 30 cm EL capillary. In-capillary derivatization: 5 s hydrodynamic injection (1 kPa) of 50 µL sample + 50 µL 200 µM Gly, followed by any one of OPA/BME	230	3 µM D-Ser.	[33]

	aminooxyacetic acid hemihydrochloride; were injected in CE for in capillary **OPA/BME** labeling.	(30/60 mM, in 25% ACN), 6 kV, 1 min. BGE: 50 mM sodium tetraborate (pH 9.7), 40 mM 2-hydroxypropyl-γ-CD. 12 kV			
L-carnosine, mimosine, 6-aminonicotinic acid (ANA), 3-ANA, 2-ANA, 4-aminobenzoic acid, 2- amino-benzoic acid,5-aminosalicylic acid, D/L Trp, D/L-homoPhe, D/L Phe, 5-hydroxy D/L Trp, D/L Tyr, 3,4 dihydroxy-L-Phe	Free standard AAs	50 µm ID, 57 cm TL, 50 cm EL capillary. 100 mM sodium phosphate, pH 2.0	200	0.2-0.4 µM	[35]
Lys, Pro, Trp, OH-Pro, Leu, His, Phe, Val, Met, Gln, Ala, Thr, Ser, Asn, Cys, and Glu	Free AAs from plant extracts in 25% ethanol.	75 µm ID, 40 cm TL, 30 cm EL capillary. 10 mM benzoic acid + 1 mM myrisityltrimethyl-ammonium bromide at pH of 11.20. -15 kV.	225 (indirect)	10 µM (Val) 45 µM (Lys)	[36]
20 AAs, Orn, GABA, β-Ala, 3-Me-His, Hcys, cystine, glutathione, anserine, carnosine, Hcys, δ-hydroxylysine, citruline	100 µL plasma or supernatant of cultivated macrophages + acetone, centrifuged, supernatant 5× diluted in water.	75 µm ID, 87 cm TL, 80.5 cm EL, capillary. 8 mM *p*-aminosalicylic acid + 2 mM $NaCO_3$, pH 10.15. 15 kV.	254 (indirect)	1.9 µM (Glu) 20.1 µM (Gly	[37]
Gabapentin	bulk drug, diluted in water and filtered.	75 µm ID, 74 cm TL, 62.5 cm EL capillary. 5 mM 5-sulphosalicylic acid and 0.5 mM cetyltrimethylammonium bromide (CTAB), pH 11. -20 kV.	215 (indirect)	5 µM	[38]
Glu, Asp	100 µL human serum + 200 µL methanol/ACN, centrifuged. Supernatant was dried, then mixed with 3 mM H_3PO_4 6% methanol.	50 µm ID, 50 cm TL, 42 cm EL, capillary. 10 mM Tris–8 mM benzoic acid–10 mM β-CD pH 7.5. 12 kV	214 (indirect)	0.4 µM	[40]
3-nitro-Tyr	Urine was centrifuged, filtered, and 1 mL spiked with 1 mL of 0.1 M NaCl.	75 µm ID, 48.5 cm TL, 40 cm EL, capillary. 50 mM HEPES/105 mM Tris	426	0.07 µM	[41]
Lys, His, Ser, Leu, Phe, Glu, Pro	100% human saliva + 5 µL sulfosalicylic acid (50% in water) centrifuged, supernatant filtered and diluted in water. 0.5 g green tea in 100 mL	50 µm ID, 65 cm TL, 57 cm EL, capillary. 50 mM $CuSO_4$ 0.05% acetic acid (pH 4.5) 15 V.	254	0.1-0.5 µM	[43]

	boiled water, infused 1 h filtered and diluted in water.				
Phe, Tyr	Phe- and Tyr-spiked urine diluted in BGE 1/1.	50 µm ID, 100 cm TL, 91.5 cm EL capillary coated with a bilayer of polybrene (hexadimethrine bromide), and 25% (m/v) aqueous solution of poly(vinylsulfonate). Injection: 1) 12.5% NH_4OH, 25 s 50 mbar. 2) sample diluted 1:1 in BGE 228 s at 50 mbar. BGE, 1 M formic acid. 30 kV	200	54 nM (Phe) 19 nM (Tyr)	[44]

Table 2: Separation and detection parameters adopted in the major publications reviewed in the chapter CE/C^4D.

(AA, amino acid; nd, not determined; ID, inner diameter of the capillary; EL, effective length of the capillary; TL, capillary total length; IS, internal standard)

AA	Sample and sample treatment	Separation conditions	LOD	Ref
20 proteinogenic AAs and Cys-Cys	Human urine and saliva, alcoholic extracts from herbs (veronica and scouring rush) Budvar beer, water solution of Panganin yeast, sonicated and then filtered.	50 µm ID, 80 cm TL, 66.5 cm EL capillary. 2.3 M acetic acid (pH 2.1) and 0.1% w/w hydroxyethylcellulose. 30 kV	9.1 µM (Lys) - 29 µM (Asp)	[51]
20 proteinogenic AAs	Urine samples were diluted 10× in BGE buffer. Beer was diluted 5× in BGE, then ultrasonicated and filtered.	0.25 µm ID, 60 cm TL capillary. Electrokinetic injection 5 kV, 7 s. 50 mM 2-amino-2-methyl-1-propanol/10 mM 3-(cyclohexylamino)-1-propanesulfonic acid (CAPS), pH 10.8. 25 kV	0.2 µM (Arg), 0.4 µM (His)	[52]
Thr, Met, Leu	Standards of AAs in standards of carbohydrate mixtures.	15 µm ID, 40 cm TL, 25 cm EL capillary. Electrokinetic injection 20 kV, 2 s. 10 mM NaOH, 4.5 mM Na_2HPO_4, 1 mM cetyltrimethyl-ammonium bromide, pH >12; 20 kV	≈1 µM	[53]

18 proteinogenic AAs, Orn citruline, creatinine, 3-Me-His	100 µL human plasma+100 µL acetone, centrifuged, supernatant, injected.	75 µm ID, 80 cm TL, 67 cm EL capillary. 1.7 M acetic acid 0.1% hydroxyethylcellulose, pH 2.2. 20 kV	4.3 µM (Arg) 42.9 µM (Cys)	[54]
3-Me-His, 1-Me-His, His	Urine diluted 1/1 in ACN, filtered.	75 µm ID, 80 cm TL, 65 cm EL capillary. 0.5 M acetic acid, 20 mM NH_4OH, 0.1% m/v hydroxyethyl-cellulose (pH 3.4). 20 kV.	≈7 µM	[55]
20 proteinogenic AAs, 3-Me-His, 1-Me-His, b-Ala, citruline, creatinine, choline, Orn, 4-hydroxy-Pro, Cys-Cys	50 µL human plasma + 100 µL CAN, centrifuged, supernatant filtered. Cerebrospinal fluid, urine, and saliva, filtered. 50 µL of these fluids+50 µL ACN.	25 µm ID, 33 cm TL, 18 cm EL capillary. 4 M acetic acid. 20 kV.	0.2 µM (Lys) 0.6 µM (Asp)	[56]
Carnitine, acetyl-carnitine, propionyl-carnitine, isovaleryl-carnitine, hexanoyl-carnitine, valproyl-carnitine, octanoyl-carnitine	50 µL human plasma + 50 µL ACN/methanol (3/1) centrifuged. Supernatant diluted 4× in BGE. Human urine samples centrifuged, diluted 4× in BGE.	50 µm ID, 40 cm TL, 32 cm EL capillary. 0.5 M acetic acid, 1 mM hydroxypropyl-β-cyclodextrin; 0.05% Tween, pH 2.6. 15 kV.	1 µM carnitine 3.2 µM octa-noylcarnitine	[57]
β-Ala, His, GABA, Gly, Ala, 2-amino-isobutyric acid, Val, Ser, isovaline, Leu, Glu, Asp	Subcritical extraction of ocean water.	50 µm ID, 64 cm TL, 43 cm EL capillary. 5 M acetic acid. 30 kV	nd	[59]
D/L-Arg, D/L-Val, D/L-Ser, D/L-Phe, D/L-Tyr, D/L-Aps, D/L-Thr, D/L-Met, D/L Trp	Standard AAs	10 µm ID, 48 cm TL, 43 cm EL capillary. 10 mM (+)-(18-crown-6)-2, 3, 11, 12-tetracarboxylic acid, 10 mM citrate/Tris at pH 2.2. 15 kV	2.5-20 µM	[60]
cis-1,2-diaminocyclohexane, 3-cyclohexyl-D-Ala, prolinol, 2-adamantanamine, 1-cyclohexylethylamine	Amines and non proteinogenic standard AAs.	25 µm ID, 60 cm TL, 55 cm EL capillary. Electrokinetic injection 5 kV, 7 s. 0.5 M acetic acid, 50 mM(+)-(18-crown-6)-2,3,ll,12-tetracarboxylic acid, pH 2.5. 15 kV	≈1 µM	[61]
Lys, His, Arg, Gly, Ala, Leu, Glu. (Gly solely quantitated)	2.5 µL periaqueductal gray matter microdialysate (2.5 mM KCl, 125 mM NaCl, 1.18 mM $MgCl_2$ and 1.26 mM $CaCl_2$) + 7.5 µL, shaken and analyzed.	75 µm ID, 43 cm TL, 30 cm EL capillary. 1.7 M acetic acid 12% m/v PEG (pH 2.1).	3.3 µM	[63]
GABA, Gly, Glu, 2-amino-isobutyric acid	2.5 µL periaqueductal gray matter microdialysate (2.5 mM KCl, 125 mM NaCl, 1.18 mM $MgCl_2$ and 1.26 mM $CaCl_2$) + 7.5 µL, shaken and analyzed.	50 µm ID, 43 cm TL, 28 cm EL capillary. Injection 100 s, 50 mbar. The ACN sample zone was forced out at 50 mbar, 100 s at 25 kV. 4.0 M acetic acid (pH 1.9). 25 kV.	29 nM (GABA, Gly), 37 nM (Glu)	[64]

Ala, Val, Ile, Leu, Ser, Gln, Glu, Phe, Pro, Tyr	10 µL plasma+30 µL 10 mM HCl in ACN, 30 µL supernatant injected.	25 µm ID, 31 cm TL, 14.5 cm EL coated capillary with poly(acrylamide-co-(3-acrylamidopropyl) trimethyl-ammonium chloride) (PAMAPTAC) containing 1% m/m (3-acrylamidopropyl) trimethylammonium chloride (APTAC). 3.2 M acetic acid +10% v/v MeOH. -30 kV	≈ 0.6 µM	[66]
Lys, Ala, Pro, Glu, Asp	1 g honey/50 mL water, centrifuged, supernatant filtered.	50 µm ID, 60 cm TL, 48 cm EL capillary. 2 M lactic acid (pH 1.4)	39 ng/g (Lys) 90 ng/g (Asp)	[67]
Choline, taurine	Milk (powdered, fresh), rice, energy drink. 1 g powder in 10 mL water, sonicated, filtered, diluted with water. Liquids filtered, diluted with water.	50 µm ID, 60 cm TL, 45 cm EL for the two capillaries. Capillary 1 (taurine) 150 mM Tris/Lac (pH 8.96). Capillary 2 (choline) 150 mM Tris/Ace (pH 9.5). -10 kV	0.27 mg/L taurine 0.35 mg/L choline	[68]

Table 3: Separation and detection parameters adopted in the major publications reviewed in the chapter CE/fluorescence.

(AA, amino acid; nd, not determined; ID, inner diameter of the capillary; EL, effective length of the capillary; TL, total length of capillary; SFC, sheath flow cell; IS, internal standard; SR, serotonin; DP, dopamine; NP, norepinephrine; NA, noradrenaline)

AA	**Sample and sample treatment**	**Separation conditions**	**Excitation λ (nm)**	**LOD**	**Ref**
Serotonin, Trp, hydroxy-indole-3-acetic acid	Standard	50 µm ID, 67 cm TL, 60 cm EL capillary. 20 mM borate buffer, pH=9. 23 kV	Pulsed 266	5 nM (SR) 2 nM (Trp)	[77]
Tyr, Trp	CSF, filtered, diluted 20× in water .	75 µm ID, 60 cm TL, 57 cm EL capillary. 10 mM CAPS, 15 mM sodium tetraborate, pH 9.2. 15 kV.	Pulsed 266	0.15 nM (Trp)	[78]
Trp, tryptamine, SR acetyl-serotonin, 5-hydroxyindole-3-acetic acid, melatonin, Tyr, DP, octopamine, epinephrine,	Single metacerebral cell in microvial, homogenized with tungsten needle manipulation and damages of the BGE as hypoosmotic buffer.	150 µm ID, 80 cm TL, capillary. SFC. Electrokinetic injection 2.1 kV 10 s. 50 mM borate pH=8.7. 21 kV	Pulsed 248,6[1]	27 nM(SR) 8 µM (DP)	[79]

[1] Wavelength-resolved fluorescence

5,6,7,8-tetrahydrobiopterin, flavin mono-nucleotide), Flavin adenine dicucleotide, β-nicotinamide adenine dinucleotide, β-nicotina-mide adenine dinucleotide phosphate.					
D/L Trp	Standards: D-Trp/L-Trp=1/400	50 µm ID, 10 cm TL, 5 cm EL capillary. 1.0 mM phosphate with 0.15% HS-γ-CD at 6 kV.	Pulsed 266	70 pM	[80]
Tryptamine, SR, NR, octopamine, N-acetylserotonin, DP epinephrine, Trp, Tyr, Phe, 3,4-dihydoxyphenylalanine, NP	Individual cerebral ganglion neurons in the 300-nL vial homogenized with BGE	50 µm ID, 80 cm TL, capillary. SFC. Electrokinetic injection 2.1 kV 10 s. 50 mM citrate buffer at pH 3. 21 kV	257[1]	4.4 nM tryptamine 3.9 µM NP	[82]
Trp and proteins	Standard	75 µm ID, 60 cm TL, 50 cm EL capillary. 40 mM sodium phosphate. pH 11.3.	XeHg lamp 280	6.7 nM	[84]
DP, 3,4-dihydroxy-DL-phenyl-alanine (DOPA), epinephrine, 5-hydroxyindole-3-acetic acid, 5-hydroxytryptamine 3-indoxyl sulfate	10 µL urine diluted in 100 mM citric acid and 89% ACN.	75 µm ID capillary. Electrokinetic injection 15 kV, 360 s. 400 mM propanoic acid 20% glycerol.	Pulsed 266	0.3 nM (epine-phrine), 17 pM (tryptamine)	[88]
DP, NA, dihydroxybenzylamine (SI)	0.5 µL 500 mM borate (pH 8.6) + 0.45 µL, 10 mM NaCN + 3.6 µL (3.25 µL microdialysate + 0.35 µL 0.1 M perchloric acid) + 0.1 µL 5 mM NDA.	50 µm ID, 72 cm TL, 52.5 cm EL capillary. 110 mM phosphate buffer, pH 7. 15 kV	442	0.37 nM (NP)	[93]
Asp, Glu, GABA, Gly, NA, DP, Ser	5 µL microdialysate + 160 µL 125 mM borate pH 8.7, 40 µL 43 mM KCN + 33 µL 5 mM NDA.	50 µm ID, 65 cm TL, 50 cm EL capillary. 22.5 mM lithium tetraborate, 20 mM lithium dodecylsulfate. 10 kV/7 min then 20 kV/8 min.	442	0.22nM (Gly) 0.42nM (GABA)	[95]
Ser, Thr, His, Glu, Ala, Asp, Tyr, Val, Met, Ile, Leu, Phe, Lys, Arg	700 µL 100 mM borate buffer pH 9.5 + 100 µL (10 mM NaCN, 10 mM borate buffer) + 100 µL 2.5 µM standard AA + 100 µL 1 mM NDA in ACN	50 µm ID, 57 cm TL, 50 cm EL capillary. 100 mM borate, pH 9.5, 50 mM SDS	LED 405	≈10 nM	[96]

Arg, histamine, agmatine, methylamine; His; Gln, Ser, propylamine, GABA; Gly, Thr, Ala; Tyr, Val, Glu	Beer diluted 50×. 100 µL mixed with 900 µL (0.6 mM NDA, 1 mM sodium tetraborate, 0.6 mM NaCN). Water diluted 10× prior to injection.	75 µm ID, 40 cm TL, 30 cm EL capillary. 100 mM Tris–borate pH 7, 14 mM CTAB, 25% CAN, 1.2% PEO.-15 kV.	LED 405	9.5 nM (GABA) 50.5 (Thr)	[97]
Phosphorylated Ser (P-Ser), Phosphorylated Tyr (P-Tyr), Phosphorylated Thr (P-Thr)	80 µL standard phospho-AA + 20 µL 20 mM sodium tetraborate (pH 10.0) + 20 µL 40 mM KCN + 20 µL 3.5 mM, 15 min at 65 ºC	75 µm ID, 40.5 cm TL, capillary. 30 mM sodium tetraborate 2 mM β-CD. pH 9.2. 18 kV.	Hg Lamp 400-490	P-Tyr 5.6 nM P-Ser 7.2 nM	[101]
Asn, Ser, Gln, Thr, His, cystine, Glu, Gly, Tyr, Ala, Asp, Taurine, Ala-Gln, Val, Met, norVal, Trp, Ile, Leu, Phe, Arg, Lys	2 µL human plasma (or culture media of in vitro cultivation of human embryos) + 8 µL MeOH/2-propanol (IPA) (4/1), centrifuged. Supernatant diluted 1/1 in 100 mM H_3BO_3/NaOH, pH 9.8, 2 µM norvaline.	50 µm ID, 66 cm TL, 45 cm EL capillary. BR: 200 mM H_3BO_3/NaOH, pH 9.8 EMMA: i) injection 30 s 100 mbar (3000 bar.s),100 mM SDS in BR, ii) 1200 mbar.s, 1 mM NDA in (BR, 12.5% (v/v) MeOH/IPA (4:1)), iii) 350 mbar.s AA sample, iv) 400 mbar.s 1 mM NDA in (BR, 12.5% (v/v) MeOH/IPA (4:1)), v) 1900 mbar.s 2.5 mM NaCN in BR. Then -5 kV for 65 s capillary inlet with 2.5 mM NaCN. No voltage for 3 min. BGE 73 mM SDS, 6.7% (v/v) 1 P, 0.5 mM HP-β-CD, 135 mM H_3BO_3/NaOH of pH 9.00. 30 kV.	488	5.6 nM (Tyr, His) 48 nM (Asp)	[103]
Asp, Glu	One blotted dry planarian, sonicated in 100 µL 0.1 M HCl + 150 µL ACN, centrifuged. 5 µL supernatant + 45 µL borax, 2 µL 0.1 M HCl, 3 µL ACN, 25 µL 12 mM KCN, then 10 µL 10 mM NDA in MeOH.	25 µm ID, 25 cm TL, 20 cm EL capillary. 10 mM sodium phosphate buffer, pH 7.5. 20 kV.	445	400 nM (Glu) 300 nM (Asp)	[108]
Lys; 1-Me-His, citruline, Gln; L-anserine, 3-Me–His, Tyr; Orn, β-Ala, carnosine, Hcy, Ser; Gly; Ala; taurine, L/D-α-amino-butyric acid , Val, Hcy, Met; Thr; Nor-Val, Ile; Phe; Leu, L-α -aminoadipic acid; Nor-Leu; Glu; Arg, Asp	100 µL human plasma + 25 µL (160 g/L sulfosalicylic acid 200 µM norvaline). Vortexed, centrifuged; neutralized to pH 9 with 5 M NaOH. 30 µL sample + 30 µL 30 mM CBQCA (10-fold molar excess AA), + 6 µL 75 mM KCN, 65 °C. Diluted 7.5× in 10 mM borate.	50 µm ID, 67 cm TL, 60 cm EL capillary. 160 mM borate, 130 mM SDS, 20 mM NaCl, and 7.5 mM γ-CD. 30 kV	488	40 nM (Arg)	[111]

Arg	Standard Arg. 2.5 µL AA, 11.5 µL MeOH, 1 µL 50 mM KCN, 10 µL 10 mM CBQCA.	50 µm ID, 41.5 cm TL capillary. SF. 18 mM Borate, 10 mM SDS, pH 9.3. 29 kV.	488	26 pM	[112]
Ser, Gln, Met, Asn, Thr, Tyr, Ala, Gly, Val, His, Pro, Cys, Ile, Leu, Phe, Norleucine, Glu, Arg, Asp.	Culture medium of *Brevibacterium linens* strain BL2 2 µL sample, 10 µL 420 µM CBQCA (in MeOH), 5 µL 420 µM KCN, 6 µL MeOH, 11 µL H_2O, 0.5 µL 1 mM norleucine.	75 µm ID, 107 cm TL, 99 cm EL capillary. 6.25 mM sodium borate, 150 mM SDS, 10 mM THF, pH 9.66. 24 kV.	488	17 pM (Ile, Leu, Phe) 383 pM (Glu)	[113]
Arg, His, Ala, taurine, Gly, Glu, Asp	Tear sample collected via phenol red thread and inserted in a pipette tip, rinsed with 20 mM phosphate buffer pH 8. Centrifuged. 10 µL sample + 10 µL 10 mM CBQCA +10 µL 10 mM KCN	50 µm ID, 50 cm TL, 40 cm EL capillary. 25 mM borate buffer, pH 9.2. 24 kV	LED 480	89 nM (taurine) 4.4 µM (Asp)	[114]
Glu, Asp, taurine, GABA, O-methyl l-threonine (IS)	10 µL microdialysate of suprachiasmatic nucleus of hamsters + (75 µg FQ in 10 µL MeOH), + 5 µL (80 mM KCN 150 nM IS), 65 °C 60 min.	50 µm ID, 60 cm TL, 50 cm EL capillary. 155 mM borate, 20 mM SDS. pH 9.5. 20 kV	488	8 nM GABA 110 nM (Glu)	[115]
Asp, Glu	Standards	25 µm ID, 8 cm EL separation capillary. Flow-gated injection interface/mixing tee. 7.5 mM OPA/BME, and AA 1.2 µL/min, in 100 µm reaction capillary 30 cm long to interface. Crossflow interface 1 mL/min (10.0 mM phosphate, pH 7.40). 1 kV/cm	LED 365	11 nM (Asp) 10 nM (Glu)	[119]
Lys, Arg, Glu, Asp	Japanese beer.	50 µm ID, 30 cm TL, 20 cm length for laser drilled hole for post column derivatization, 25 cm EL, capillary. BGE 10 mM SDS and 50 mM borate (pH 9.5). Derivatization reagents, 10 mM OPA, 1% BME 9% ethanol v/v in BGE, derivatization voltage 4 kV. Separation voltage 10 kV.	LED 365	≈5 µM	[120]

Hcy	0.8 mL urine + 7 mL 20 mM CH_3COOH pH 4.7 + 200 µL 2.0× Tween 20-Au nanoparticals (aminothiol high selectivity). 2 h equilibration. Centrifuged, supernatant removed. 20 µL precipitate in 20 µL 2 mM thioglycollic acid. Supernatant in 0.1 mM OPA (no nucleophile addition)	75 µm ID, 50 cm TL, 40 cm EL capillary. 10 mM SDS, 10 mM phosphate buffer, pH 12. 10 kV	Diode laser 355	4 nM (Hcy)	[122]
Arg, Gln, His, Pro, Ala, Asp	Standards. 1 µL 5 mM FITC (in acetone) + 5 µL sample diluted 1/1 in 0.4 M carbonate buffer (pH 9.0) +24 µL acetone + 20 µL 0.2 M carbonate buffer (pH 9.0). 40 °C 3 h	50 µm ID, 57 cm TL, 50 cm EL capillary. Phosphate/borate buffer pH 9. 20 kV	SFC 488	0.1 nM(Arg) 0.4 nM(Pro)	[125]
Ammonia, Ala, Asn, Asp, Arg, citruline, Gln, Glu, Gly, Leu, Lys, Orn, Phe, SEr, taurine, Thr, Tyr, tyramine, Val	50 µL cerebrospinal fluid + 50 µL 0.21 mM FITC (acetone). 2 h; diluted 1000× with water.	50 µm ID, 75 cm TL, 42 cm EL capillary. 100 mM boric acid, 100 mM SDS, pH = 9.3. 20 kV	488	≈5 pM each AA	[136]
Arg, cysteine, Ile, His, Pro, Tyr, Phe, Gln, Ala, Gly, Glu	Standards. Derivatization media 55.5 µM FITC + 10 µM AA in 0.022 M phosphate pH 9.4. 12 h. Extraction: 0.2 mL liquid ion-exchange Amberlite resin LA-2 (selective extract FITC excess).	75 µm ID, 57 cm TL, 50 cm EL capillary. 0.4% boric acid, 0.3% sodium tetraborate pH 9.5.	488	0.5 nM (Arg) 0.3 nM (Pro)	[138]
Homocysteic acid (IS), Ala, Ser, Gly, taurine, Glu, Asp	100 µL human plasma + 50 µL 200 µM IS filtered using Vivaspin 500. 50 µL supernatant + 40 µL 200 mM Na_2HPO_4 pH 9.5 + 10 µL 80 mM FITC. 20 min, 100 °C. 100× water diluted. 100 µL cerebrospinal fluid, saliva, or vitreous humor was vacuum dried, and reswollen in 20 µL 200 mM Na_2HPO_4 pH 9.5 + 10 µL 80 mM FITC. 20 min, 100 °C.	75 µm ID, 57 cm TL, 50 cm EL capillary. 18 mM Na_3PO_4, pH 11.8. 28 kV.	488	25 nM (Gly) 67 nM (Ser and Asp)	[139]
Gly, Ala, methylamine, tyramine, hexylamine, dibutylamine, putresceine,	800 µL sonicated beer + 495 µL 0.2 M carbonate buffer (pH 9), 1 mL 10 mM FITC + 1 mL acetone. 50 °C, 2 h, 5× water diluted	75 µm ID, 40.5 cm TL, 40 cm EL capillary. 30 mM sodium borate, 0.001% hexadimethrin bromide, 15% isopropanol, pH 9.3. -25 kV.	488, LED 470	0.9 µM (Ala) 3 µM (putrescine)	[143]

cadaverine, 1,6 hexanodiamine, agmatine					
Glu, Asp, P-Tyr, P-Thr, P-Ser. (P= phosphorylated)	0.2 g *Nicotiana tabacum* calcium/calmodulin-binding protein kinase (NtCBK2) from Tobacco cells, in 100 µL 25 mM Tris–HCl (pH 7.5), 0.5 mM dithiothreitol, 10 mM magnesium acetate, 100 µM ATP and 1 mM $CaCl_2$, 30 min, 30 ºC. Hydrolyzed in 6 M HCl at 110 ºC for 4 h. Aliquot dried and dissolved in 100 µL of 10 mM borate (pH 9.3). 5 µL sample + 5 µL 0.2 M borate buffer (pH 9) and 2 µL 5 mM DTAF. 50× diluted in water.	50 µm ID, 65 cm TL, 50 cm EL capillary. Borate buffer (20 mM, pH 9.35), Brij35 (10 mM). 25 kV	488	0.5 nM (P-Tyr), 5 nM (Asp)	[146]
Gabapentin, Phenylpropanolamine (IS)	0.5 mL plasma + 1 mL ACN, vortexed, centrifuged. 90 µL supernatant + 10 µL 15 µM IS. 50 µL of this solution + 10 µL 10 mM 6-carboxyfluorescein succinimidyl ester + 40 µL 50 mM borate buffer, pH 9.5.	50 µm ID, 60 cm TL, 40 cm EL capillary. 50 mM sodium borate, pH 9.5; 25 kV.	488	60 nM gabapentin	[150]
ethylamine; ethanolamine; n-hexylamine; methylamine; n-pentylamine; n-propylamine	Filtered beer. 50 µL + 10 µL 1 mM 6-oxy-(N-succinimidyl acetate)-9-(2'-methoxy carbonyl) fluorescein (SAMF) +75 µL H_3BO_3 pH 8.	75 µm ID, 57 cm TL, 50 cm EL capillary. 25 mM boric acid, 24 mM SDS, pH 9. 22.5 kV	488	80 pM (methylamine) 400 pM (n-butylamine)	[151]
Hcy, D-penicillamine, cysteamine, Cys, glutathione	100 µL plasma + 10 µL 35 mmol/L tris(2-carboxy ethyl)phosphine + 5 µL 10 mM IS, Vortexed. + 60 µL 0.8 M 5-sulfosalicylic acid. Vortexed, centrifuged. 100 µL supernatant + 50 µL 1 g/L 6-IAF(in DMSO), 2 h, 5000× diluted in water.	50 µm ID, 75 cm TL, 43 cm EL capillary. 10 mM SDS, 50 mM boric acid, 20 mM 3-(cyclohexylamino)-1 propanesulfonic acid pH 9.5. 25 kV	488	nd	[152]
Glutathione, Hcy, N-acetyl-Cys, cystamine (IS)	0.5 mL plasma + 50 µL 500 µM IS + 250 µL dithiothreitol (in 0.9% NaCl), vortexed 15 min. + 100 µL (2.34 M perchloric acid, 2 mM EDTA), vortexed, centrifuged. 100 µL supernatant + 1 mL (0.42 mM fluorescein-5-maleimide, 50 mM phosphate, pH 7.5), 15 min., 100× diluted with water.	75 µm ID, 57 cm TL, 50 cm EL capillary. Acetonitrile/10 mM phosphate, 50 mM SDS [27:73 (v/v); pH 7.0], 45 ºC, 25 kV.	488	3 µM	[153]

Homocysteine, Cys glutathione, Cys-Gly, γ-Glu-Cys, penicillamine, mercaptopropionyl Gly, cysteamine, mercapto acetic acid (IS)	75 µL urine + 125 µL 16 µM IS + 30 µL 17.5 mM tris(carboxyethyl)phosphine. 100 µL of this solution + 100 µL 1.5 M perchloric acid, vortexed, centrifufed. 50 µL supernatant + 33 µL 1M NaOH + 10 µL 5 mM 5-bromo methylfluorescein (in N,N-dimethyl formamide). 10 min reaction.	25 µm ID, 27 cm TL, 20 cm EL capillary. 60 mM borate, 15 mM SDS, 2-amino-2-methyl-1-propanol, pH 10. 30 kV.	488	76 nM (Hcy) 183 nM (penicilamine)	[154]
D/L Val, D/L Ala, D/LAsp, D/L Glu, Gly	10 µL AA Mars7 standard with 40 µL 50 mM borate buffer (pH 9.5), 10 µL of water and 50 µL 1.8 mM fluorescamine (in acetone).	72 µm ID, 6.2 cm EL microchip; 10 mM Na_2CO_3, 15 mM HP-β–CD, pH 8.9. 700V/cm	Diode laser 404	83 nM (Val)	[156]
Hcy, Cys, glutathione	100 µM AA standards in 100 mM borate pH 8, 2 mM EDTA. 2 Na. 400 µM 4-aminosulfonyl-7-fluoro-2,1,3-benzoxadizole (ABDF) in 100 mM borate pH 8.	50 µm ID, 45 cm TL, 30 cm EL capillary. On-column derivatization: injection ABDF 30 s (15 cm siphoning), sample AA 15 s (15 cm siphoning), ABDF 20 s (15 cm siphoning). Voltage 1 min each +1 kV, -1 kV, +1 kV, 38 °C, 10 min. Separation: 20 mM Tris, 0.1 M H_3PO_4 pH 2.1; 15 kV	363.8	2.5 nM (Hcy) 5 nM (Cys)	[158]
methylamine, dimethylamine, ethylamine pyrrolidine, isobutyl amine, isoamylamine, ammonia	20 µL beer + 20 µL (MeOH, CH_3COONa saturated) + 20 µL 7-chloro-4-nitrobenzo-2-oxa-1,3-diazole (NBD-Cl) 5 mM in MeOH. 60 °C 2 h, 4× diluted with water.	75 µm ID, 81 cm TL, 74.5 cm EL capillary. 50 mM SDS, 10 mM borate pH 9.3. 24 kV.	488	10 µM (isoamylamine)	[160]
Val, Ala, Glu, Asp, buccaline, amyloid-β	Standard	75 µm ID, 47 cm TL, 40 cm EL capillary. In capillary derivatization: 4s (0.1 psi) injection (0.1psi) AA in BGE, 1 s (0.1psi) ethanol, 2 s (0.1 psi) 52 mM NBD-F (in ethanol) Separation: BGE: 20 mM borate buffer pH ranging from 7.7 to 10.0. 15 kV. 45 °C	488	0.1 µM (Ala) 0.6 µM (Asp)	[162]
D/L-Ser	30–60 mg male rat cerebrum tissue in 150 µL 0.1 M HCl, homogenized, sonicated, centrifuged. 100 µL supernatant + 30 µL 30% (w/v) trichloro acetic acid solution vortexed, centrifuged, + 20 µL 1 M NaOH to pH 9. 10 µL	50 µm ID, 75 cm TL, 50 cm EL capillary. Separation 100 mM borate, pH 10, 40 mM HP-β-CD. 15 kV	457.9	0.3µM (D-Ser)	[163]

	of this solution + 40 µL 0.1 M borate pH 9 + 50 µL 2 mM NBDF. 60 °C, 5 min.				
Gly, Ser, Val, Gln	Standards. Molar ratio AA/NBDF = 0.1.	75 µm ID, 45 cm TL, 25 cm EL capillary. EMMA on column injection with inkjet microchip. Two droplets 25× times of 180 pL (44 V 20-µs injections) of 1 mM NBDF (in ethanol) (droplet 1) and AA in 10 mM borate pH 8.5 (droplet 2) 3 kV, 2 s incubation 5 min.	473	0.2 nM(Gln) 5 nM(Val, Ser)	[165]
D/L Tyr, L-Lys, L-His, L-Val, Gly, L-Glu, L-Asp	100 µL commercial pharmaceutical preparation of AA, 880 µL ACN/water (1:1, v/v) + 20 µL trimethylamine, vortexed, sonicated, centrifuged. 10 µL supernatant + 10 µL 10 mM R(−)-4-(3-isothiocyanatopyrrolidin-1-yl)-7-(N,N dimethylaminosulfonyl)-2,1,3-benzoxadiazole. 55 °C 20 min. 30 µL 1 mM CH_3COOH (in 1/1, ACN/water)	75 µm ID, 45 cm TL capillary. 15 mM borate pH 10.5. 14 kV.	LED 460	2.9 µM D-Tyr	[166]
glutathione	20 µL centrifuged saliva, or exhaled breath condensate + 1 µL 10 µM eosin-5-maleimide (in DMF)	50 µm ID, 50 cm TL, 25 cm EL capillary. 15 mM HEPES, pH 7. 15 kV.	Diode laser 515	0.59 nM (glutathione)	[167]

Table 4: Separation and detection parameters of the main publications cited in the chapter CE/MS generalities.

(AA, amino acid; nd, not determined; ID, inner diameter of the capillary; TL, total length of capillary; SF, sheath liquid flow rate; AmAc, ammonium acetate; IS, internal standard; SR, serotonin; DP, dopamine; NP, norepinephrine; NA, noradrenaline)

AA	**Sample and sample treatment**	**Separation conditions**	**ESI +/-**	**LOD**	**Ref**

All proteinogenic AAs (except Gln), β-Ala, sarcosine, GABA, hydroxyPro, Orn, α-aminoadipic acid, allo-δ-hydroxylysine, 1-methylHis, citrulline, cystathionine, carnosine, anserine	Soy sauce, beer, sake, and human urine.	50 µm ID, 100 cm TL capillary. 1 M FA, 30 kV. SF 10 µL/min 5 mM AmAc in 50% (v/v) MeOH/water	+	0.3 µM (Arg, His) 11 µM (Asp)	[170]
All proteinogenic AAs	Infant food samples, 10× diluted with water, vortexed, centrifuged. Supernatant injected for CE.	50 µm ID, 70 cm TL capillary. 300 mM FA, 100 mM trimethylamine. 20 kV. SF 4 µL/min 0.0%–1.0% FA 2-propanol/water 80:20% v/v	+	≈1 µM	[173]
D/L Arg, D/L Thr, D/L Val, D/L Trp, D/L Leu, D/L Tyr, D/L Lys, D/L Phe.	Standard	20 µm ID, 130 cm TL capillary. 30 mM 18-C-6-TCA. 30 kV	+	nd	[175]
All proteinogenic AAs, L- canavanine	Dried blood spot + 100 µL water (10 min.). 20 µL this solution + 180 µL (ACN/water/FA, 49.9/49.9/0.2; v/v/v).	20 µm ID, 115 cm TL capillary. 1 M FA. 30 kV	+	2.5 µM (Tyr) 35 µM (Gly)	[176]
All proteinogenic AAs and 80 other molecules	*Xenopus* embryo + 55 µL (ACM/water/MeOH, 2/2/1), triturated, vortexed, centrifuged. Supernatant collected.	50 µm ID, 45 cm TL capillary. 1 M acetic acid. 26.5 kV. SF 10 mM ammonium acetate/MeOH, electrokineticaly driven	-	nd	[178]
All proteinogenic AAs + methionine sulfone (IS), β-Ala, Orn, sarcosine, GABA, hydroxy-Pro	Human urine, diluted in water.	50 µm ID, 100 cm TL capillary. 1 M FA, 30 kV. SF 10 µL/min 5 mM ammonium acetate (50% MeOH-water, v/v)	+	0.7 µM (Ser) 11 µM sarcosine	[180]
Ng-nitroso-Arg, citruline, cyano-Orn, Ng-Hydroxy-Arg, 1-3 cyclo-hexadiene	50 µL Ng-hydroxy-l-Arg (10g/L) in PBS, +/- 10 µL 1-3-cyclohexadiene (formamide 50/50)	50 µm ID, 105 cm TL capillary. 50 mM. 30 kV. FA 10 µL/min, 0.1% FA (50% water–MeOH, v/v)	+	nd	[181]
All proteinogenic AAs, methionine sulfone (IS)	50 mg preweighed deep-frozen human tissue homogenized in 500 µL 20 µM IS in MeOH. Then + (200 µL water/500 µL chloroform), vortexed, centrifuged. 480 µL supernatant filtered (using a 5-kDa filter) + 50 µL water.	50 µm ID, 100 cm TL capillary SF 10 µL/min 0.1 µM hexakis(2,2-difluorothoxy) phosphazene in (50% MeOH-water, v/v)	+	0.1 µM (Ile, Leu, Phe, Arg…) 1.4 µM (Gln)	[182]
All proteinogenic AAs, GABA, tyramine	*E. coli* (BL-21) in Luria-Bertani broth, centrifuged. Supernatant 20× diluted in 200 mM ammonium acetate	50 µm ID, 80 cm TL capillary. 1 M FA, 23 kV. SF 10 µL/min 5 mM ammonium acetate (50% MeOH/water, v/v)	+	1 nM (Lys) 25 nM (Glu)	[184]

Pro, uridine, hippuric acid, pyroglutamic acid, flavin adenine dinucleotide, glucose-6-phosphate, uric acid, glutathione, glutaric acid, citrate	Human urine, centrifuged, mixed 1/1 in 25 mM trimethylamine (TEA)	50 µm ID, 100 cm TL capillary. 25 mM trimethylamine. 30 kV. SF 5 µL/min 5 mM TEA (50% MeOH/water, v/v)	-	3.2 µM (Pyro-Glu) 4 µM (Pro)	[185]
^{13}C labelled AA	10 flaxseed embryos cultured with ^{13}C-glutamine, washed, extracted in 1 mL 0.01% HCl 95 °C. Lyophilized, resuspended in 1 mL sodium acetate (50 mM pH 5.5), loaded on Dowed 50×8, lyophilized, resuspended in 500 µL water.	50 µm ID, 125 cm TL capillary. 1 M FA, 25 kV. SF 8 µL/min 2.5 mM ammonium acetate (50% MeOH/water, v/v)	+	nd	[186]
All proteinogenic AAs, Orn, β-Ala, sarcosine, GABA, N,N-dimethylglycine, creatinine, betaine, homo-Ser, citrulline, homo-Arg, N^6-trimethyl-Lys, 3-hydoxybutyrate, 2-hydoxybutyrate, lactate, fumarate	350 µL plasma + 3.15 mL 10 µM 2 AM in MeOH + 3.5 mL chloroform + 1.4 mL water, vortexed, centrifuged. Aqueous layer collected. AM: authentic material for migration-time alignment	50 µm ID, 80 cm TL capillary. Anions: 50 mM ammonium acetate (pH 8.5). Cations: 1 M FA. 30 kV SF 10 µL/min.	+/-	3.3 nM (Arg 473 nM (Gly)	[187]
All proteinogenic AAs, acyl-carnitine, L-allo-Ile, 4-OH-Pro, pyro-Glu	100 µL (1/1 MeOH/H_2O) on Dried Blood Spot from Guthrie card, 20 min. Directly CE injected	50 µm ID, 80 cmTL capillary; 1.4 M FA, 30 kV. SF 10 µL 0.1% FA (50% MeOH/ water, v/v)	+	60 nM (Arg) 11.7 µM (Val)	[188]
All proteinogenic AAs, atenolol, O-butyryl-L-carnitine, L-carnitine, L-carnosine, creatinine, *p*-chloro-L-Tyr, L-citrulline, L-cystathionine, 2,3-dihydroxy-L-phenylalanine (DOPA), DP, guanosine, histamine, Hcy, Orn, 5-hydroxyl-L-tryptophan, metoprolol, N-methyl-L-Asp, 3-methyl-L-His, 1-methyl-adenosine, L-methionine sulfone, nicotinamide, nicotinic acid, p-nitro-L-tyrosine, O-octoyl-L carnitine, oxytetracycline, tyramine, *m*-L Tyr, *o*-L-Tyr, SR, L-theanine, glutathione	Washed RBC lysed in 3-fold-volume excess water (0 °C) vortexed, centrifuged. Supernatant ultracentrifugation using 3-kDa filter (protein removing). Filtrate diluted 1:1 with 400 mM ammonium acetate, pH 7.0.	50 µm ID, 80 cm TL capillary; 1.4 M FA, 30 kV. SF 10 µL 0.1% FA (50% MeOH/ water, v/v)	+	nd	[189]
All proteinogenic AAs, Orn, N,N-diaminobutane, ethanolamine, carnosine, β-Ala, GABA, sarcosine, α	50 mg pineapple leaves were ground + 500 µL MeOH/water 1/1 (v/v), vortexed, centrifuged. Supernatant utracentrifuged in 5-kDa ultrafilter.	50 µm ID, 100 cm TL capillary. 1 M FA 30 kV. SF 10 µL/min (50% MeOH/ water, v/v)	+/-	≈1 µM	[190]

aminobutyrate, cystathionine, homo-Ser, methionine sulfone, hydroxy-Pro, Phe-Gly, phosphoethanolamine, urea, taurine, succinate, lactate, malate, isocitrate, fumarate, tartrate, cis-aconitate					
Orn, β-Ala, Allo-Ile, citrulline, pyro-Glu.	40 g vegetable oils + 160 mL of methanol:chloroform (2:1, v/v) vortexed, left overnight, centrifuged. Upper phase collected + (40 mL chloroform, 100 mL water), vortexed centrifuged. Supernatant dried. + 1 mL Butanolic-HCl, vortexed, 80 ºC, 30 min., dry and diluted in 500 µL of acetonitrile/water (40:60, v/v)	50 µm ID, 60 cm TL capillary. 0.1 M FA, 25 kV. SF 3.3 µL/min 0.1% FA (isopropanol/water, 1/1, v/v)	+	40 pg/g (Orn, β-Ala, GABA). 190 pg/g (citruline)	[191]
All proteinogenic AAs, Chloro-Tyr (IS), 4 hydroxy-Pro,	Clean Mylar strips (10 × 2 cm) + 8 µL 1.6 mM IS in BGE, left to dry + 1 mL (EtOH/water, 6/4, v/v), filtered, dry. + 50 µL BGE	50 µm ID, 100 cm TL capillary. 1 M FA, 25 kV. SF 10 µL/min 0.1% FA (methanol /water, 1/1, v/v)	+	20 ng/strip (Lys) 180 ng/strip (Met)	[192]
D/L proteinogenic AAs without Asn, Arg, Allo-Ile	500 µL vinegar filtred (3 kDa filter), water diluted (1/1).	50 µm ID, 100 cm TL capillary. 1 M FA 30 mM 18C6H4, 24 kV. SF 10 µL/min (50% MeOH/ water, v/v)	+	0.15 µg/mL (Met) 0.83 µg/mL (Val)	[194]
D/L Ser, D/L Glu, D/L Gln, D/L Asn, D/L Asp	100 µL artificial cerebrospinal fluid, + 10 µL 30 mM sodium tetraborate (pH 9.2) + 90 µL 6 mM (+)-1-(9-fluorenyl)ethyl chloroformate (in acetone/ACN, 1/2, v/v)). Vortexed 1 h. Diluted in 0.5 mL water.	50 µm ID, 80 cm TL capillary. BGE 150 mM acetic acid, pH 3.7 (NH_4OH), 30 kV. Inlet: 17 mbar negative pressure. SF 3 µL/min 0.1% NH_4OH in (50% MeOH/ water, v/v)	-		[195]
D/L Arg, D/L Lys, D/L Ala, D/L Glu, D/L Asp	100 mg grounded soya kernels + 1 mL 0.37 M trichloroacetic acid, vortexed. + 0.2 mL 3.6 mM sodium deoxycholate. Centrifugation. 625 µL supernatant + 675 µL water + 1.5 mL 355 mM	50 µm ID, 85 cm TL, capillary. 5 mM 3-monodeoxy-3-monoamino-β-CD, 50 mM, HCO_3, NH_4 pH 8. 30	+	nd	[197]

	sodium tetraborate (pH 10). + 1 M NaOH pH 10 + water to final volume = 10 mL. 250 µL of this solution + 50 µL 3.75 mM FITC (in acetone). Reaction overnight.	kV. SF 4 µL/min (50% isopropanol/ water, v/v).			
Zn-Gly, Zn Met, Zn galacturonate, Zn caffeate, Zn pterostilbene, Zn piceatannol, Zn isorhamnetin, Zn zeaxanthin glucoside	50 mg grounded goji berry + 2 mL 30 mM Tris-HCl pH 7.4. Vortexed 2 h. Ultrafiltrated (10 kDa filter) immediately analyzed.	50 µm ID, 100 cm TL, capillary. 20 mM ammonium formate (pH 9), 10 kV. SF 10 µL/min 5 mM ammonium formate, in 50% methanol/water (v/v)	+/-	nd	[199]
17 AAs	Standards	20 µm ID, 120 cm TL, porous tip capillary. 1 M FA 15 mM 18C6H4, 20 kV.	+	nd	[200]
D/L Asp, D/L Phe, D/L Tyr	~20 µg silk digested in 6 N HCl at 110 °C, 2 h, dried, resuspended in 0.1 N HCl.	20 µm ID, 120 cm TL, porous tip capillary. 30 mM 18C6H4. 30 kV	+	nd	[201]
Proteinogenic AA, spermine, hypoxanthine, glutathione, adenosine, creatine, hydroxyl-Pro, anthranilate, spermidine, cytosine, adenine, homo-Ser, tyramine	50 µL of known HepG2 cell lysate (in MeOH/water, 4/1, v/v) + 50 µL 0.2 µg/mL isotope-labeled AAs + 100 µL cold water/chloroform (1.5/1 v/v), vortex, centrifuged, supernatant ultrafiltered (5 kDa filter), dried + 50 µL 250 mM ammonium acetate, pH 7.	30 µm ID, 91 cm TL, porous tip capillary. 10% acetic acid pH 2.2, 30 kV	+	1-42 nM, except for Asp 412 nM	[203]
All proteinogenic AAs (except Cys, Asn, Gln) D_3-Met (IS), α-keto-glutarate, pyruvate, succinate, fumarate, lactate	2×10^6 washed bovine aortic endothelial cells (or human tissue from stemotomy) + 600 µL cold [MeOH/water (4/1), 5 µM IS], sonicated, centrifuged. 20 µL supernatant were dried. Dry sample + 100 µL anhydrous DMF with (300 mM 1-chloro-N,N,2-trimethyl-1-propenylamine, 300 mM 3-(diethylamino) propionic acid) + 4 µL pyridine.	50 µm ID, 80 cm TL capillary. 5 mM ammonium formate, 10% MeOH, pH of FA adjusted to 2.5.	+	9 nM (Ile, Leu) 225 nM (His)	[205]
Trp, Tyr, Phe, Ala, Pro, Val, The, Leu, Ile, Arg, Met	Standards	50 µm ID, 40 cm TL capillary fitted in union comprising a conductive-hole. 5 mM ammonium acetate, pH 10.8. 25 kV.		0.11 µM (Phe) 1.62 µM (Ala)	[206]